

POLITECNICO DI TORINO

MASTER's Degree in BIOMEDICAL ENGINEERING



MASTER's Degree Thesis

Neural Signals Classification through
Machine Learning: Distinguishing
Voluntary and Involuntary Movements
EEG Correlates

Supervisors

Prof.ssa Gabriella OLMO

Prof. Vito DE FEO

Candidate

Viviana FORNELLI

July 2023

Abstract

This thesis is focused on the development of a Machine Learning (ML) model with the primary goal of accurately classifying voluntary and involuntary movements by means of the EEG signal, contributing to the larger project of diagnosing the level of consciousness in non-responsive patients. Some tens of thousands of patients across the globe have been incorrectly labeled as "awake but unaware" for long periods, when they have actually remained conscious the entire time [1]. The high prevalence of misdiagnosis highlights the need for improved diagnostic methods in this field.

The goal is to minimize misdiagnoses, leading to improved patient outcomes and care in the field of Brain Injuries. This project is based on the Readiness Potentials (RPs): slow negative EEG potentials found in the seconds preceding voluntary actions [2], as indicators of volition and consciousness.

In addition to the classification task, this work also undertakes the evaluation of the performance of the improved EEGLAB plug-in (Matlab toolbox).

Proper signal preparation is crucial before classification: the signals go through pre-processing to remove artifacts and noise, followed by feature extraction. These features are selected based on their statistical significance or chosen from existing literature. The effectiveness of the optimal pre-processing chain is assessed in the classification task, ensuring the reliability and validity of the classification results. Subsequently, feature selection methods are applied to refine the feature set. The machine learning algorithms employed are: Decision Tree (DT), Support Vector Machines (SVM) and K-Nearest Neighbors (k-NN). These models are evaluated and compared based on their performance.

The developed ML model can be part of the BCI framework: it offers opportunities for improving the diagnosis in non-responsive patients and gains a more reliable understanding of their state of consciousness and cognitive state.

Table of Contents

List of Tables	v
List of Figures	vi
1 Anatomy and function of the Brain	1
1.1 Brain anatomy	1
1.2 Cells of the brain	7
1.2.1 Nerve cells and neural signals	7
1.2.2 Glia cells	8
1.3 Brain states and Cortical activities	9
1.3.1 Voluntary and Involuntary movements	9
2 The enigma of Mind and Consciousness	12
2.1 What is Consciousness?	12
2.1.1 The brain's processing of external world information	13
2.1.2 States of consciousness	14
2.1.3 Disorders of Consciousness	15
2.1.4 Assessment methods	16
3 EEG signals and Readiness Potential	18
3.1 EEG signals	18
3.1.1 EEG recordings and International 10-20 System	19
3.2 Readiness Potential and free will	20
3.2.1 Main features of the RP	21
3.2.2 Main Characteristics of the RP	21
3.2.3 Movement-Related Cortical Potential (MRCP)	23
3.2.4 Libet's Experiment	23
4 Readiness Potential: Experimental Procedures and Techniques	26
4.1 Tasks and Protocol	27
4.1.1 2012 - 2015 Protocol	27

4.1.2	2015 - 2018 Protocol	27
4.1.3	2018 Protocol	28
4.2	Dataset classification	28
4.3	Experimental setup	29
4.4	Signal Processing Software for Data Analysis	31
4.4.1	EEGLAB	31
4.4.2	MRCPLAB	32
5	Classification Project: State-of-the-Art and Machine Learning	34
5.1	State of the art	34
5.2	Machine learning	35
5.2.1	Overview of Essential Machine Learning Techniques	35
5.2.2	Machine Learning in Brain-Computer Interfaces (BCI)	35
5.2.3	The Overall Architecture of BCI	36
5.3	Classification Methods Involved	36
5.3.1	Support Vector Machine	37
5.3.2	K-Nearest Neighbors	38
5.3.3	Decision Tree	39
6	Method and Project Development	41
6.1	Dataset Preprocessing	41
6.1.1	Residue Iteration Decomposition (RIDE)	43
6.1.2	How does RIDE overcome the problem of Jitter in ERPs?	44
6.1.3	Understanding the RIDE Flowchart	45
6.2	Data Normalization with Z-score method	46
6.3	Feature Extraction	47
6.3.1	RP Time-Domain features	48
6.3.2	RP Frequency-Domain features	49
6.3.3	PCA for Feature Construction	49
6.4	Feature selection	50
6.4.1	ReliefF method	51
6.5	Classification	52
6.5.1	Leave-One-Out Cross-Validation	52
7	Results and Discussion	53
7.1	Outcomes with the Improved EEGLAB plug-in	53
7.1.1	Feature Extraction and Feature Selection	53
7.1.2	Classification	55
7.2	Outcomes with the Old EEGLAB plug-in	61
7.2.1	Short explanation of the old plugin	62
7.2.2	Feature Extraction and Feature Selection	62

7.2.3	Classification	62
7.3	Comparison between the New and Old EEGLAB Plugins	68
7.3.1	RP and SNR of voluntary subjects	68
7.3.2	RP and SNR of involuntary subjects	76
8	Conclusions	87
8.0.1	Special Case	89
8.0.2	Issues and limitations	90
8.0.3	Ideas for the future	90
	Bibliography	91

List of Tables

5.1	Table summarizing the performance of the Zanetta's classification[32].	34
6.1	ERP's components.	45
6.2	The combinations of averaged RPs representing different areas of the brain, to better understand data management and the graphical representation of results.	48
7.1	Table of all the extracted features: from voluntary MI993011 and involuntary dataset RG865070.	54
7.2	Table of classification performances with the algorithm for feature selection (<i>4 features</i>).	60
7.3	Table of classification performances without the algorithm for feature selection (<i>17 features</i>).	61
7.4	Table of classification performances of the <i>old</i> plug-in with the algorithm for feature selection (<i>4 features</i>).	67
7.5	Table of classification performances of the <i>old</i> plug-in without the algorithm for feature selection (<i>17 features</i>).	67

List of Figures

1.1	The brain has three main parts: the cerebrum, cerebellum and brainstem[5].	2
1.2	The two hemispheres of the brain are interdependently[7].	3
1.3	The cerebrum is divided into four lobes: frontal, parietal, occipital and temporal[8].	4
1.4	The folded appearance of the cortex[9].	5
1.5	Deep structures. [3]	5
1.6	Deep structures[10].	7
1.7	Structure of neurons[11].	7
1.8	The black line in the graph represents the Action Potential curve: the stimulus from the pre-synaptic neuron depolarizes the target neuron. Sodium channels open and sodium enters the cell. This results in depolarization. At the peak, the potassium channels open and the ion exits out of the cell. The colored ones represent the Post-Synaptic Potential curves: A) positive ions (Na+) enter the neuron, causing membrane depolarisation (red curve); B) inhibitory negative ions (Cl-) enter the neuron, causing hyperpolarisation of the membrane hyperpolarisation (blue curve).	8
1.9	Brain activity in voluntary movements.	10
1.10	Voluntary movement is controlled by brain circuits. [14]	11
2.1	The two main components of consciousness: wakefulness and awareness. The X axis represents the Content of Consciousness, while the Y axis represents the Level of Consciousness or wakefulness[4]. . . .	14
3.1	Scheme of the 10-20 System[25].	19

3.2	A representation of the electrode placements for different regions of the scalp according to the International 10-20 system. F - Frontal, C - Central, T- Temporal, P - Parietal, O - Occipital, Z - Mid-line, Fp - Frontal Polar, L - Odd, R - Even, Mid-line to Lateral Numbers Increase; C1 medial to C3, C2 medial to C4; CP3 means 1/2 way in between proportional, CPi - ipsilateral to site, CPc - central lateral [26].	20
3.3	Bereitschaftspotential (BP) with the superposition of the Pre-Motor Positivity (PMP) and the Motor Potential (MP)	21
3.4	Representation of the early and late components of a RP[27].	22
3.5	MRCP waveform components[28]. Movement onset is defined at the time point 0s. The MRCP comprises RP and MMP sections. (In RP section, (-2 ~ -1)s is early BP, (-1 ~ 0)s is late BP, (-0.5 ~ 0)s is motor potential (MP), and after movement onset, (0 ~ 1)s is MMP section) [29]	24
3.6	Graph showing the results of Libet's experiment [30].	25
4.1	2018 Protocol for EEG, EOG and EMG recordings.	28
4.2	Experimental setup[34].	30
4.3	EEGLAB GUI with MRCPLAB plug-in.	32
5.1	General BCI system architecture[38].	36
5.2	Hyper-planes in 2D and 3D feature space[39].	37
5.3	Example of a Dataset for which it is wise to use the Kernel[41] . . .	38
5.4	Example of a kNN application[43]	39
5.5	The general structure of a decision tree[44].	39
6.1	Trial-to-trial latency variability in ERP components can lead to two consequences. In Case 1, it blurs the waveforms and attenuates amplitude differences between conditions. In Case 2, it can mimic amplitude differences between conditions even when the underlying amplitudes are identical. [47].	44
6.2	Conventional average ERP (left) from single trials with latency jitter, decomposition by RIDE (middle) and reconstructed ERP after correcting for latency variability (right). [47].	45
6.3	Flow-chart of RIDE decomposition [47].	47
6.4	Pseudo code of the ReliefF algorithm[52].	51
7.1	Left: SNR of C line; Right: PCA1(PSD).	55
7.2	Left: SNR of Fc line; Right: Area (C line).	55
7.3	Confusion Matrix for Linear SVM Model.	56
7.4	ROC curve of Linear SVM Model.	56

7.5	Confusion Matrix for Cubic SVM Model.	57
7.6	ROC curve of Cubic SVM Model.	57
7.7	Confusion Matrix for k-NN Model.	58
7.8	ROC curve of k-NN Model.	58
7.9	Confusion Matrix for Decision Tree Model.	59
7.10	ROC curve of Decision Tree Model.	59
7.11	Left: SNR of C line; Right: PCA1(PSD) (old plug-in).	62
7.12	Left: SNR of Fc line; Right: Area (C line) (old plug-in).	62
7.13	Confusion Matrix for Linear SVM Model (old plug-in).	63
7.14	ROC curve of Linear SVM Model (old plug-in).	63
7.15	Confusion Matrix for Cubic SVM Model (old plug-in).	64
7.16	ROC curve of Cubic SVM Model (old plug-in).	64
7.17	Confusion Matrix for k-NN Model (old plug-in).	65
7.18	ROC curve of k-NN Model (old plug-in).	65
7.19	Confusion Matrix for Decision Tree Model (old plug-in).	66
7.20	ROC curve of Decision Tree Model (old plug-in).	66
7.21	Subject graph AL858070 (old plugin). Left: RP; Right: SNR. . . .	68
7.22	Subject graph AL858070 (new plugin). Left: RP; Right: SNR. . . .	68
7.23	Subject graph AP996111 (old plugin). Left: RP; Right: SNR. . . .	69
7.24	Subject graph AP996111 (new plugin). Left: RP; Right: SNR. . . .	69
7.25	Subject graph SD874070 (old plugin). Left: RP; Right: SNR. . . .	70
7.26	Subject graph SD874070 (new plugin). Left: RP; Right: SNR. . . .	70
7.27	Subject graph MI993011 (old plugin). Left: RP; Right: SNR. . . .	71
7.28	Subject graph MI993011 (new plugin). Left: RP; Right: SNR. . . .	71
7.29	Subject graph RB890071 (old plugin). Left: RP; Right: SNR. . . .	72
7.30	Subject graph RB890071 (new plugin). Left: RP; Right: SNR. . . .	72
7.31	Subject graph MS861070 (old plugin). Left: RP; Right: SNR. . . .	73
7.32	Subject graph MS861070 (new plugin). Left: RP; Right: SNR. . . .	73
7.33	Subject graph GF892070 (old plugin). Left: RP; Right: SNR. . . .	74
7.34	Subject graph GF892070 (new plugin). Left: RP; Right: SNR. . . .	74
7.35	Subject graph TC995011 (old plugin). Left: RP; Right: SNR. . . .	75
7.36	Subject graph TC995011 (new plugin). Left: RP; Right: SNR. . . .	75
7.37	Subject graph AP996111 (old plugin). Left: RP; Right: SNR. . . .	76
7.38	Subject graph AP996111 (new plugin). Left: RP; Right: SNR. . . .	76
7.39	Subject graph LL993111 (old plugin). Left: RP; Right: SNR. . . .	77
7.40	Subject graph LL993111 (new plugin). Left: RP; Right: SNR. . . .	77
7.41	Subject graph RG865070 (old plugin). Left: RP; Right: SNR. . . .	78
7.42	Subject graph RG865070 (new plugin). Left: RP; Right: SNR. . . .	78
7.43	Subject graph LF864071 (old plugin). Left: RP; Right: SNR. . . .	79
7.44	Subject graph LF864071 (new plugin). Left: RP; Right: SNR. . . .	79
7.45	Subject graph AP996120 (old plugin). Left: RP; Right: SNR. . . .	80

7.46	Subject graph AP996120 (new plugin). Left: RP; Right: SNR. . .	80
7.47	Subject graph GO862071 (old plugin). Left: RP; Right: SNR. . .	81
7.48	Subject graph GO862071 (new plugin). Left: RP; Right: SNR. . .	81
7.49	Subject graph FM893061 (old plugin). Left: RP; Right: SNR. . .	82
7.50	Subject graph FM893061 (new plugin). Left: RP; Right: SNR. . .	82
7.51	Subject graph SP880071 (old plugin). Left: RP; Right: SNR. . .	83
7.52	Subject graph SP880071 (new plugin). Left: RP; Right: SNR. . .	83
7.53	Subject graph AL858070 (old plugin). Left: RP; Right: SNR. . .	84
7.54	Subject graph AL858070 (new plugin). Left: RP; Right: SNR. . .	84
8.1	Subject graph LF864071 (new plugin). Left: RP; Right: SNR. . .	89

Chapter 1

Anatomy and function of the Brain

The brain is the central control center of the body; it is responsible for managing bodily functions and processing external information. It is composed by three main parts: the cerebrum, cerebellum, and brainstem. Through the five senses, the brain receives sensory input and integrates the messages it receives. It controls various aspects such as thoughts, memory, speech, movement, and the proper functioning of numerous organs within our body. The brain and spinal cord compose the central nervous system (CNS), instead of the peripheral nervous system (PNS) which comprises spinal nerves branching from the spinal cord and cranial nerves branching from the brain[3].

The four control systems of the brain (in relation to consciousness):

- cerebrum control system, subdivided into: right hemisphere (autobiographical self, procedural-intuitive functionality) and left hemisphere (high-level consciousness, declarative-abstract functionality) [4];
- limbic control system: it controls sensorial-emotional learning with emotional valuation [4];
- cerebellum control system: it controls sensorimotor reflex learning (protoself reflex level) [4];
- brainstem control system: it controls hormone-based mechanisms (protoself innate level) [4].

1.1 Brain anatomy

The brain is composed by the cerebrum, cerebellum, and brainstem (Figure 1.1).

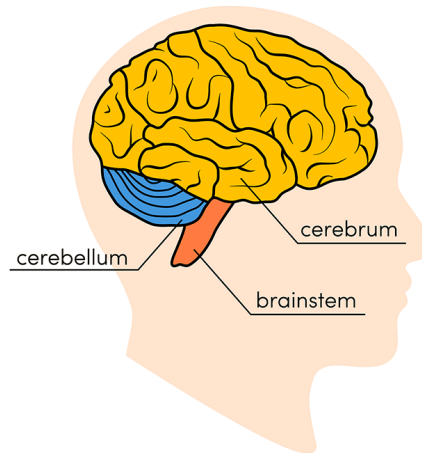


Figure 1.1: The brain has three main parts: the cerebrum, cerebellum and brainstem[5].

- Cerebrum: this is the largest part of the brain and is composed by two (right and left) hemispheres. It performs functions like interpreting touch, vision and hearing, as well as speech, reasoning, emotions, learning, and fine control of movement[3, 6].
- Cerebellum: this is situated beneath the cerebrum, specifically positioned at the posterior and inferior region of the brain, directly behind the brainstem and beneath the occipital lobe. It plays a crucial role in coordinating muscle movements, maintaining posture, and balancing the body. In the event of damage, it can lead to impaired muscle control and movement, abnormal eye movements, headaches, speech difficulties or slurred speech, challenges with walking and mobility, ataxia, and dysmetria.[3, 6].
- Brainstem: it connects the cerebrum and cerebellum to the spinal cord and carries out numerous involuntary functions such as breathing, heart rate regulation, body temperature control, sleep-wake cycles, digestion, reflex actions including sneezing, coughing, vomiting, and swallowing. The brainstem is divided into three sections: the midbrain (mesencephalon), the pons (metencephalon), and the medulla oblongata (myelencephalon). In case of damage, it can result in speech disorders, vestibular disturbances, dysphagia (difficulty or pain in swallowing), altered consciousness, demyelination (as in multiple sclerosis), infections, respiratory disturbances, visual problems, issues with other sensory functions, and difficulties in vasomotor control.[3, 6].

Right brain – Left brain The cerebrum is divided into two parts: the right and left hemispheres. They are connected by a bundle of fibers called the "corpus callosum," which helps transmit messages between them. Each hemisphere controls the opposite side of the body. For example, if there is a stroke on the right side of the brain, the left arm or leg may become weak or paralyzed.

In general, the left hemisphere handles speech, comprehension, math, and writing. The right hemisphere is responsible for creativity, spatial skills, art, music, and has a greater involvement in regulating negative emotions[3].

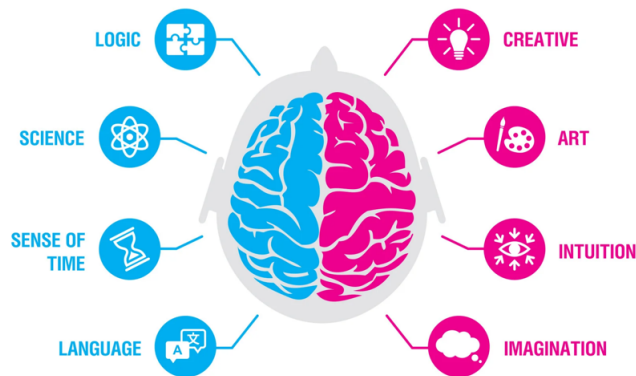


Figure 1.2: The two hemispheres of the brain are interdependently[7].

Lobes of the brain

The cerebral hemispheres have distinct fissures, which divide the brain into lobes. Each hemisphere has 4 lobes: frontal, temporal, parietal, and occipital (Figure 1.3). Each lobe may be divided into areas that serve very specific functions[3].

Frontal lobe The frontal lobe is the largest lobe in the human brain and it is located behind the forehead, specifically in the frontal lobe there is the Broca's area, which controls the muscles in the mouth used for speech. The frontal lobe is responsible for speech and language production, motor skills, understanding and reacting to the feelings of others, forming personality, maintaining a sense of motivation, and managing attention. Unfortunately, the frontal lobe is the most common area for damage in the brain that can be paralysis, Broca's Aphasia (inability to express language), inability to focus, Adynamia (reduced motivation), changes in personality, mood fluctuations, and difficulty controlling impulse[6].

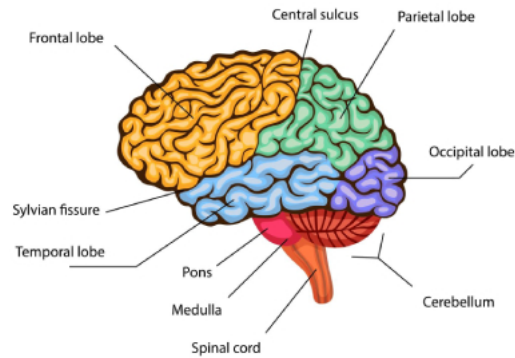


Figure 1.3: The cerebrum is divided into four lobes: frontal, parietal, occipital and temporal[8].

Parietal lobe The parietal lobe is located near the back/top of the head, behind the frontal lobe, and separated by the parieto-occipital central sulcus. It is responsible for sensations, such as touch, pressure, pain, heat, and tension, navigating and controlling the body through spatial awareness, understanding written language, and solving math problems. If damaged, there could be difficulties in distinguishing left from right, spatial disorientation, alexia (problems with reading,) dyscalculia (difficulty with mathematics), and apraxia (difficulty with complex movements)[6].

Occipital lobe The occipital lobe is in the rear part of the upper brain. The central cerebral fissure divides the 2 lobes, and the *tentorium cerebelli* separates them from the temporal lobe and cerebellum. It contains the primary visual cortex, which sends and interprets information through our eyes. It is responsible for depth perception, color determination, distance perception, face recognition, object recognition, and combining the images from both eyes into one image. If damaged, there can happen blindness and difficulty in understanding basic colors and shapes, recognizing familiar faces, detecting moving objects, recognizing words, hallucinations, Riddoch syndrome (can't see stationary objects,) and epilepsy can occur[6].

Temporal Lobe The temporal lobes is located at the bottom middle portion of the brain, behind the temples. There are structures including the auditory cortex and Wernicke's area. The auditory cortex performs basic and higher functions of hearing and Wernicke's area interprets written and spoken speech. It is responsible for long term memory, emotion, understanding and giving meaning to voices and sounds, and is an essential part of the limbic system. If damaged, these problems can occur: impaired musical skills, learning, tverbal memory, trouble with direction,

deafness, auditory hallucination, life-threatening bleeding, dyslexia, Pick's disease, and aphasia[6].

Cortex

The surface of the cerebrum is called the cortex. It looks folded due to a resemblance to hills and valleys. The cortex contains 16 billion neurons that are organized in specific layers. The nerve cell bodies color the cortex grey-brown giving it its name (gray matter). Beneath the cortex are long nerve fibers (axons) that connect brain areas to each other (white matter)[3].

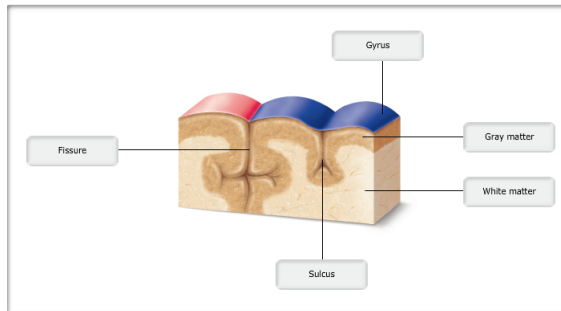


Figure 1.4: The folded appearance of the cortex[9].

Deep structures

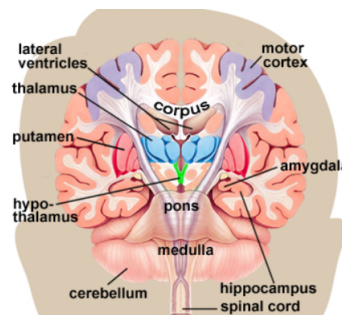


Figure 1.5: Deep structures. [3]

As said before, white matter connects different areas of the cortex to each other., acting as a sort of pathway that allows messages to travel from one gyrus to another, from one lobe to another, from one side of the brain to the other, and to structures deep in the brain.

- Hypothalamus: is located in the floor of the third ventricle and is the master control of the autonomic system. It plays a role in controlling behaviors such as hunger, thirst, sleep, and sexual response. It also regulates body temperature, blood pressure, emotions, and secretion of hormones[3].
- Pituitary gland: it is located in a small pocket of bone at the skull base called the *sella turcica*. The pituitary gland is connected to the hypothalamus of the brain by the pituitary stalk. It controls other endocrine glands in the body and secretes hormones that control sexual development, promote bone and muscle growth, and respond to stress[3].
- Pineal gland: is located behind the third ventricle. It helps regulate the body's internal clock and circadian rhythms by secreting melatonin[3].
- Thalamus: it is like a station for the information that comes and goes to the cortex. It plays a role in pain sensation, attention, alertness and memory[3].
- Basal ganglia: includes the *caudate*, *putamen* and *globus pallidus*. These nuclei work with the cerebellum to coordinate fine motions, such as fingertip movements[3].
- Limbic system: is the center of our emotions, learning, and memory. It is composed by the *cingulate gyri*, *hypothalamus*, *amygdala* (emotional reactions) and *hippocampus* (memory)[3].

Meninges

The meninges are Dura Mater, Arachnoid Mater, and Pia Mater, three layers of tissue that cover and protect the brain and spinal cord. They are arranged from the outermost layer inward.

- Dura mater: it is a tough membrane that lines the inside of the skull. It has two layers, the periosteal and meningeal dura, which are fused together. The dura also forms folds called the *falx* and *tentorium*. The falx divides the brain's hemispheres, while the tentorium separates the cerebrum from the cerebellum[3].
- Arachnoid mater: is a thin membrane that covers the entire brain, made of elastic tissue. The space between the dura and arachnoid membranes is called the subdural space[3].
- Pia mater: it hugs the surface of the brain following its folds and grooves and has many blood vessels that reach deep into the brain.

The space between the arachnoid and pia is called the subarachnoid space that contains the cerebrospinal fluid bathes and cushions the brain[3].

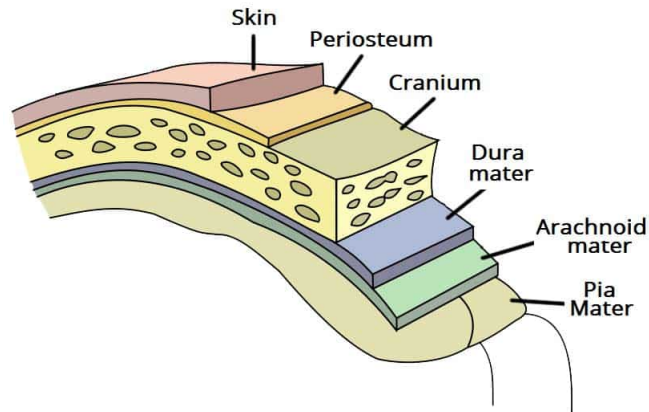


Figure 1.6: Deep structures[10].

1.2 Cells of the brain

The brain contains two types of cells: Nerve cells (neurons) and Glia cells.

1.2.1 Nerve cells and neural signals

Neurons is made of three main parts: cell body, dendrites and an axon. They transmit information through electrical and chemical signals. Neurons transmit their energy across a tiny gap called a synapse. A neuron has many arms called dendrites that act like antennae picking up messages from other nerve cells. These messages are passed to the cell body which determines if the message should be passed along. Important messages are passed to the end of the axon where sacs containing neurotransmitters open into the synapse. Neurotransmitter molecules traverse the synapse to specific receptors on the receiving nerve cell so the message can pass[3]. The information is propagated in neurons through chemical or electrical

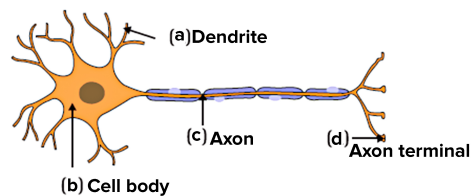


Figure 1.7: Structure of neurons[11].

signals. Neurons receive and send information through two different kinds of signals: action potential (AP) and post-synaptic potentials. APs are short electrical signals that propagate along the axons. They are the fundamental units (spikes) through which neurons interact with each other.

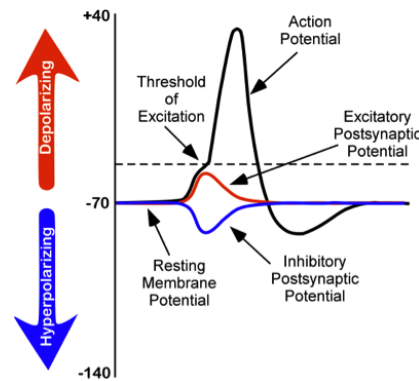


Figure 1.8: The black line in the graph represents the Action Potential curve: the stimulus from the pre-synaptic neuron depolarizes the target neuron. Sodium channels open and sodium enters the cell. This results in depolarization. At the peak, the potassium channels open and the ion exits out of the cell. The colored ones represent the Post-Synaptic Potential curves: A) positive ions (Na^+) enter the neuron, causing membrane depolarisation (red curve); B) inhibitory negative ions (Cl^-) enter the neuron, causing hyperpolarisation of the membrane hyperpolarisation (blue curve).

Post-synaptic potentials are formed when the neurotransmitter binds to the receptor on the membrane of the post-synaptic cell. They can be excitatory if they increase the probability that a post-synaptic neuron will produce an action potential, or inhibitory if they decrease this probability.

1.2.2 Glia cells

Glia cells provides neurons with nourishment, protection, and structural support. There are about 10 to 50 times more glia than nerve cells. Astrocytes regulate the blood-brain barrier and control homeostasis, neuronal defense and repair, scar formation, and also affect electrical impulses. Oligodendroglia cells create myelin that insulates axons allowing electrical messages to travel faster. Ependymal cells secrete cerebrospinal fluid (CSF) and line the ventricles. Microglia cells protect the brain and clean up dendrites [3].

1.3 Brain states and Cortical activities

The signal obtained from the scalp appears highly distorted and chaotic, as it represents the accumulation of multiple concurrent activities taking place within the brain. Additionally, external sources introduce electrical potentials into the signal, along with instrument-induced electrical activities during recording. Anything that does not originate from brain activity is classified as noise. The EEG typically exhibits an amplitude ranging from 10 to 100 microvolts. It is captured using silver or silver chloride electrodes positioned on the scalp. In order to ensure data comparability across different research groups, standardization of sampling techniques has been emphasized over the years. These standards allow for electrode placement that covers the entire skull, enabling measurements to be adjusted according to the anatomical variations among individuals.[12].

Brain waves The most frequent spectral components in EEG/MEG are:

- *Gamma rhythm* (30–100 Hz): it represents the binding of different populations of neurons to perform a certain function.
- *Beta rhythm* (12–30 Hz): it is associated with active attention and focus on the exterior world. Beta is also present during states of tension, anxiety, fear and alarm.
- *Alpha rhythm* (8–12 Hz): it is the basic rhythm amplified by closing the eyes and by relaxation.
- *Theta rhythm* (4–8 Hz): it is usually associated with drowsy, near-unconscious states, such as the threshold period just before waking or sleeping. Awake theta is associated with relaxed, meditative, and creative states.
- *Delta rhythm* (0.5–3Hz): it is associated with deep sleep or unconsciousness.
- *Gamma waves* ($\geq 40\text{Hz}$): they are not spontaneous rhythms, but are induced by sensory stimulation.
- *Sensorimotor rhythm wave* (13–15Hz): is an idle rhythm of synchronized electric brain activity, which appears over the sensorimotor cortex.

1.3.1 Voluntary and Involuntary movements

There are two types of movements that can occur: 1) *Voluntary movements* are usually self-initiated but may also be induced in response to cue signal or stimulus; 2) *Involuntary movements* are automatic, such as postural reflexes, defense responses, and other non-conscious motor activities or pathological.

This thesis is based on the distinction between voluntary and involuntary movements.

Voluntary action

Voluntary action is like as a collection of processes linked to particular brain regions (Figure 1.9). The main motor cortex (**M1**) is the most involved essential part because it is the motor and the last common pathway to carry out commands by sending them to the muscles and spinal cord. The granular frontal cortex, on the backside of the frontal lobe, contains motor regions.

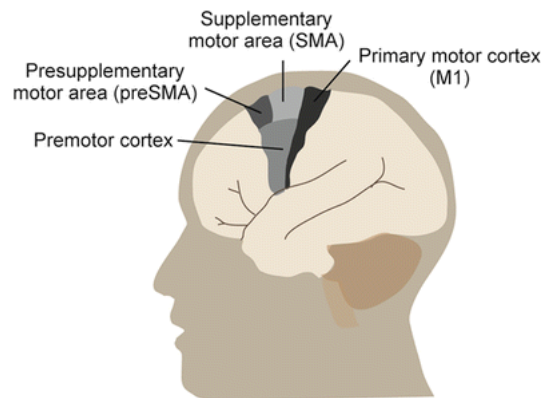


Figure 1.9: Brain activity in voluntary movements.

The pre-supplementary motor area (**pre SMA**), which in turn receives input from the pre-frontal cortex and basal ganglia, receives one input prior to reaching M1. The development of intentions, which come before and guide acts, would be based on the neural substrate that the pre-frontal areas represent.

The **readiness potentials** are generated in association with the premotor area. The information is transmitted from the motor cortex to the basal ganglia and the cerebellum that will control the motor action. It is then relayed to the motor cortex through the thalamus. Additionally, a final output is generated and sent to the parietal cortex for comparison with proprioceptive feedback. Finally, the neural signal travels from the primary motor cortex to the spinal cord and contralateral muscles, initiating the actual movement[13].

Neuroimaging studies have shown that self-paced actions activate the pre-SMA more strongly than triggered stimuli, indicating its role in voluntary movement control. The readiness potential (RP) graph demonstrates a negative slope in the pre-SMA prior to movement, suggesting a cascade of neuronal activity from the pre-SMA to the SMA and M1. Another cortical circuit, involving the posterior parietal areas, contributes to immediate sensory guidance of actions. The frontal

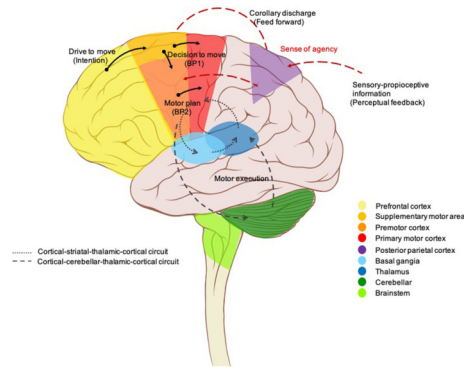


Figure 1.10: Voluntary movement is controlled by brain circuits. [14]

and posterior parietal cortices form parallel circuits for integrating sensory and motor information, with the prefrontal and cingulate regions playing crucial roles in cognitive control processes[15, 16].

In summary, the brain guides the conscious execution of voluntary movements, which start with the creation of an intention to move in the prefrontal cortex and limbic area. The subsequent programming of the necessary movement sequences involves both the presupplementary and supplementary motor areas.

Involuntary action

These movements are often reflexive or automatic, triggered by sensory stimuli or internal unconscious activity of the nervous system. These are generated by subcortical and spinal circuits in the brain: specifically, it was discovered that the sensorimotor cortex (S1-M1) is crucial to the development of focal dystonia, essential tremor, Parkinson's tremor, and cortical myoclonus. S1-M1 is the active driver of cortical myoclonus, while S1-M1 is the mediator of essential tremor and Parkinson's tremor. It is possible "negative motor areas" in the PMA and pre-SMA are involved in the control of voluntary movement and the generation of negative involuntary movements, respectively.[17]

Chapter 2

The enigma of Mind and Consciousness

The relationship between brain and consciousness is a crucial topic in cognitive science: it involves many fields as psychology, linguistics, anthropology, neuropsychology and neuroscience. The problem of explaining why any physical state is conscious rather than nonconscious is called the "hard problem of consciousness"[18]. Consciousness is hard to define because it is a subjective experience that can not be directly observed or measured. However, there are many theories that try to explain what consciousness is and how it arises. Some theories suggest that consciousness arises from complex computations in the brain, while others suggest that it emerges from the integration of information across different brain regions. Various cells and pathways of mind are engaged: has become increasingly clear and shared among researchers that consciousness is not confined to only one region of the brain. Today, this concept includes any kind of cognition, experience, feeling or perception. It can manifest as different forms: basic awareness, awareness of own awareness, or self-awareness and it can be constantly changing or remain stable.[19].

2.1 What is Consciousness?

Steven Rose, a professor of biology and the director of the Brain and Behaviour Research Group at the Open University, suggests that the concept of "Consciousness" is a continuous process that involves interaction between minds/brains and the environment. This process depends on temporary changes (like alterations in sleep/wake states) or permanent changes (like developmental factors during childhood or social influences during adulthood), that are based on various circumstances. At any given moment in an individual's life, "Consciousness" represents the overall activity of the mind/brain as it interacts with the environment. The

level of consciousness in an organism may be influenced by the quantity and quality of neuronal cells and connections, potentially involving specific types of neurons within the association cortex. [20]

In the field of medicine, Consciousness is evaluated by observing a patient's level of arousal and their ability to respond following a "range of states", starting from full alertness and comprehension, then progressing through disorientation, delirium, loss of coherent communication, and ultimately leading to the absence of response to painful stimuli.[19].

According to New Scientist, the orthodox scientific view today is that consciousness is a property of physical matter, an idea we might call physicalism or materialism. The integrated information theory suggests that consciousness arises from the ability of a system to generate integrated information. Finally, predictive processing suggests that consciousness arises from our ability to predict what we will experience based on our past experiences.

2.1.1 The brain's processing of external world information

The brain constantly receives and processes signals from our senses, allowing us to perceive and interpret the world around us. A simplified representation of how the brain processes information from the external world can be described in several steps:

1. **Sensation:** the process begins with the capture of sensory information through our sense organs, such as the eyes, ears, nose, skin, and tongue. Recently, scientists recognize other kinds of sensations, including pain, pressure, temperature, joint position, and movement.

2. **Transduction:** sensory information is converted into electrical or chemical signals that can be understood by the nervous system. This transduction occurs within the sense organs, where specialized cells called receptors convert the stimulus into nerve impulses. Different types of sensory input are combined in the brain, enabling us to make sense of a large amount of information and generate appropriate motor responses.

3. **Perception:** nerve impulses generated by the receptors are sent to the brain through sensory nerves. The brain processes this information and interprets it to create our perception of the external world. This process involves different specialized brain areas to process specific types of sensory information, such as the visual area for visual information or the auditory area for auditory information.

4. **Integration:** the various sensory information from different sense organs is integrated in the brain to create a complete and coherent picture of the external world. The brain combines information from different sensory systems to provide a unified and understandable representation of the surrounding environment.

5. **Interpretation:** the brain interprets and assigns meaning to the sensory

information based on past experiences, accumulated knowledge, and the current context. This interpretation allows the brain to identify objects, people, sounds, and other features of the environment and respond accordingly (in a voluntary or involuntary way).

2.1.2 States of consciousness

Consciousness has several dimensions that they can measure by localizing them into a specific state, characterized by a variety of electrical (voltage frequency spectrum) and physiological (blood flow, neurotransmitter concentrations) parameters in a model of the human brain.

Three dimensions of consciousness Consciousness has three main distinct measurable dimensions:

- wakefulness (physiological arousal)
- awareness (the capacity to have conscious mental experiences, such as thoughts, emotions, and sensations)
- sensory organization (how perceptions and abstract concepts form a connected conscious experience)

These three dimensions work together to shape our consciousness in every moment. For instance, when fully awake, we experience high awareness, but when the sleep begins, both wakefulness and awareness decrease[21].

A standard scale that can be used to measure consciousness levels is helpful.

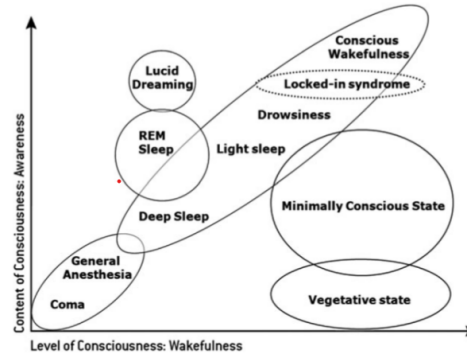


Figure 2.1: The two main components of consciousness: wakefulness and awareness. The X axis represents the Content of Consciousness, while the Y axis represents the Level of Consciousness or wakefulness[4].

The normal state of consciousness comprises either the state of wakefulness (the ability to open your eyes and have basic reflexes such as coughing), awareness (associated with more complex thought processes and is more difficult to assess), or alertness in which most human beings function while not asleep or one of the recognized stages of normal sleep from which the person can be readily awakened[22].

The abnormal state of consciousness is difficult to define; it includes: clouding of consciousness, confusional state, delirium, lethargy, obtundation, stupor, dementia, hypersomnia, vegetative state, akinetic mutism, locked-in syndrome, coma, and brain death. Many of these terms mean different things to different people, and may prove inaccurate when transmitting and recording information regarding the state of consciousness of a patient[22].

When a patient has a altered level of consciousness, three main steps are executed in order to asses the level of consciousness: 1) determining the level of consciousness itself; 2) examining the patient to identify possible causes of confusion or coma; 3) determining whether there is a focal disorder, considering the degree of dysfunction throughout the brain and involvement of cortical or brainstem structures.[22]

2.1.3 Disorders of Consciousness

A disorder of consciousness is a state where consciousness has been affected by damage to the brain. The main disorders of consciousness are:

- **Coma** When a person shows no signs of being awake and no signs of being aware; this condition leads the patient to lie with the eyes closed, totally unable to answer to external environment, voices or pain. A coma usually lasts for less than 2 to 4 weeks, during which time a person may wake up; if not, it means that the condition is evolving into a vegetative state or minimally conscious state[23].
- **Vegetative state** A vegetative state refers to a condition in which an individual is awake but lacks any indications of consciousness. Someone in a vegetative state may: 1) open their eyes, 2) alternate between periods of wakefulness and sleep, and 3) exhibit basic reflexes (such as blinking in response to a loud noise). They are also capable of independently regulating their heart rate and breathing. However, a person in a vegetative state does not display meaningful responses or any signs of emotional experience. If an individual remains in a this state for an extended period, it may be considered as:
 - a continuing vegetative state when it's been longer than 4 weeks
 - a permanent vegetative state when it's been more than 6 months if caused by a non-traumatic brain injury, or more than 12 months if caused by a

traumatic brain injury. In this case, the recovery is extremely unlikely but not impossible[23].

- **Minimally conscious state** When a person demonstrates limited or inconsistent awareness. There may be periods during which they can communicate or respond to instructions, such as moving a finger when prompted. Transitioning into a minimally conscious state can occur after being in a coma or vegetative state. While in some cases a minimally conscious state is considered a phase towards recovery, in others it becomes a permanent condition. Similar to a vegetative state, a minimally conscious state is deemed ongoing if it has persisted for more than 4 weeks. Generally, a minimally conscious state is considered permanent if it lasted for several months without any signs of improvement. The prognosis for someone believed to be in a permanently minimally conscious state is usually similar to that of an individual in a vegetative state. The longer they remain in this state, the lower the chances of recovery[23].

Why they happen Damage to the parts of the brain that are involved in consciousness can lead to disorders of consciousness. Common scenarios include: traumatic brain injury, non-traumatic brain injury (where the brain is injured because of a health condition, like a stroke), and progressive brain damage (where the brain gets worse over time, like Alzheimer’s disease)[23].

Locked-in syndrome Locked-in syndrome shares similarities with disorders of consciousness, but it is recognized and treated differently. Individuals with this syndrome are conscious and aware, but they experience complete paralysis and inability to speak. They often can just retain eye movement and communicate through blinking[23].

2.1.4 Assessment methods

These scales help healthcare professionals quantify and monitor changes in a patient’s level of consciousness over time.

Instrumental Assessment methods

The diagnosis of a state of consciousness requires a comprehensive clinical evaluation that may include neurological examinations, stimulation tests, behavioral tests, recordings of brain activity such as electroencephalography (EEG), and brain imaging techniques such as magnetic resonance imaging (MRI).

1. *Neurological examinations*: these are essential for assessing brain function and the nervous system. This may involve evaluating motor responses, reflexes,

sensory functions, and sensory integration, useful to test the integrity of the nervous system.

2. *Stimulation tests*: these are used to assess an individual's responses to sensory stimuli, that may involve auditory, visual, or tactile stimuli to evaluate whether the person demonstrates perception or response to environmental stimuli.

3. *Behavioral tests*: these are used to assess an individual's behavioral responses to stimuli and the surrounding environment. These tests may involve specific tasks that require interaction with the environment or communication through gestures or movements.

4. *Recordings of brain activity*: such as electroencephalography (EEG), allow for monitoring of the brain's electrical activity. It can be helpful in assessing the presence of epileptic activity or identifying signs of consciousness by analyzing the shape of the signal.

5. *Brain imaging*: techniques that provide detailed information about brain structure and function, such as Magnetic Resonance Imaging (MRI), that can detect abnormalities or brain lesions, or Functional Magnetic Resonance Imaging (fMRI), that can be used to map brain activity and identify regions involved in consciousness.

The combined use of these diagnostic tools can provide a comprehensive assessment of an individual's state of consciousness, helping medical professionals to make an accurate diagnosis and plan appropriate interventions or treatments.

Assessment Scales

There are several assessment scales used to evaluate the degree of consciousness in patients. Some commonly used scales include:

1. *Glasgow Coma Scale* (GCS): this is one of the most widely used scales for assessing consciousness. It evaluates three aspects: eye opening, verbal response, and motor response. The total score ranges from 3 to 15 (lower score indicating a lower level of consciousness). There is also the Pediatric Glasgow Coma Scale (PGCS), specific for pediatric patients, that is similar to the GCS.

2. *Coma Recovery Scale-Revised* (CRS-R): this scale is specifically designed to assess patients with disorders of consciousness, such as coma or vegetative state. It evaluates different behavioral responses and has scales for auditory, visual, motor, verbal, communication, and arousal functions.

3. *Full Outline of UnResponsiveness* (FOUR) *Score*: this scale assesses four categories a) eye response, b) motor response, c) brainstem reflexes, d) respiration. It is more specific compared to the GCS.

Chapter 3

EEG signals and Readiness Potential

In the previous chapter, the theme of consciousness and various disorders has been described. When dealing with patients who have a disorder of consciousness (DOC), it is crucial to obtain an accurate diagnosis as early as possible in order to develop personalized treatment plans. However, it is very difficult for clinicians to accurately diagnose patients in Coma, Vegetative State, or Minimal Conscious State: diagnostic errors are common. This thesis is based on exploring the Readiness Potential, an event-related potential (ERP) component associated with volitional movement intentions, as a way to evaluate cognitive function in unresponsive patients. This is done through electromyography (EMG) recordings during voluntary and involuntary movements following a specific experimental protocol.

In summary, understanding the RP in different types of movements could be crucial to improve the correct diagnosis of DOC, but in general it is fundamental for our understanding of motor control and consciousness, challenging traditional notions of free will and investigate the neural processes that conduct actions.

3.1 EEG signals

EEG signals, or electroencephalography signals, are electrical brain activity recorded from electrodes on the scalp. EEG is a technique to study brain function and it is especially valuable for analyzing the timing and patterns of neural activity. Extracting EEG signals from the brain is essential to obtain the reconstruction of the functional state of the mind, to gain knowledge about the mental health and consciousness.

One important aspect of EEG signals is the phenomenon called Readiness Potential (RP) that is a type of brain wave pattern that occurs before the execution

of a voluntary movement. This potential (firstly discovered by the neurophysiologist Kornhuber and Deecke in the 1960s, and used by Libet in the famous experiment that will be discussed in the following paragraphs) appears as a gradual increase in electrical activity, predominantly in the motor cortex, and can be observed in the EEG signal several hundred milliseconds before the actual movement[24].

3.1.1 EEG recordings and International 10-20 System

There are two method to record EEG: it can be non-invasively by placing electrodes on the scalp or invasively using techniques like electrocorticography, where electrodes are positioned directly on the brain cortex.

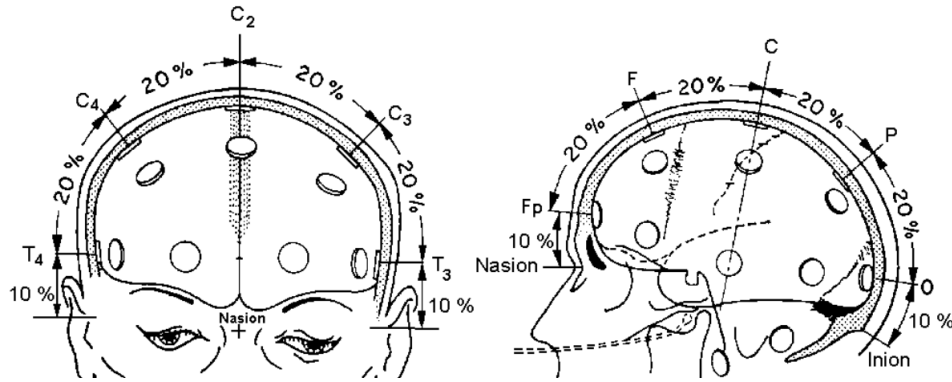


Figure 3.1: Scheme of the 10-20 System[25].

The International 10-20 system is an standardized internationally recognized method to describe and apply the location of scalp electrodes in the context of an EEG exam, (polysomnograph sleep study, or voluntary lab research) in order to ensure consistency and accuracy across different studies. The system is based on the relationship between electrode location and the underlying area of the cerebral cortex whilst ensuring that all brain regions are covered. The system provides a uniform map to cover the entire surface of the scalp into "regions" that are measured into ratios of 10 to 20 percent recommended anatomical *landmarks* measurements that allows one to map the head with precision to determine electrode placement for stimulating and recording of neuroelectric potentials[26].

These regions are labeled with letter-number combinations such as Fp, F, C, P, and O, representing frontal, central, parietal, and occipital areas (Figure 3.2). Electrodes are positioned at specific locations within these regions, with odd numbers representing electrodes on the left side and even numbers on the right side. The numbers increase from front to back: C1 is medial to C3 is medial to C5, C2 is medial to C4 is medial to C6. The system also includes additional electrodes

positioned at the midline and near the earlobes. These midline electrodes are denoted with the letter *z*, while the earlobe electrodes are labeled as A and B[26].

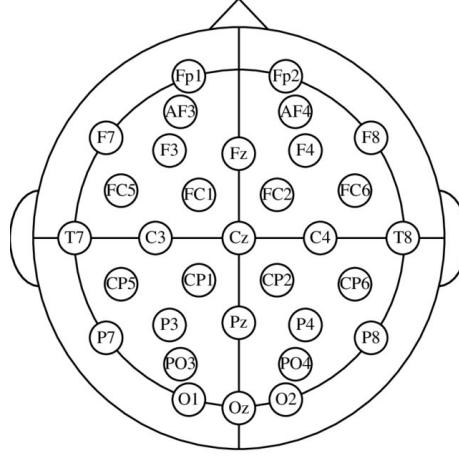


Figure 3.2: A representation of the electrode placements for different regions of the scalp according to the International 10-20 system.

F - Frontal, C - Central, T- Temporal, P - Parietal, O - Occipital, Z - Mid-line, Fp - Frontal Polar, L - Odd, R - Even, Mid-line to Lateral Numbers Increase; C1 medial to C3, C2 medial to C4; CP3 means 1/2 way in between proportional, CPi - ipsilateral to site, CPc - central lateral [26].

3.2 Readiness Potential and free will

The readiness potential (RP) is an electrical potential recorded on the scalp using EEG, specifically a type of slow negative cortical potential, which indicates neural activity of preparation for movement and precedes movement by anywhere from 0.5 to 1.5 seconds. This phenomenon was first discovered by Benjamin Libet and his colleagues in the late 1960s[24]. This electrical activity (in the motor cortex) challenges the traditional view of conscious free will and raises questions about the relationship between conscious awareness and the underlying neural activity[24], because it suggests that the brain prepares for a voluntary action even before the individual is aware of their own decision to perform it, suggesting that motor preparation processes occur at an unconscious level.

This concept is crucial and it is fundamental for this work: researchers have used Readiness Potential in various studies to investigate different aspects of motor control, decision-making, and consciousness. Studying the timing of the Readiness Potential and its characteristics, provides important insights into how the brain initiates actions and the interaction between conscious and unconscious processes.

This explains why the RP is considered an electrophysiological *marker* of motor preparation, specifically because the typical waveforms is different from involuntary movements.

3.2.1 Main features of the RP

The Readiness Potential (RP) is characterized by specific features. Some important characteristics and timing aspects of the RP are:

1. *Onset*: the RP typically emerges shortly before the execution of a voluntary movement. According to various studies, it occurs approximately 1 to 2 seconds prior to the actual movement.
2. *Location*: the RP is primarily observed in the motor cortex, specifically in the supplementary motor area (SMA) and the primary motor cortex (M1).
3. *Polarity*: the RP is a slow negative cortical potential, meaning that it manifests as a negative deflection in the recorded EEG signal[24].

3.2.2 Main Characteristics of the RP

Kornhuber and Deeke identified three distinct components in the cortical signals preceding the EMG onset, indicating movement preparation:

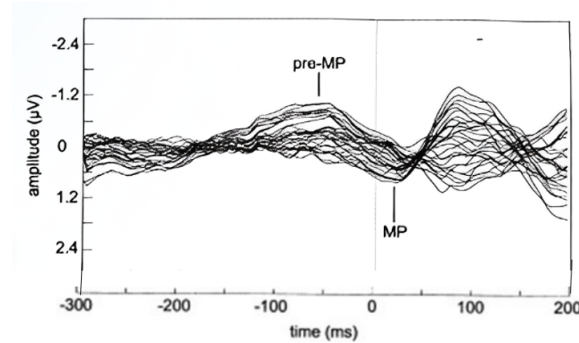


Figure 3.3: Bereitschaftspotential (BP) with the superposition of the Pre-Motor Positivity (PMP) and the Motor Potential (MP)

1. **Bereitschaftspotential** (BP): this slow cortical negativity occurs approximately 2 seconds or 1.5 seconds before the voluntary movement, and it is bilateral even for unilateral movements (strictly related to the motor intention).
2. **Pre-Motion Positivity** (PMP): this bilateral cortical positivity appears around 90-80 ms before the EMG onset; the predominant component over the hemisphere ipsilateral to the motion side.

3. **Motor Potential (MP)**: this unilateral negative potential becomes visible about 60-50 ms before the movements. It is present only in the motor cortex contralateral to the side of movement and is superimposed on the BP, along with the PMP.

Shibasaki et al. took a different approach to the Bereitschaftspotential (BP) by dividing it into two segments: the "early BP" and the "late BP". The *early BP* is associated with cognitive processes such as attention, preparatory state, movement selection, and unconscious intention to act. It exhibits bilateral symmetry and originates from the pre-supplementary motor area (pre-SMA). The *late BP*, which occurs leading up to the peak of the BP, is influenced by movement-related factors such as precision, effort, and complexity. It represents the conscious will to act and reaches its maximum amplitude over the contralateral primary motor cortex for hand movements, and at the midline for foot movements. Coles referred to this asymmetrical distribution as the Lateralized Readiness Potential (**LRP**), which was identified by subtracting the potentials recorded at C4 and C3 for left and right hand movements separately.[27].

The “early BP” and the “late BP”

Shibasaki et al. used a different method while referring to BP, dividing it into two segments: the “early BP” and the “late BP”:

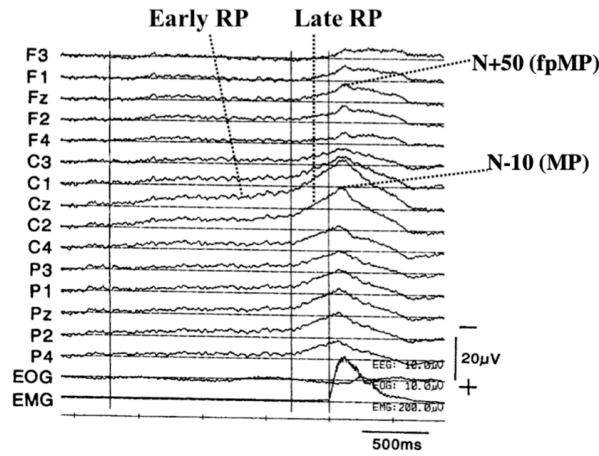


Figure 3.4: Representation of the early and late components of a RP[27].

- *early BP* represents the subconscious preparatory state to act. It is bilaterally symmetrical, originating from the pre-SMA[27];
- *late BP*, leading up to the peak of the BP, represents the conscious preparation for intended movement. It presents highest intensity over the contralateral

primary motor cortex for hand movements and at the midline for foot movements[27].

Considerations on the Bereitschaftspotential (BP) in Movement Analysis

The BP magnitude and time course are influenced by preparatory factors, movement discreteness, speed (generally, the faster the movement, the later the BP onset), and complexity. All these factors need to be studied in order to know the neurophysiological processes that lead to the motor preparation and execution.[27].

3.2.3 Movement-Related Cortical Potential (MRCP)

The RP is considered a form of a Movement-Related Cortical Potential (**MRCP**); the latter is time-locked to a movement event; its detection can be instrumental in the development of Brain Computer Interfaces (BCI). Furthermore, the MRCP can be detected even in cases where the patient lacks physical capability to execute the movement, making it a promising candidate for application in Brain-Computer Interface (BCI) systems.[28].

The MRCP waveform typically consists of several components that reflect different stages of motor processing and execution. These components (Figure 3.5) are resumed into two main components that are: 1) readiness potential (RP) 2) movement-monitoring potential (MMP). As explained before, RP is a negative cortical potential which has two fundamental parts before the movement onset: Negative Slope (NS), called ‘early BP’ that begins about 1~2s before voluntary movement onset; ‘late BP’ or ‘motor potential’ (MP) about 1s before the movement onset. After the movement onset, MMP, that is a positive cortical potential (which reflected an outcome of the motor process) increases deflection for coming back to initiate state[29].

3.2.4 Libet’s Experiment

In the early 1980s, Benjamin Libet conducted experiments in order to investigate the role of consciousness in motor action generation, to detect the relationship between the readiness potential (RP) and the actual movement. This famous experiment suggests that brains start making voluntary movements before consciously decide to move. This raises controversies and doubts about the effectiveness of our willpower and free will. The Libet experiment was influenced by the findings in the 1960s that revealed a gradual increase in electrical activity over the motor cortex before making a voluntary movement, beginning as much as a second earlier before individuals consciously initiate voluntary movements[30]. The study was

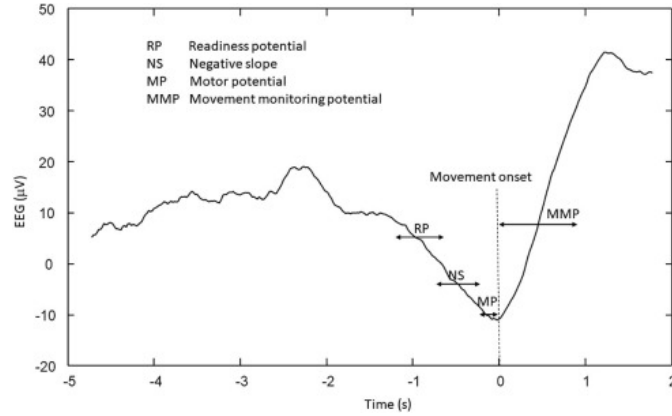


Figure 3.5: MRCP waveform components[28]. Movement onset is defined at the time point 0s. The MRCP comprises RP and MMP sections. (In RP section, (-2 ~ -1)s is early BP, (-1 ~ 0)s is late BP, (-0.5 ~ 0)s is motor potential (MP), and after movement onset, (0 ~ 1)s is MMP section) [29]

done using a clock with a rapidly rotating dot, where subjects had to note the dot's position when they became consciously aware of the decision to move a finger. Scalp EEG and finger EMG were used to monitor brain activity and finger flexion during the experiment. The results showed a pre-movement build-up of electrical potential known as readiness potential (RP), starting approximately 550 ms before the movement. Surprisingly, the conscious awareness of the decision to move emerged only 200 ms before the actual movement (Figure 3.6), creating a time lag of around 350 ms between the initial rise of RP and conscious awareness. Libet and colleagues interpreted the early rise in RP as an unconscious neuronal preparation for voluntary action [31, 30]. Based on their findings, researchers concluded that conscious decisions take too long to initiate actions. As a result, they inferred that voluntary acts may originate from unconscious processes in the brain rather than conscious intentions. This interpretation raised doubts about the reliability of our intuitive perception of conscious will, indicating that it could potentially be an illusion. As said before, these findings have greatly influenced the prevailing belief that both conscious "will" and subsequent actions are caused by prior neural activity. [30, 32].

The presence of RP is considered indicative of voluntary intention to move because of this experiment, and consequently the absence of this potential suggests the absence of voluntary action. Differentiating between voluntary and involuntary movements could potentially serve as a method to determine the presence of consciousness[33].

All these concepts are presented and explained in order to clarify why this

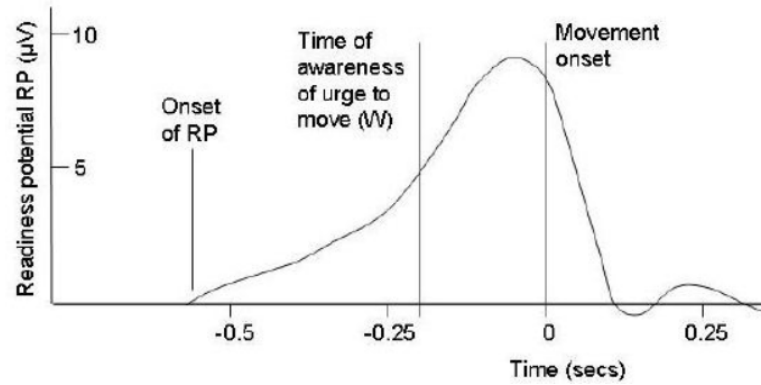


Figure 3.6: Graph showing the results of Libet's experiment [30].

thesis focuses on the RP, with the aim of creating an algorithm that can detect the difference between movements in non-responsive patients, demonstrating the presence or absence of consciousness, thus assisting doctors in diagnosing disorders of consciousness.

Chapter 4

Readiness Potential: Experimental Procedures and Techniques

The primary focus of this project is to obtain clear brain signals through meticulous pre-processing, establish a neural response template under various conditions, and classify the subject's cerebral state based on the resulting waveform.

The initial stage involves recording biosignals from participants. This experimental phase took place at *Centro Puzzle* in Turin and involved recruiting healthy volunteers from both genders, ranging in age from 18 to 65 years. Galileo NT and its software were used to record and display the potentials on a screen[31][34].

The study required three distinct types of biopotentials:

- **Electroencephalography** (EEG) signals were collected using an EEG cap that had either 4, 8, or 32 passive Ag/AgCl electrodes, depending on the specific protocol being used. The EEG datasets were recorded at a sampling frequency of 512 Hz.
- **Electrooculography** (EOG) signals were obtained by attaching two adhesive electrodes above and below each eye. This was done to enhance the removal of ocular artifacts. Please note that EOG signals were only recorded in the last protocol.
- **Electromyography** (EMG) signals were captured by placing adhesive electrodes near the muscles from which the electrical activity was to be recorded. In the case of the last protocol, the electrodes were positioned on the front and back of the second phalanx of the index finger, as the task involved lifting the right index finger.

4.1 Tasks and Protocol

Over the years, various protocols have been implemented, each involving distinct tasks and experimental configurations.

4.1.1 2012 - 2015 Protocol

The computer screen displays a timer, and the participant is instructed to flex their right index finger every 10 seconds for a duration of 6 minutes. This process generates 40 epochs that can be utilized for evaluating the Event-Related Potentials (ERPs). Additionally, several alternative tests were conducted:

- *Using the mouse*: the movement is obtained by clicking the mouse button;
- *Using both hands*: the participant is instructed to use both hands, with the experimenter indicating which hand to use on each occasion;
- *Short trials*: the experiment follows the standard procedure but with shorter trial durations of 5 seconds. The goal is to validate the hypothesis of the absence of free will, where the subject becomes aware of the intended action only after the brain has already prepared for it, as observed in the Libet experiment;
- *Bimanual*: the experiment involves simultaneous movement of both hands. This task is useful to detect the cognitive conditions of patients with anosognosia for hemiplegia, a temporary condition that can occur in individuals where stroke has damaged the motor area of the right hemisphere of the brain. In these patients, there is paralysis on the left side of the body, but they are unaware of it and confidently claim to have no problem and can move both the paralyzed arm and leg correctly. To capture the EMG signal from these patients who are only paralyzed on the left side of the body, they are asked to move both hands in the "Bimanual" task. The unaffected hand performs the task, allowing the signal to be recorded, while the paralyzed hand is imagined to be moving by the patient, who genuinely believes they are performing the movement. It's important to note that patients with this condition have complete right-sided impairment. If the stroke affects the left hemisphere, which also compromises the language center, they are unable to express their level of awareness regarding the paralysis[31][34].

4.1.2 2015 - 2018 Protocol

The participant watches a clock displayed on a screen and is instructed to perform a specific movement every 10 seconds for a duration of 6 minutes and 40 seconds.

The movements can include flexing the index finger, voluntary movement of the foot or leg, coordinated movement of the hand and leg, or the patellar reflex of the knee. In some cases, blindfolded participants are guided by an operator to perform the tasks[31][34].

4.1.3 2018 Protocol

The participant moves finger while the EMG signal is recorded. Neurologically healthy volunteers are assigned three tasks in each test session: - Voluntary task: The subject is required to move the index finger within a specific time window of 10-13 seconds, initiated by a beep. This task sets a specific time limit for the subject to complete an action while also giving them the freedom to choose their own course of action, which can differ from person to person and from one attempt to another. - Semi-voluntary task: Similar to the previous task, the subject repeats the index finger movement upon hearing the beep, but without the voluntary element. - Involuntary task: In this task, the subject's patellar reflex is stimulated by a gavel hitting the tendon. Only the experimenter wearing headphones can hear the acoustic signal, ensuring that the subject cannot predict the exact moment of the stimulus. Each experimental session includes 40 repetitions for each task, with the acoustic signal randomized to prevent subject adaptation[31][34].

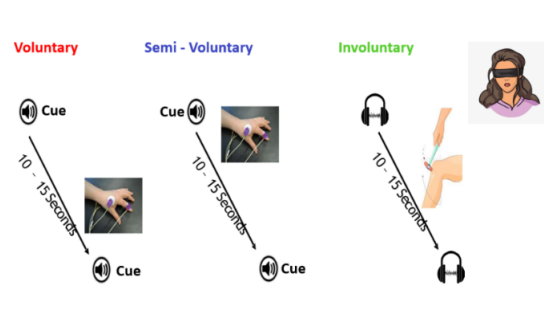


Figure 4.1: 2018 Protocol for EEG, EOG and EMG recordings.

4.2 Dataset classification

The collected data were categorized based on subject information, acquisition type and mode, and the specific instrumentation utilized. In this particular protocol, the inclusion of Labjack, a USB-based measurement and automation device with digital input/output capabilities, facilitated the initiation of movement while connected to a Data Acquisition System (DAQ). The classification of the recorded data involved assessing the quality of both Labjack and EMG signals on a scale of 0

to 3, considering factors such as signal variability and noise. Each dataset was assigned a 45-character string composed of various elements:

- **8 characters** the subject's information was anonymized by utilizing the first letter of their name, the first letter of their surname, the last digit of the recording year, the last two digits of their year of birth, the month of registration, and a binary indicator (0/1) denoting their gender.
- **5 characters** the type of EEG electrode mounting can be identified by the following abbreviations: 32C18 refers to 32 channels, while OBE12 indicates the use of bridge electrodes.
- **4 characters** the protocol used can be identified by the following abbreviations: A18C represents the 2018 protocol, B18C represents the 2015-2018 protocol, and VOPC stands for Very Old Protocol, indicating the protocol used from 2012 to 2015.
- **3 characters** the condition of the subject during the experiment is described as either blindfolded (FOL) or not blindfolded (UNF).
- **5 characters** the type of task performed by the subject is identified as either voluntary (VOL18), semivoluntary (SEM18), or involuntary (INV18).
- **4 characters** the tasks performed by the subject are classified as follows: right forefinger (RFOF), left forefinger (LFOF), bimanual forefinger (BFOF), mouse click with the right hand (RMOU), right leg (RLEG), left leg (LLEG), right foot (RFOO), left foot (LFOO), right hand and leg (RHLE), and left hand and leg (LHLE).
- **4 characters** the EMG channels used for recording are labeled as EMG1 for channel 1, EMG2 for channel 2, and EMGX for channels without a specific number.
- **4 characters** the quality of the EMG signal is classified using the notation E0/E1/E2/E3, while the Labjack signal quality is classified as L0/L1/L2/L3 [31][34].

4.3 Experimental setup

The data recording has been conducted using the following instrumentation: - *Data Acquisition device*: Galileo Suite, EB Neuro with Brain Explorer amplifiers. - *Galileo Software* for processing and displaying the EEG traces. - *Stimulation system*: Labjack and OpenSesame software for the acoustic signal. - *Synchronization system*:



Figure 4.2: Experimental setup[34].

Labjack and photocoupler circuit. - *Recording tools*: EEG cap, adhesive electrodes (4 for EOG signal and 2 for EMG signal), ground electrode for EMG (placed on the wrist for voluntary and semi-voluntary tasks, and on the ankle for involuntary tasks), and two earlobe reference electrodes for EEG. - *Additional accessories*: conductive paste TEN20, abrasive paste NUPREP, conductive EEG gel, and a syringe with a blunt needle. The subject is on a chair which ensure that their feet do not touch the floor. One computer is dedicated to running the *OpenSesame* software, which initiates the task and emits the acoustic signal. Another computer is connected to the EEG cap and runs the *Galileo* software, which allows for the visualization, processing, and exporting of the EEG signal. The subject is positioned behind the first computer, with the computer on their left side [31][34]. The electrode placement begins with the positioning of the EMG and EOG sensors. Then, the earlobe and wrist (or ankle) electrodes are attached using TEN20 conductive paste. Following that, the EEG cap is placed, with the Cz electrode positioned in the middle between the *nasion*, *inion*, and the two earlobes. The skin is cleaned using the abrasive paste to remove sebum and dead cells. Subsequently, the cap is filled with conductive gel using a blunt needle to enhance signal conduction and improve adhesion to the skin [31][34]. The conductive EEG gel serves two purposes:

1. It improves signal conduction by reducing electrode impedance, ensuring a good coupling between the electrodes and the skin. Prior to recording the EEG signal, the experimenter must verify that the impedance of the electrodes does not exceed a specified threshold, typically set at $10\text{ k}\Omega$. Lower impedance leads to better signal quality and reduces noise.
2. It enhances adhesion between the electrodes and the skin, preventing detachment issues caused by movement. The gel helps to maintain a stable

connection throughout the recording session, ensuring reliable and continuous signal acquisition.

By addressing both signal conduction and adhesion concerns, the conductive EEG gel plays a vital role in obtaining high-quality EEG recordings during the experiment [31].

Once the biosignals have been acquired and made compatible with the Matlab environment, they undergo meticulous processing to enhance their quality and remove any unwanted elements that may interfere with subsequent analysis and classification. For the purpose of analyzing these signals, the project utilizes the EEGLAB toolbox, a powerful tool in EEG signal processing. Specifically, the MRCPLAB plugin, developed specifically for this project, is employed [31][34].

4.4 Signal Processing Software for Data Analysis

The signal processing tasks in this project are performed using Matlab, an important programming language and environment for scientific computing. Matlab provides a comprehensive set of functions and tools for signal processing, data analysis, and visualization.

Within Matlab, the project utilizes the EEGLAB toolbox, which is specifically designed for processing and analyzing EEG signals. EEGLAB offers advanced techniques for filtering, artifact removal, event-related potential analysis, and other signal processing tasks relevant to EEG data.

4.4.1 EEGLAB

EEGLAB is an interactive toolbox developed by the *Swartz Center* for Computational Neuroscience (SCCN) that operates within the MATLAB environment. It is specifically designed for processing and analyzing various types of electrophysiological signals, including EEG (electroencephalography) and MEG (magnetoencephalography).

Thanks to the user-friendly graphical interface (GUI), this toolbox allows users to perform a set of operations on EEG and other electrophysiological signals in both the time and frequency domains in order to model and visualize event-related brain dynamics. This enables researchers to investigate and understand the brain's response to specific events or stimuli. Additionally, EEGLAB supports the development and integration of new methods and algorithms through the creation of plug-in functions, promoting collaboration and innovation among researchers [31][34].

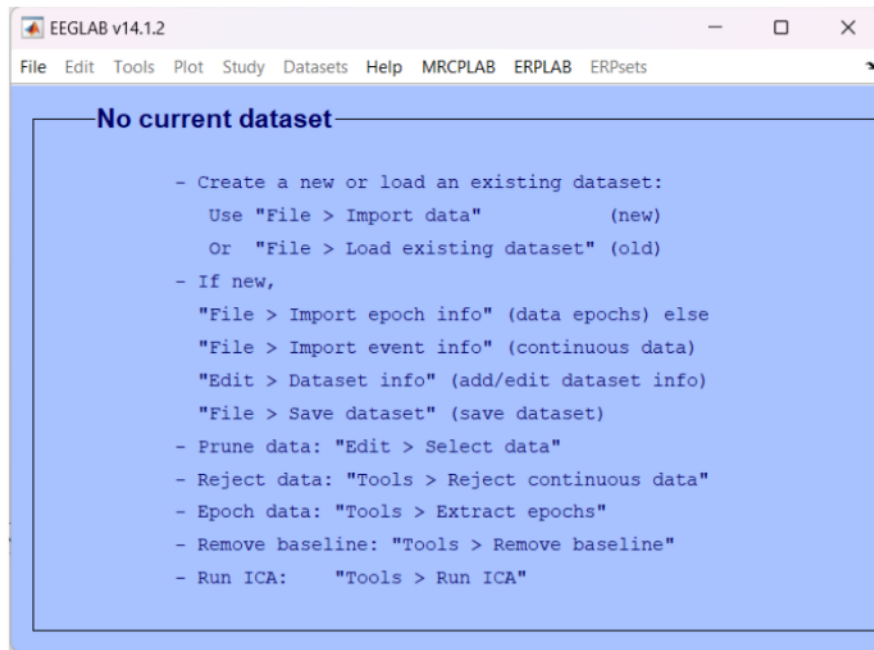


Figure 4.3: EEGLAB GUI with MRCPLAB plug-in.

4.4.2 MRCPLAB

MRCPLAB is a specialized plug-in for EEGLAB that has been developed specifically for this project. It builds upon the functionality provided by EEGLAB while introducing new functions that are tailored to the project's requirements.

When running EEGLAB, MRCPLAB can be accessed from the menu, offering the following functions:

1. *Import/Save Data:*

- Import from ASCII file: Processes ASCII file data by resampling and filtering EEG, EMG, and EOG signals, evaluating events, initializing the EEG structure with the necessary data, and creating a .set file for faster subsequent uploads.
- Import from .set file: Imports a previously processed EEG structure from an ASCII file.

2. *EEG Channel Operation:*

- Channel data (scroll): Opens a window to visualize the EEG and onsets obtained from the EMG.

- Seek noisy channels: Helps evaluate and identify bad channels that need to be rejected for accurate results.
 - Select or reject data: Allows the rejection of bad channels.
 - Artifact Correction: Detects and corrects artifacts using Independent Component Analysis (ICA).
 - Interpolate electrodes: Interpolates previously rejected channels by considering the closest electrodes.
3. *Spatial Filter*: Applies different types of spatial filters, such as Single Input Spatial Filter (SISF), Single Lead Spatial Filter (SLSF), and Large Lead Spatial Filter (LLSF), with a variable number of electrodes and coefficients. SNR-dependent coefficients can only be used if SNR has been estimated beforehand; otherwise, spatial filtering can be applied with equal coefficients.
4. *Epoch Operation*:
- Epoch and filter: Creates epochs based on the onsets evaluated through the EMG.
 - Jitter compensation: Allows the application of different methods for delay correction, including RIDE (Residue Iteration Decomposition) and Woody's method for aligning epochs.
 - ERP and SNR evaluation: Calculates the Event-Related Potential (ERP) and corresponding Signal-to-Noise Ratio (SNR) through averaging.
 - ERP viewer: Plots the ERP and SNR.
5. *Topographies and Energy Considerations*: Plots topographies and provides energy considerations that are useful for calculating LRP (Lateralized Readiness Potential).

These functions provided by MRCPLAB enhance the capabilities of EEGLAB, enabling specialized processing and analysis of EEG data for the specific requirements of the project [31][34].

Chapter 5

Classification Project: State-of-the-Art and Machine Learning

5.1 State of the art

This thesis work is a continuation of the Master's thesis in Biomedical Engineering from Politecnico di Torino of Alessandra Zanetta. Our thesis are parts of a larger project that aims to investigate the level of consciousness in non-responsive patients (Vegetative State or Minimal Conscious State). The Zanetta's thesis describes the development of a Brain Computer Interface (BCI) that uses Readiness Potentials (RP), which arise just before the start of a voluntary movement as a marker of presence of consciousness. The aim of her thesis was to create a robust machine learning algorithm that can predict whether a movement is voluntary or not[32]. The results achieved are resumed in the following table:

Classification	Specificity	Sensitivity
Linear SVM	73.3%	63.3%
Cubic SVM	73.3%	80%
K-NN	93.3%	73.3%
Decision Tree	73.3%	53.3%

Table 5.1: Table summarizing the performance of the Zanetta's classification[32].

5.2 Machine learning

Machine Learning was defined in the 1950s by AI pioneer Arthur Samuel as “the field of study that gives computers the ability to learn without explicitly being programmed” [35].

5.2.1 Overview of Essential Machine Learning Techniques

There are several techniques commonly used in machine learning:

1. *Supervised machine learning*: this category involves training algorithms using labeled datasets to classify data, avoiding overfitting or underfitting through cross-validation. Supervised learning is widely used to solve real-world problems. Common methods in this category could be neural networks, naïve Bayes, linear regression, logistic regression, random forest, and support vector machine (SVM)[36], techniques used in this work.
2. *Unsupervised machine learning*: this category involves training algorithms using cluster unlabeled datasets, discovering hidden patterns and groupings in the data without human intervention. An important example is the principal component analysis (PCA) that can also reduce the number of features in a model through dimensionality reduction. Common algorithms in this category are neural networks, k-means clustering, and probabilistic clustering methods[36].
3. *Semi-supervised learning*: it is a mix of supervised and unsupervised learning. It uses a smaller labeled data set to guide the classification and feature extraction process from a larger unlabeled data set. This approach is useful when there is an insufficient labeled data for a traditional supervised learning algorithm[36].

5.2.2 Machine Learning in Brain-Computer Interfaces (BCI)

Brain-Computer Interface (BCI) technology is an emerging field that integrates human cognition with machines by providing a direct communication between brain and control external devices, thus surpassing the limitations of the human body and traditional tools. This interaction is bidirectional: the external devices provide continuous feedback information to the brain, allowing the brain to adjust its control strategies in real-time. This type of interface between the brain and the outside world is based on the conversion of brain signals into output commands to execute a specific task. This technology holds vast possibilities for applications such as health monitoring and advanced human-computer interaction[37].

5.2.3 The Overall Architecture of BCI

Unlike traditional methods that rely on peripheral nerves and muscles for signal transmission, BCI establishes a direct connection between the brain and peripheral devices using EEG signals, as described before. The user's intentions are captured through EEG signals, which are then converted into output formats[38].

A typical BCI system consists of four main components: *signal acquisition* from the biological brain, *signal processing*, *control device* (identified biological intentions are converted into control signals, enabling direct control of the peripheral device) and *feedback link*[38].

The signal processing component consists of three stages: preprocessing, feature extraction, and feature classification to predict the intentions of the user. The BCI system is capable of recognizing specific patterns within the brain signals[38]. An illustrative representation of the BCI system architecture is shown in Figure 5.1.

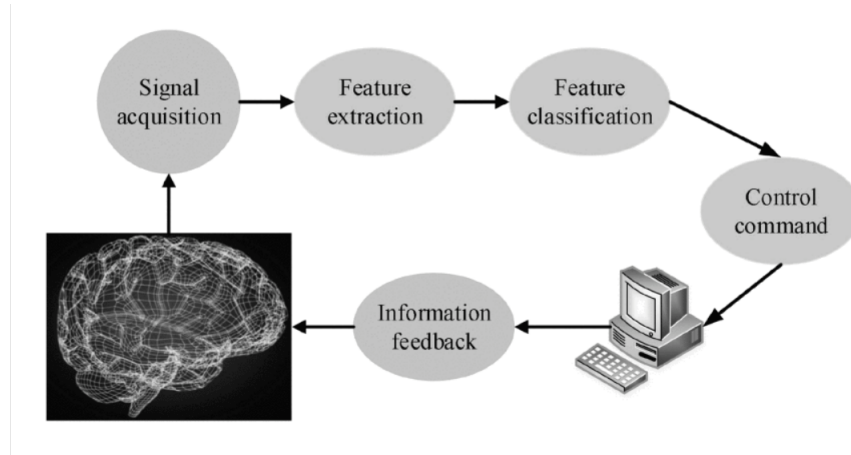


Figure 5.1: General BCI system architecture[38].

Brain-Computer Interface (BCI) can be categorized into three distinct ways of information transmission: from the biological brain to the peripheral device, from the peripheral device to the biological brain, and from one biological brain to another biological brain[38].

5.3 Classification Methods Involved

The classifiers used in this study are: Support Vector Machine (linear SVM and cubic SVM), K-Nearest Neighbors (K-NN) and the Decision Tree (DT).

5.3.1 Support Vector Machine

The goal of the Support Vector Machine (SVM) algorithm is to identify a hyperplane in an N-dimensional space (where N represents the number of features) that effectively separates the data points into different classes. There are multiple potential hyperplanes that can be chosen to separate the two classes of data points: the best hyperplane is one that maximizes the distance between subjects of the two classes [39]. In **linear SVM**, the algorithm is suitable when the data points

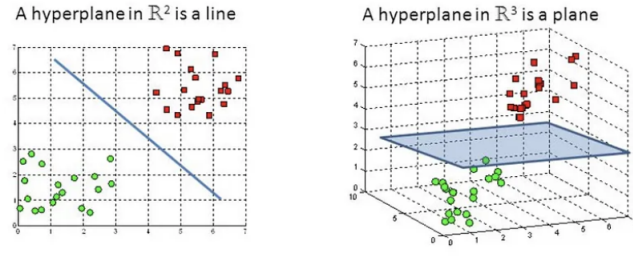


Figure 5.2: Hyper-planes in 2D and 3D feature space[39].

are perfectly linearly separable, meaning they can be accurately classified into two classes using a single straight line (in two-dimensional space)[40].

On the other hand, **non-linear SVM** is used when the data points are not linearly separable. This occurs when a straight line (in two-dimensional space) cannot effectively separate the data into two distinct classes; it consists of converting this lower dimension space to a higher dimension space using some quadratic functions to find a decision boundary that clearly divides the data points. In such cases, advanced techniques like *kernel* tricks are employed (specifically in this thesis)[40], for more accurate classification.

In fact, in most real-world applications, data points are not linearly separable, making non-linear SVM with kernel tricks a common choice to handle complex classification tasks. By utilizing the kernel, non-linear SVM can effectively classify data points that cannot be separated by a straight line in their original feature space.

Polynomial kernel for cubic SVM In this study, also a Cubic SVM was used. SVM using a polynomial kernel of degree 3 refers to the specific choice of a polynomial function with a degree of 3 as the kernel for the support vector machine algorithm. It is defined as:

$$K(x, y) = (\alpha \cdot x^T y + c)^3$$

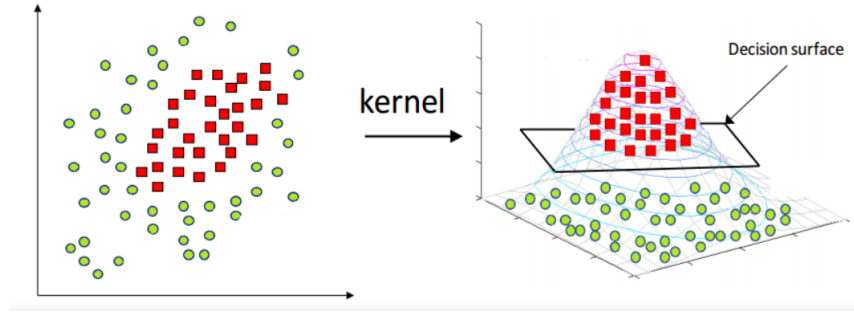


Figure 5.3: Example of a Dataset for which it is wise to use the Kernel[41]

The kernel function computes the cubic transformation of the dot product between the input data points: the variables x and y represent the input data points, α is a scaling factor, and c is an offset (free parameter)[42].

5.3.2 K-Nearest Neighbors

The k-nearest neighbors algorithm (k-NN) is a Supervised Learning Classifier that operates on the principle of proximity: it determines the class membership of a new data point by examining the classes of its k nearest neighbors, because it is based on the idea that objects with similar features belong to the same class. It is a non-parametric method, meaning that it does not make any assumptions about the data distribution. Instead, it relies on the notion that data with similar characteristics need to be located close to each other in the feature space[43].

The k-NN algorithm can be described using the following steps (Figure 5.4):

1. Determine the value of K , which represents the number of neighbors to consider.
2. Calculate the Euclidean distance between the new data point and all other data points in the dataset.
3. Select the K data points with the shortest Euclidean distance as the nearest neighbors.
4. Count the number of data points in each category (or class) among the selected K neighbors.
5. Assign the new data point to the category with the highest count among the neighbors.
6. The k-NN model is now trained and ready for classification or prediction tasks[43].

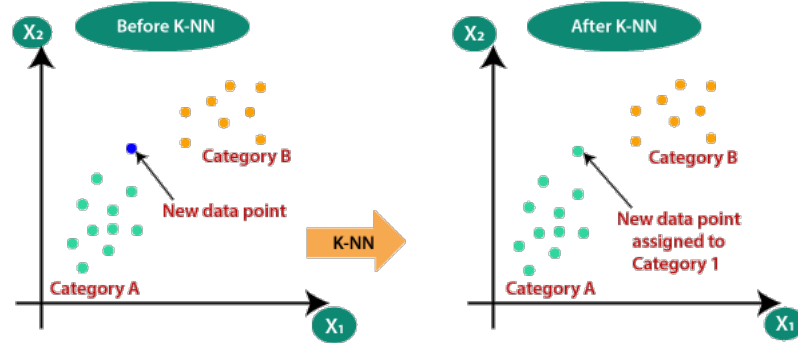


Figure 5.4: Example of a kNN application[43]

5.3.3 Decision Tree

The decision tree is a Supervised Learning classifier with a tree-like structure, where each node can be either a leaf node or an internal node: if it is a leaf node, it represents the assigned class value for the instance. If it is an internal node, it specifies the attribute test to be performed. For each possible attribute value in a test, the algorithm creates a branch and its corresponding subtree [44]. The main focus of the decision tree algorithm is to choose the most useful attributes to be tested at each internal node of the tree using a top-down strategy, which involves a greedy search for attributes without revisiting the previous choices[44].

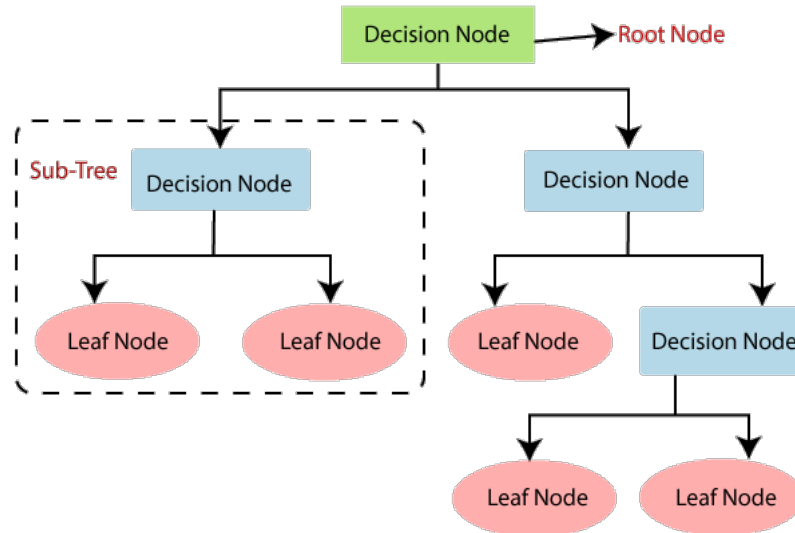


Figure 5.5: The general structure of a decision tree[44].

Decision Tree Terminologies

- **Root Node:** the starting point of the decision tree. It represents the entire dataset and serves as the initial decision-making point, which leads to further divisions.
- **Leaf Node:** the terminal nodes of the decision tree. They represent the final outcome or prediction, and no further splitting or classification is performed beyond these nodes.
- **Splitting:** the process of dividing the root node or decision node into sub-nodes based on specific conditions or attributes.
- **Branch/Sub Tree:** when a node is split into multiple sub-nodes. Each sub-node represents a possible path or outcome based on the attribute condition.

How does the Decision Tree algorithm Work?

The steps for building the tree can be summarized as follows:

1. Begin with the root node, denoted as S , which contains the complete dataset.
2. Determine the best attribute to split the dataset.
3. Divide the dataset into subsets based on the possible values of the selected attribute.
4. Create a decision tree node corresponding to the selected attribute.
5. Recursively repeat steps 2 to 4 for each subset of the dataset, creating new decision trees.
6. Continue this process until a stopping condition is met, such as reaching a stage where further classification is not possible. These final nodes are referred to as leaf nodes[44].

Chapter 6

Method and Project Development

This thesis aims to classify signals from a selected dataset, that were processed before classification with the new EEGLAB plugin and the old EEGLAB plugin. The objective is to evaluate the performance of the updated and improved plug-in to determine if the signals are classified more accurately in the new version, which includes new and improved preprocessing steps.

The project can be resumed in four major steps: data preprocessing, feature extraction, feature selection and classification. These steps will be described in detail.

Analyzed subjects

The set of data for the classification is composed by 9 subjects from involuntary and 8 subjects from voluntary task groups; these were chosen based on data acquisition process quality. The EEG signals are from the 2015 and 2018 protocols.

6.1 Dataset Preprocessing

Various iterations of preprocessing steps have been tried in order to identify the optimal preprocessing pipeline that cleans the EEG signal, so every adopted step is chosen in order to increase the accuracy and quality of results. The first step is loading of the dataset to analyze. The operations performed (with the new EEGLAB plug-in) are as follows:

Seek noisy channels

The "*Seek Noisy Channels*" function in EEGLAB detects noisy channel through a series of statistical and visual checks on each channel to determine its noise level. It calculates measures such as signal variance, kurtosis, and spectral power, to assess the level of noise present in each channel. Once the analysis is complete, the function provides a report with the channels with high noise levels. Thanks to this report, it is possible to see the list of "bad" channels that contain noise or artifacts. [34, 16, 31].

Select or reject data

It allows to choose or delete specific portions of data in EEG dataset, but in this case, the "*Select or Reject Data*" option is used to remove channels that have been identified as noisy in the previous analysis. This allows to focus on the remaining channels that provide more reliable and meaningful data for the analysis. [34, 16, 31].

Artifact correction

Artifacts are undesired phenomena that can contaminate EEG signals and impact the accuracy and interpretation of the analysis, that can be 1) muscle artifacts, caused by muscle activity, such as contractions or involuntary movements of cranial or facial muscles; 2) eye artifact, such as rapid eye movements or slow eye movements; 3) external interference, like electrical noise by electronic devices; 4) baseline artifacts, resulting from fluctuations in the EEG signal's baseline, such as signal drift or baseline shifts [34, 16, 31].

Interpolate electrodes

This function consists in using previously eliminated channels (that were noisy) for filling in missing or imperfect electrode channels based on the information from the excluded channels. This approach is based on the concept that the excluded channels contain important information that can contribute to the study [34, 16, 31].

Spatial filtering

It is useful for increasing signal quality by reducing noise and artifacts. It is important when distinguishing between voluntary and involuntary signals. By isolating the desired brain activity and minimizing interference, *Spatial Filtering* improves the accuracy of classification and allows the identification of distinct

patterns associated with voluntary and involuntary states. In this specific case, the **SLSF** filter with 8 electrodes was used. [45].

6.1.1 Residue Iteration Decomposition (RIDE)

The Residue Iteration Decomposition (RIDE) method, developed by Ouyang, Sommer, and Zhou, addresses trial-to-trial latency variability in event-related brain potentials (ERPs). It decomposes ERPs into component clusters with different latency variability and re-synchronizes them into a reconstructed ERP. RIDE combines event markers and estimated latencies for component extraction, preventing distortions and enabling targeted analysis of specific sub-processes within defined time windows. RIDE is a convenient and informative method for decomposing ERPs, providing single trial analysis, and facilitating the study of brain-behavior relationships using EEG data. It effectively mitigates the smearing effect caused by trial-to-trial variability in averaged ERPs, preserving temporal precision and enhancing waveform clarity for more accurate analysis of neural activity and subtle amplitude effects [46].

The impact of latency variability on ERPs

ERPs are typically obtained by averaging multiple EEG epochs, assuming that the signal of interest remains consistent across trials while background noise varies independently. However, ERP components can exhibit trial-to-trial latency variability, which has significant implications for condition effects.[47].

The first consequence of latency variability is that it blurs the waveforms, resulting in attenuated ERP component amplitudes and reduced amplitude differences between conditions. This reduction in amplitude differences can make experimental effects less discernible and diminish the statistical significance of findings (Figure 6.1, first case)[47].

The second consequence is that different levels of latency variability across conditions can mimic amplitude effects in ERPs. Even if conditions have identical amplitudes, variations in single trial latencies can create artificial amplitude differences in the average ERP, leading to erroneous interpretations. These amplitude differences may be mistakenly attributed to differences in underlying neural activity rather than to differences in temporal variability across trials (Figure 6.1, second case)[47].

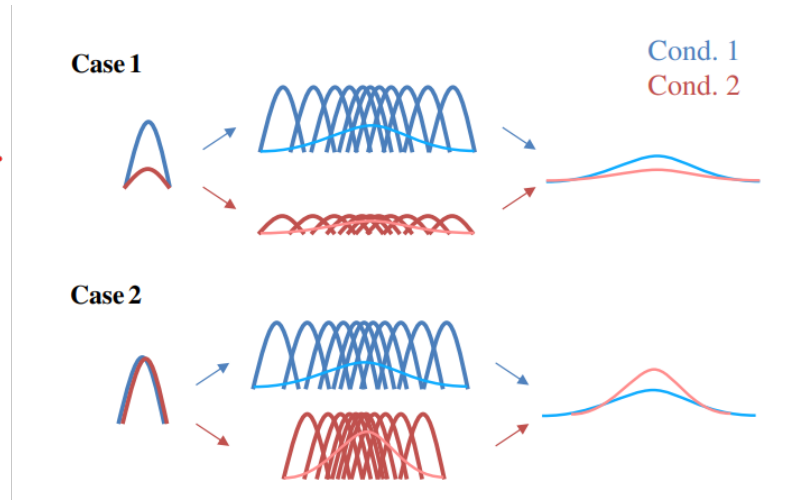


Figure 6.1: Trial-to-trial latency variability in ERP components can lead to two consequences. In Case 1, it blurs the waveforms and attenuates amplitude differences between conditions. In Case 2, it can mimic amplitude differences between conditions even when the underlying amplitudes are identical. [47].

6.1.2 How does RIDE overcome the problem of Jitter in ERPs?

According to the article "Reconstructing ERP amplitude effects after compensating for trial-to-trial latency jitter: A solution based on a novel application of residue iteration decomposition" [46], RIDE overcomes several limitations of conventional approaches for compensating trial-to-trial latency jitter in ERPs. Here are the advantages of RIDE:

1. Decomposition into component clusters: this allows for a more accurate representation of the underlying neural activity.
2. Reconstructed ERP: this process helps to mitigate the smearing effect caused by trial-to-trial variability and increases the quality of the ERP waveforms.
3. Combination of event markers and latencies: this approach improves the accuracy of component extraction.
4. Distortion prevention: this leads to more accurate and reliable decomposition of ERPs.
5. Targeted analysis: this targeted analysis increases the identification and analysis of specific neural processes.

6.1.3 Understanding the RIDE Flowchart

RIDE generally divides the ERP into three distinct component clusters: the stimulus-locked component cluster S, the response-locked component cluster R, and the central component cluster C, which does not align with either the stimulus or the response but exhibits noticeable latency variability that can be identified through template matching [47].

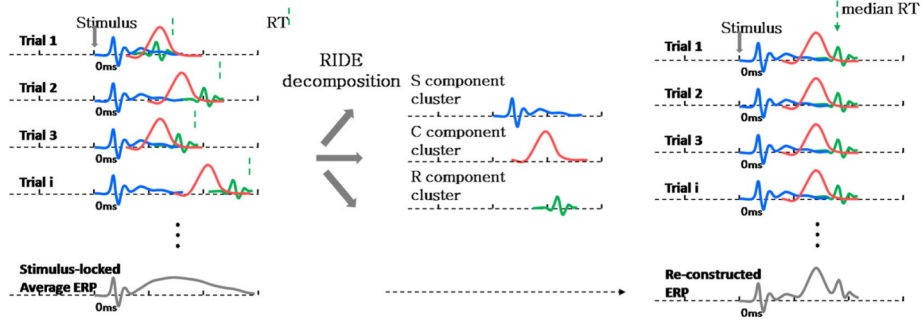


Figure 6.2: Conventional average ERP (left) from single trials with latency jitter, decomposition by RIDE (middle) and reconstructed ERP after correcting for latency variability (right). [47].

Components	Description
S component	It is a positive peak at around 100 ms after stimulus onset over the occipital region. It reflects the initial processing of visual information.
C component	It is a negative peak at around 200 ms after stimulus onset over the central region. It reflects the processing of motor information.
R component	It is a positive peak at around 300 ms after response onset over the central region. It reflects the processing of feedback information.

Table 6.1: ERP's components.

The algorithm follows an iterative process, with the decomposition module acting as the inner iteration loop and the latency estimation module as the outer

iteration loop. The steps involved in each module are described below:

Decomposition Module:

1. Initialize the decomposition process by randomly selecting initial values for the component clusters S, C, and R.
2. Estimate the mixing matrix that represents the contribution of each component cluster to the observed ERPs.
3. Perform Independent Component Analysis (ICA) to separate the observed ERPs into their underlying component clusters.
4. Update the component clusters S, C, and R based on the extracted independent components and the estimated mixing matrix.
5. Repeat steps 2-4 until convergence is achieved, optimizing the decomposition of the observed ERPs into the component clusters [31, 47].

Latency Estimation Module:

1. Initialize the latency estimation process by setting initial latency values for the C component clusters in single trials.
2. Based on the current estimates of the component clusters S, C, and R obtained from the decomposition module, align each C component cluster to its most probable latency in each trial.
3. Update the latency values for the C component clusters based on the alignment results.
4. Repeat steps 2-3 until convergence is achieved, refining the latency estimates of the C components in single trials[31, 47].

By iteratively performing the decomposition and latency estimation modules (,) the RIDE algorithm obtains information about the component clusters S, C, and R, in order to accurately estimate the C component latencies in single trials[47].

6.2 Data Normalization with Z-score method

Normalizing EEG data is a critical step in studying and interpreting signals for mental diagnosis. This step is a preprocessing technique used to standardize numerical values in the dataset, making them comparable and easier to interpret, in order to obtain classification results with high value of accuracy and optimal performance.

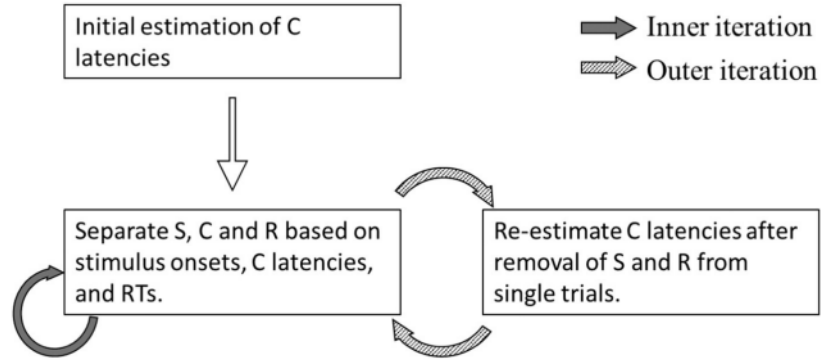


Figure 6.3: Flow-chart of RIDE decomposition [47].

The **Z-score normalization** was chosen: it consists of altering EEG data such that they have a mean of 0 and a standard deviation of 1, allowing the signals to be compared across participants and situations. When dealing with EEG signal features, using the Z-score normalization method is often preferred over the min-max method for several reasons:

1. **Preservation of Distribution:** EEG signals, in this case, have complex distributions that need to be preserved for the correct classification based on time-domain feature;
2. **Robustness to Outliers:** outliers have less impact on the normalization process;
3. **Statistical Comparisons:** as said before, statistical measures are selected and this type of normalization facilitates statistical comparisons across different feature, since they are standardized to have a mean of 0 and a standard deviation of 1.

In particular, this process was applied before the Feature Extraction on Fc line and C line, so the Pre-Motor Area Channels and Motor Area Channels (please, refer to table 6.2), the signals considered in the process of detection of attributes.

6.3 Feature Extraction

Features are individual properties generated from a data set and used as input to ML models, that refers to a measurable property, characteristic or aspect of that specific given data [48].

The features used in this context are "Numerical" type: these features represent real numeric values that quantify various aspects of the EEG data, that will be

described in the following paragraphs. The goal is to identify the features that best summarize the underlying patterns or characteristics of the data.

Proper Feature Extraction is crucial for biomedical signals: the main goal is to be able to select the appropriate features that characterize the EEG signal for our classification purposes, thereby leaving the task of Feature Selection to identify the most significant and relevant features for the problem, while discarding others.

6.3.1 RP Time-Domain features

As mentioned before, one of the purpose of the project is to demonstrate if the new plugin provides better signals than the previous ones. The selected features are the same as those previously selected by Zanetta in her thesis work (please, refer to this paragraph: 5.1), with the addition of **SNR** of C line and Fc line (in fact, through visual comparisons, the new plugin also provides better signal-to-noise ratios, so they need to be considered). Additionally, the search for the representative peak of the motor action (which in my colleague's thesis is calculated within a single interval) in this case, considering the improved shapes of the RP, has been split into two parts: the search occurs within the interval [-1500 0] and (0 1000].

Brain Area	Averaged Channels
Pre-Motor Area	Fcz, Fc3, Fc4
Motor Area	Cz, C3, C4

Table 6.2: The combinations of averaged RPs representing different areas of the brain, to better understand data management and the graphical representation of results.

The peak before 0, within the interval [-1500, 0], typically corresponds to the anticipatory or preparatory phase of the response. It captures the physiological changes that occur before the onset of the stimulus or the initiation of the task: it has been attributed to activity in the supplementary motor area and premotor cortex [24]. This anticipatory peak can reflect the individual's initial intentional and cognitive processes in response to an upcoming event or task.

On the other hand, the peak after 0, within the interval (0, 1000], represents the response to the stimulus or task itself. It reflects the physiological changes that occur after the onset of the stimulus and during the active engagement in the task. This peak is associated with the physiological reactions related to the specific stimulus or task. It is generated by activity in the primary motor cortex [24].

In conclusion, the extracted features (in time domain) are:

- **Peak amplitude before 0:** the negative peak represents the potential of neurons activated when there is an intention to move. It was evaluated in the motor area (C line).
- **Peak amplitude after 0:** it represents the physiological response to the stimulus or task, reflecting the changes and processing that occur during engagement (C line).
- **Negative Slope:** it occurs before the movement onset and for this reason is evaluated in the pre-motor area (Fc line).
- **Statistical features:** variance, area, standard deviation, mean value, skewness and kurtosis in the motor area (C line).
- Principal component analysis (**PCA**) on the signal (C line).
- **Mean value of Signal to Noise Ratio evaluation:** which is positive when the signal exceeds the noise (C line and Fc line). It is calculated within the time interval before 0.

6.3.2 RP Frequency-Domain features

The Power Spectral Density (PSD) graph is useful to see areas of higher power at specific frequencies, that represent the presence of frequency bands that are more active or dominant in the signal. In our case, the frequency band is from 1.5Hz to 3.5 Hz, suggesting that there is a notable concentration of power in that frequency range.

So, the chosen features are:

- **Power Spectral Density:** the distribution of average signal power in the band of interest was calculated (1.5 Hz - 3.5 Hz) of the C line.
- Principal component analysis (**PCA**) on the PSD.

By performing PCA on the PSD, the study aimed to reveal key components and extract valuable information from the frequency domain.

6.3.3 PCA for Feature Construction

Principal Component Analysis (**PCA**) is an unsupervised learning algorithm that is commonly used for the dimensionality reduction in machine learning: it transforms a high-dimensional dataset into a lower-dimensional one by identifying the principal components that capture the most significant variations in the data, based on statistical process that converts the observations of correlated features into a set

of linearly uncorrelated features, using the orthogonal transformation. These new transformed features are called the Principal Components[49].

As a feature construction method, PCA can be applied to extract new features that are linear combinations of the original features: it identifies important relationship in the dataset and transform these based on their importance. This methods allows us to keep the most important relationships and drop the others [50].

6.4 Feature selection

The next important step is *Feature Selection*: it is a dimensionality reduction technique, that aims to detect the most discriminative features instead of the less relevant or redundant ones for classification and problem description. The result is a small subset of meaningful features selected from a larger one obtained from Feature Extraction.

The importance of the feature indicates how much it contributes to the model prediction: it determines the degree of usefulness for the ML model and prediction. The method of selection is based on representing feature importance using a numeric value called *score*, where the higher the score value has, the more important it is for the prediction: irrelevant features are excluded [48]. This process leads to better classifier performance, lower computational cost, higher accuracy and improved interpretability of the model.

The main types of feature selection are:

1. **Filter Methods:** these methods use a *proxy measure* to determine the importance of features or feature subsets calculated from main characteristics of the training data. Filters are classified based on informations like distance, dependence, consistency, similarity, and statistical measures, leading to selected features that can be used with any modeling algorithm. Examples include information gain, chi-square, and Relief[51].
2. **Wrapper Methods:** these methods use a modeling algorithm to train predictive models with different candidate groups of feature, selected based on feature importance scores. The resulting performance are used to evaluate the feature sets. They are iterative and computationally intensive, because a new model is trained for each feature subset. Nonetheless, they can identify the optimal feature set for a specific modeling algorithm. Examples include wrappers for Naïve Bayes and Support Vector Machines (SVM)[51].
3. **Embedded Methods:** these methods consider feature selection as part of the execution of the modeling algorithm; thanks to this process they are computationally efficient. Examples include various decision tree based algorithms, CART, C4.5 and XGBoost[51].

6.4.1 ReliefF method

The chosen Feature Selection method is the ReliefF algorithm, that is a variant of the Relief algorithm (the original Relief algorithm is rarely applied in practice anymore [52]), specifically designed for feature selection tasks. It is an efficient heuristic estimator of the attribute quality that can deal with dependent and independent attributes that may be present in the dataset [53]. It works by assigning a weight (based on observed importance) to each feature in the dataset.

Here's an overview of how the ReliefF algorithm works Figure 6.4: ReliefF is

Input: for each training instance a vector of feature values and the class value

Output: the vector W of estimations of the qualities of features

1. Set all weights $W[X] = 0.0$;
2. **For** $i = 1$ **to** m **do begin**
3. Randomly select an instance R_i
4. Find k nearest hits H_j
5. **For each class** $C \neq \text{class}(R_i)$ **do**
6. From class C find k nearest misses $M_j(C)$
7. **For** $X = 1$ **to** a **do**
8. $W[X] = W[X] - \sum_{j=1}^k \text{diff}(X, R_i, H_j) / (m \cdot k) +$
9. $\sum_{C \neq \text{class}(R_i)} \frac{P(C)}{1 - P(\text{class}(R_i))} \sum_{j=1}^k \text{diff}(X, R_i, M_j(C)) / (m \cdot k)$
10. **End**

Figure 6.4: Pseudo code of the ReliefF algorithm[52].

based on the selection of nearest neighbors. The goal is to find the nearest neighbors based on important attributes. Noisy and redundant attributes can negatively impact neighbor selection, leading to bad probability estimates [53]: for this reason it has been of fundamental importance to clean the EEG signal thoroughly and extract features as accurately as possible.

To improve the reliability of probability estimation, ReliefF searches for k nearest hits/misses instead of just one, and calculate the average of their contributions. This extension significantly improves attribute quality estimation reliability (Kononenko, 1994). To simplify parameter tuning, a default value of $k = 10$ is suggested, because it was demonstrated that it confers satisfactory empirical results [53]. Indeed, in this thesis this value of k is used.

6.5 Classification

The final phase of this study is the binary classification: movement as either voluntary or involuntary. The classifiers used were the same as those chosen in the previous work (Zanetta thesis) in order to better assess whether the classification is improved or degraded and, consequently, evaluate the performance of the current plugin. For each machine learning algorithm, the leave-one-out cross-validation procedure was utilized in the prediction.

As said in the previous chapter, the classifiers used in this study are as follows: Support Vector Machine (linear SVM and cubic SVM), K-Nearest Neighbors (K-NN) and the Decision Tree (DT).

6.5.1 Leave-One-Out Cross-Validation

It is crucial to assess the predictions made by the model for classification problems.

LOOCV (Leave One Out Cross-Validation) is a cross-validation technique where each observation is used as the validation set while the remaining (N-1) observations are used as the training set. The model is trained using the training set and then used to predict the value for the observation in the validation set. This process is repeated N times, with each observation being used as the validation set once [54].

LOOCV is a special case of K-fold cross-validation. In this approach, K (number of folds) is equal to the number of observations ($K = N$), in order to reduce bias and randomness in model evaluation. Its goal is to minimize the mean-squared error rate and mitigate the risk of overfitting[54].

LOOCV offers several advantages:

1. **Reduced Bias:** it minimizes bias by repeatedly fitting models on slightly different data sets; this method reduces the risk of overestimating the test error compared to the validation set approach[55].
2. **Consistent Test Error:** the estimated test error will always be the same on the entire dataset; this leads to high consistency in the evaluation model performance.[55].

This method is employed because it is particularly useful for small datasets (indeed the dataset in this case consists of 17 subjects): LOOCV tests individually every subjects, by treating each data as a separate validation set, while the remaining data points are used for training. This approach leads to a more comprehensive evaluation of the model's performance, creating a model's generalization ability that would not otherwise exist, by minimizing the risk of overfitting.

Chapter 7

Results and Discussion

This chapter will represent and discuss the results obtained from the various stages of the work, from Feature Selection to Classification, with the aim of highlighting the differences between the plugins in order to demonstrate whether the modifications made on the improved plugin are positive or negative.

7.1 Outcomes with the Improved EEGLAB plugin

This section is dedicated to the classification results obtained from the data processed with the plugin described in the previous chapters.

7.1.1 Feature Extraction and Feature Selection

The table below shows two examples (one voluntary and one involuntary subject) and their values extracted in the Feature Extraction step with the purpose of demonstrating the differences from a quantitative point of view (Table 7.1).

Feature	Voluntary dataset	Involuntary dataset
Peak amplitude before 0	1.428	0.998
Peak amplitude after 0	3.021	1.739
Negative Slope	0.001	0.004
Variance	1	1
Mean Value	2.51E-16	5.12E-17
Standard Deviation	1	1
Area	- 1839.686	393.804
Kurtosis	1.575	2.742
Skewness	0.377	-0.476
Power Spectral Density	0.162	1.232
Mean value SNR (Fc Line)	15.913	-7.817
Mean value SNR (C Line)	15.527	-6.598
PCA1(PSD)	0.205	0.262
PCA1(Signal)	-0.518	-0.198
PCA2(Signal)	2.417	0.308
PCA3(Signal)	0.215	0.141
PCA4(Signal)	-0.018	-0.263

Table 7.1: Table of all the extracted features: from voluntary MI993011 and involuntary dataset RG865070.

It is important to note that both the variance and the standard deviation (the square root of the variance) are equal to 1. This is because, as explained earlier, when applying Z-score normalization to data, the variance becomes 1 after normalization.

The ReliefF feature selection algorithm selected the most informative features, indeed the dataset was reduced to 4 features: Mean Value of Fc SNR, Mean Value of C SNR, the Area of the C line in the time interval before zero (thus that associated with the intention [-1500ms 0ms]) and the first component extracted with PCA from the PSD.

The *scatter plots* of the selected features are shown below (Figure 7.1, Figure 7.2),

providing a graphical representation of the data arrangement. This allows for a visual comparison of the most discriminating features between the two groups, volunteer and involuntary.

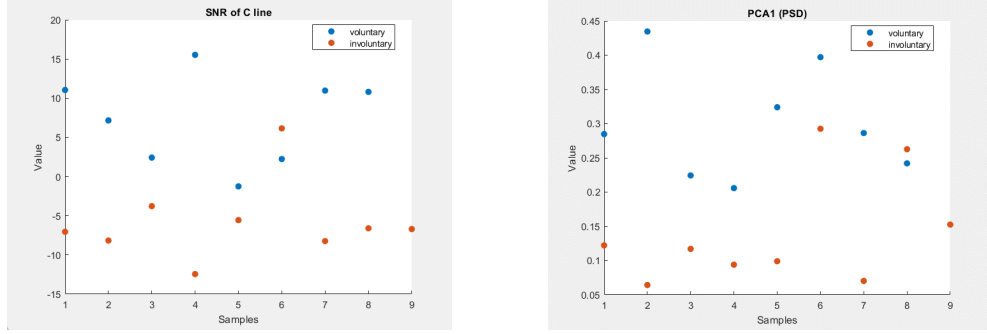


Figure 7.1: Left: SNR of C line; Right: PCA1(PSD).

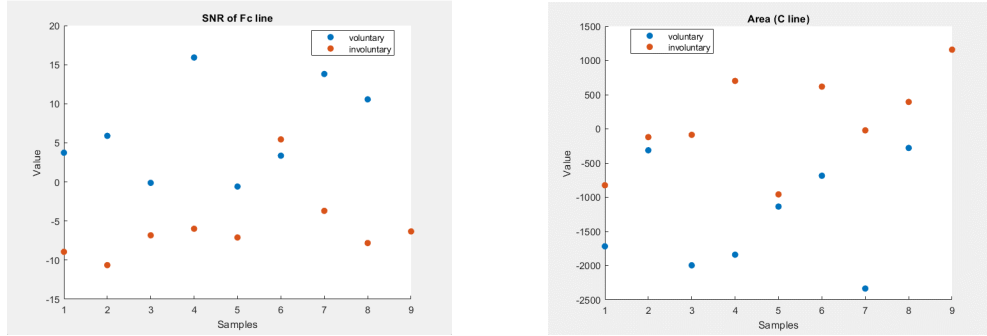


Figure 7.2: Left: SNR of Fc line; Right: Area (C line).

By observing the plots, it is evident that the features exhibit distinct patterns and separability between the voluntary and involuntary groups. This visual confirmation highlights the effectiveness of these features in distinguishing between the two classes.

7.1.2 Classification

The Classifiers were described in detail in the sixth chapter. In order, the obtained confusion matrices and ROC curves are presented.

Linear SVM

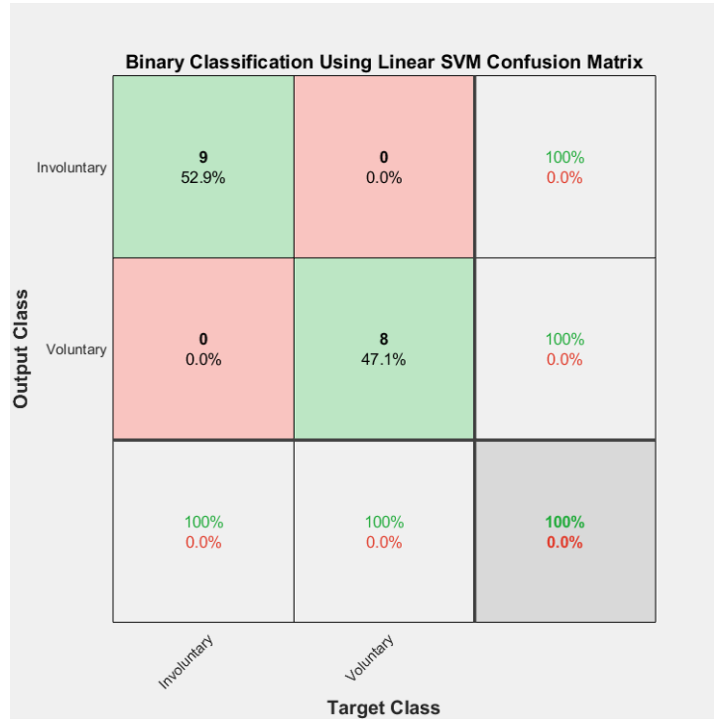


Figure 7.3: Confusion Matrix for Linear SVM Model.

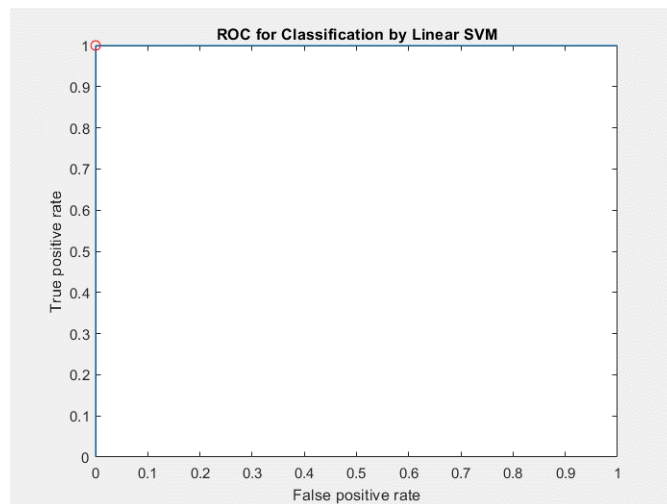


Figure 7.4: ROC curve of Linear SVM Model.

Cubic SVM

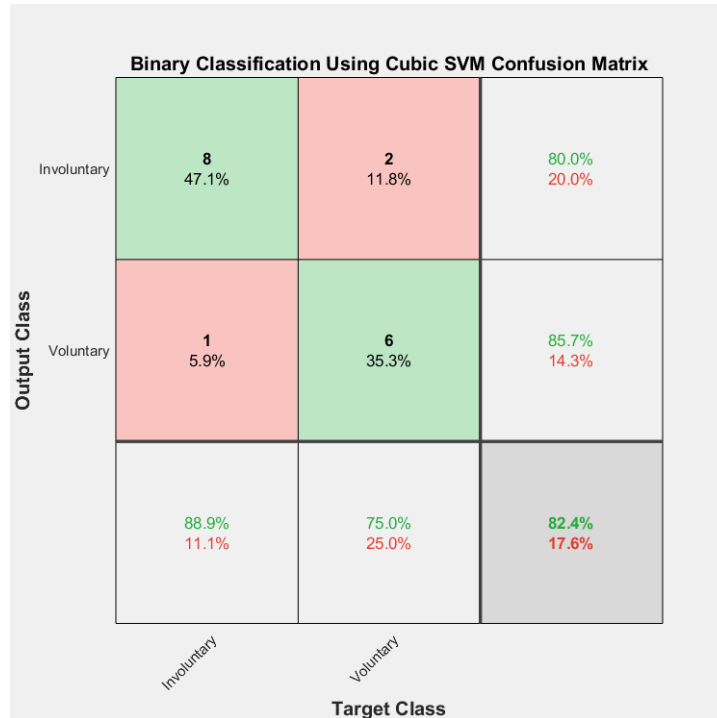


Figure 7.5: Confusion Matrix for Cubic SVM Model.

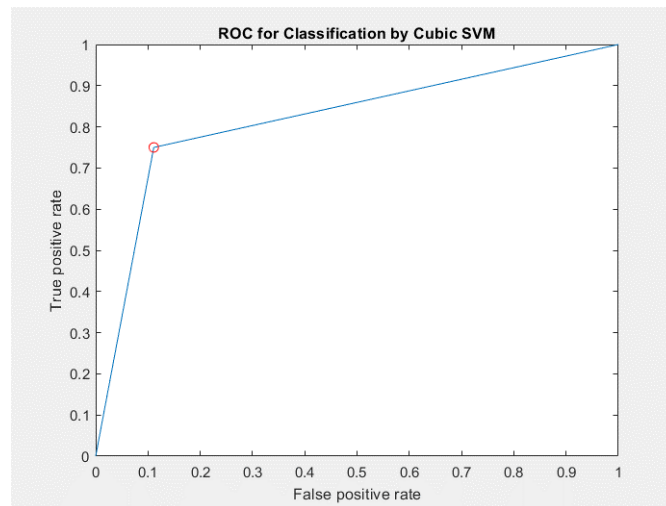


Figure 7.6: ROC curve of Cubic SVM Model.

k-NN

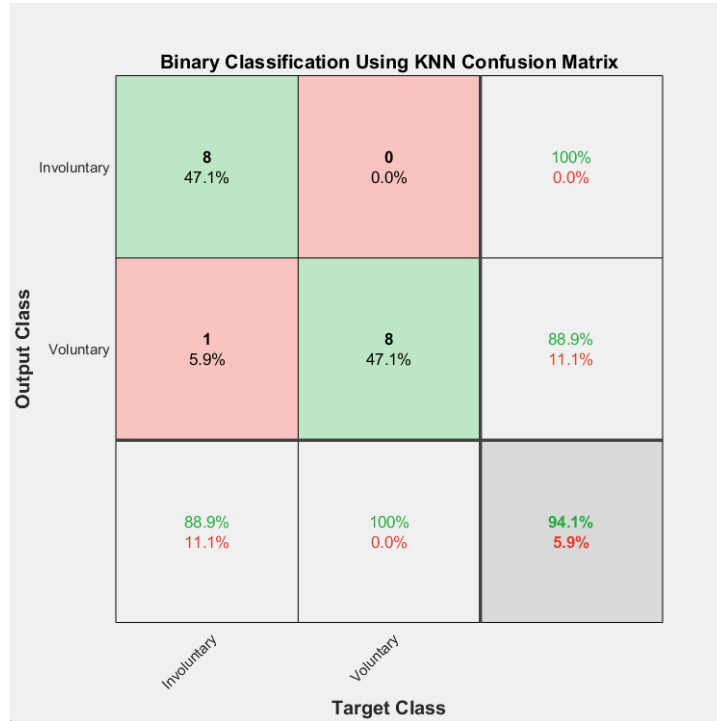


Figure 7.7: Confusion Matrix for k-NN Model.

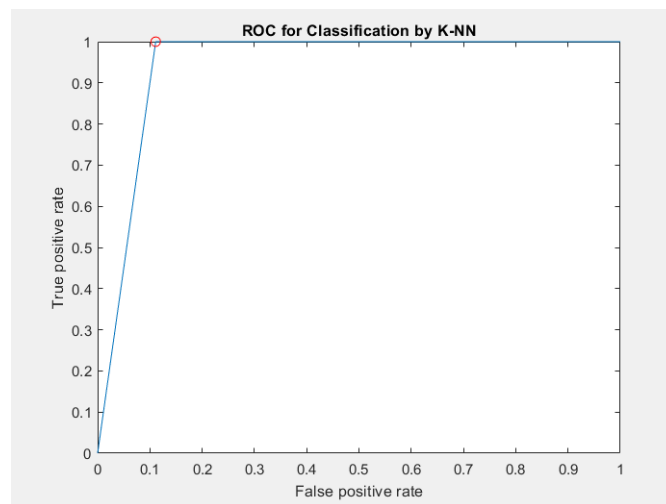


Figure 7.8: ROC curve of k-NN Model.

Decision Tree

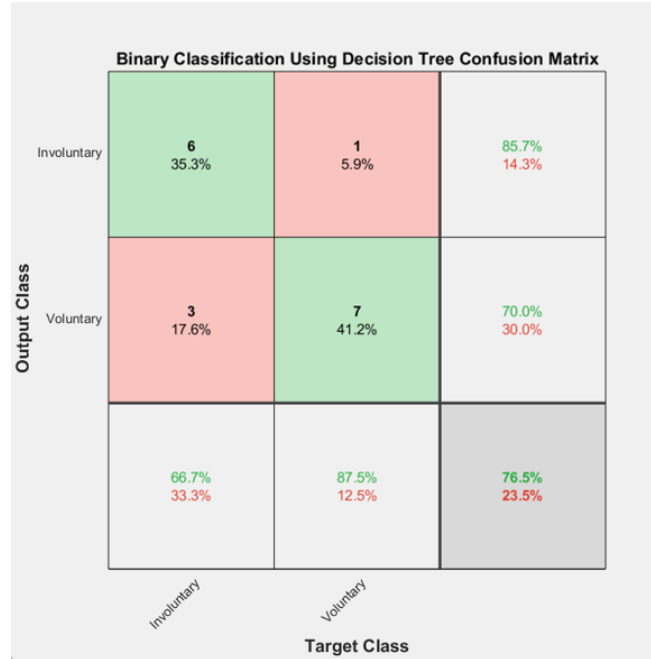


Figure 7.9: Confusion Matrix for Decision Tree Model.

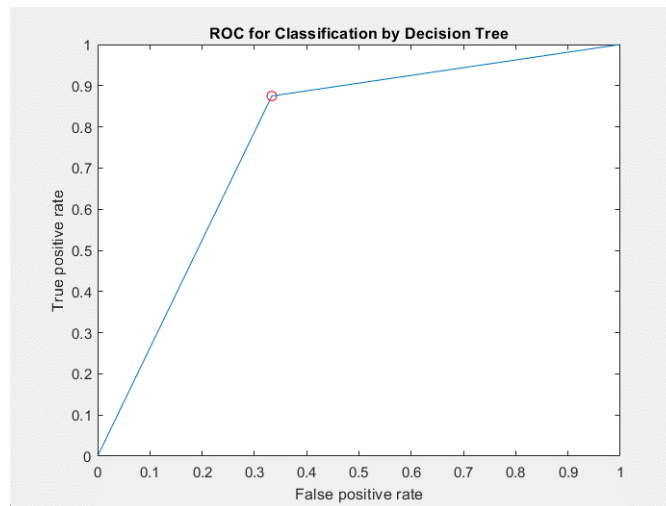


Figure 7.10: ROC curve of Decision Tree Model.

Performance Tables (with Feature Selection)

	Linear SVM	Cubic SVM	k-NN	Decision Tree
AIC	-Inf	-32.11	-44.16	-14.85
K Statistics	100%	63.89%	88.89%	54.17%
Specificity	100%	85.71%	88.89%	70.00%
Sensitivity	100%	80.00%	100%	85.71%
Accuracy	100%	82.4%	94.1%	76.5%

Table 7.2: Table of classification performances with the algorithm for feature selection (*4 features*).

1. Linear SVM: it has a very low AIC value and high percentages of K Statistics, Specificity, Sensitivity, and Accuracy; these results demonstrate that the classifier is able to distinguish between voluntary and involuntary signals and a high discriminative capacity.
2. Cubic SVM: it shows improved performance compared to Linear SVM in terms of AIC and K Statistics; the measures of Specificity, Sensitivity, and Accuracy are also high, although slightly lower than those of Linear SVM. This suggests that Cubic SVM has a good signal classification capability but it is slightly less precise than Linear SVM.
3. k-NN: it presents a negative AIC value and achieves high percentages of K Statistics, Specificity, Sensitivity, and Accuracy: this means that the classifier achieved high classification capability based on data proximity.
4. Decision Tree: it exhibits a negative AIC value and obtains high percentages of Specificity, Sensitivity, and Accuracy, but lower than the other classifiers. This indicates that the Decision Tree may have a good classification capability but it is less precise in discriminating signals compared to the other classifiers, in this case.

The classifier's performance suggests that the selected features are informative and enable good discrimination between voluntary and involuntary signals in the context of RP-based classification.

Performance Tables (without Feature Selection)

	Linear SVM	Cubic SVM	k-NN	Decision Tree
AIC	-Inf	-Inf	-56.44	1
K Statistics	100%	100%	88.89%	83.33%
Specificity	100%	100%	77.78%	66.67%
Sensitivity	100%	100%	80%	72.73%
Accuracy	100%	100%	88.2%	82.4%

Table 7.3: Table of classification performances without the algorithm for feature selection (*17 features*).

1. Linear SVM: the classifier achieves perfect values and this means that it is able to classify both signals without the need for feature selection.
2. Cubic SVM: it is similar to Linear SVM, because it also achieves perfect values in all performance metrics, instead of the previous type of classification (with feature selection).
3. k-NN: it achieves high values in terms of metrics. However, there is a slight drop in performance compared to Linear and Cubic SVM.
4. Decision Tree: it shows slightly lower values compared to the other classifiers in terms of K Statistics, Specificity, Sensitivity, and Accuracy.

In summary, Linear SVM and Cubic SVM achieved perfect results without feature selection, suggesting that they may not significantly benefit from its implementation, but on the other side k-NN and Decision Tree showed lower values without Feature Selection. In this case, it can be clear that maximizing the performance of two classifiers at the expense of the other two is pointless, especially since the phase of understanding the best discriminative features for this problem is more important. Moreover, the overall performance is better in the case of classification with the selected features rather than without feature selection, in order to also highlighting what the most meaningful characteristics of an RP are.

7.2 Outcomes with the Old EEGLAB plug-in

This section will instead present the results of the classification on signals processed with the previous plugin, which involves a different preprocessing approach that will be examined in more detail in the upcoming paragraphs.

7.2.1 Short explanation of the old plugin

The previous plugin differs from the new and improved one in the following aspects: 1) It uses an Artifact Correction code that lacks some modifications present in the recent version, which includes several robust detrending methods to remove slow derivatives from the signal [19]; 2) Spatial Filtering is not performed.

7.2.2 Feature Extraction and Feature Selection

The classification is based not only on the same subjects but also on the same features selected from the previous dataset (processed with the new plugin), allowing for performance comparison. The scatter plots of the features for this case are shown (they do not exhibit as clear of a separation).

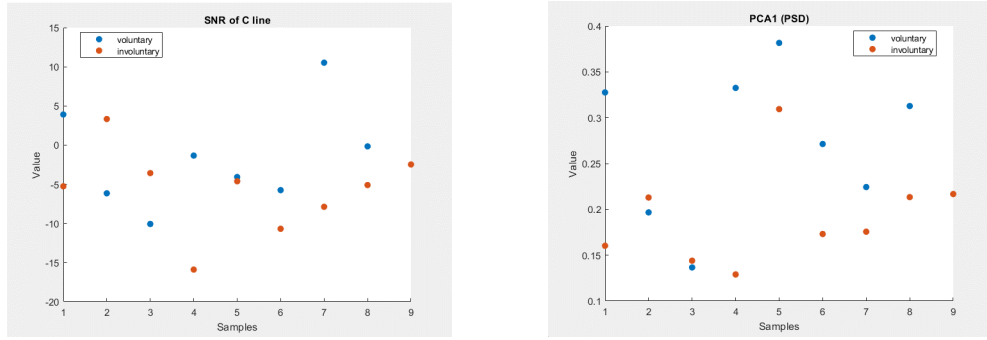


Figure 7.11: Left: SNR of C line; Right: PCA1(PSD) (old plug-in).

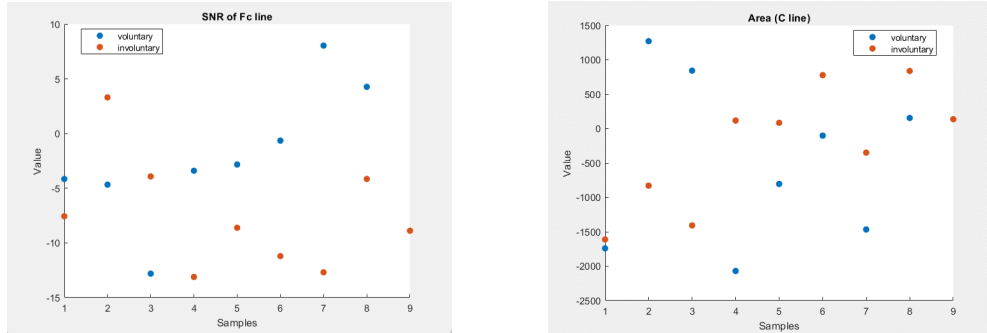


Figure 7.12: Left: SNR of Fc line; Right: Area (C line) (old plug-in).

7.2.3 Classification

Here are the classification graphs for the signals of the subjects processed with the old plugin.

Linear SVM

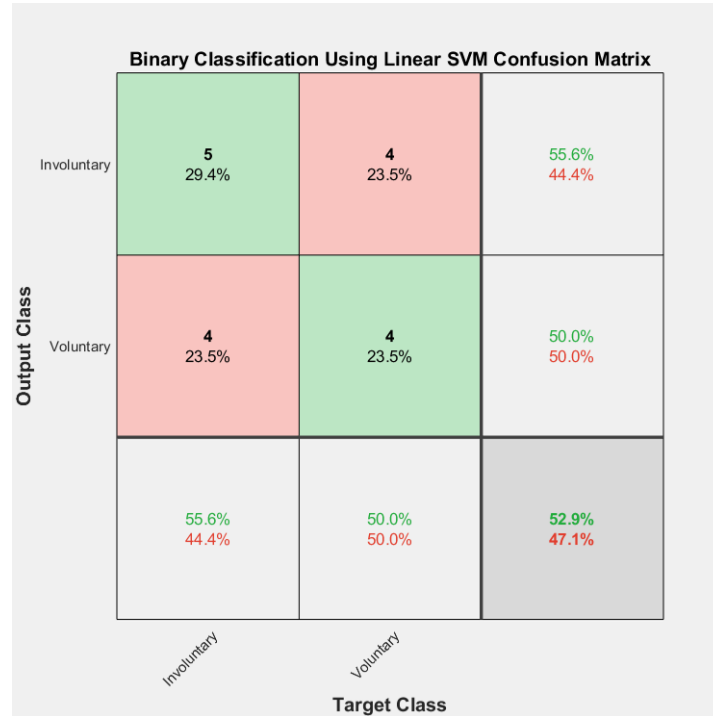


Figure 7.13: Confusion Matrix for Linear SVM Model (old plug-in).

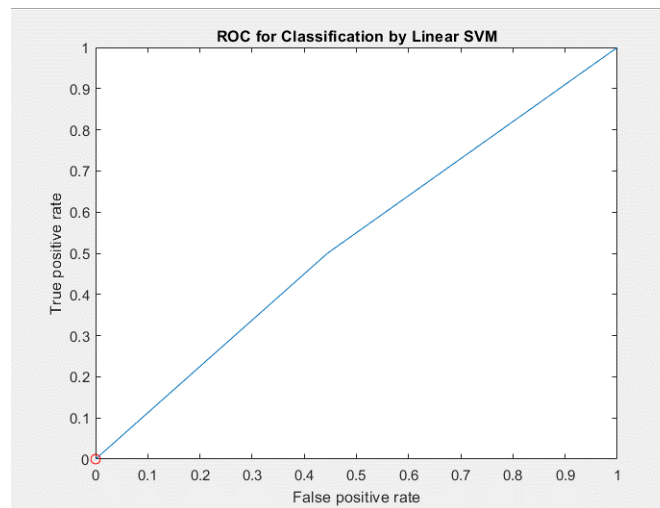


Figure 7.14: ROC curve of Linear SVM Model (old plug-in).

Cubic SVM

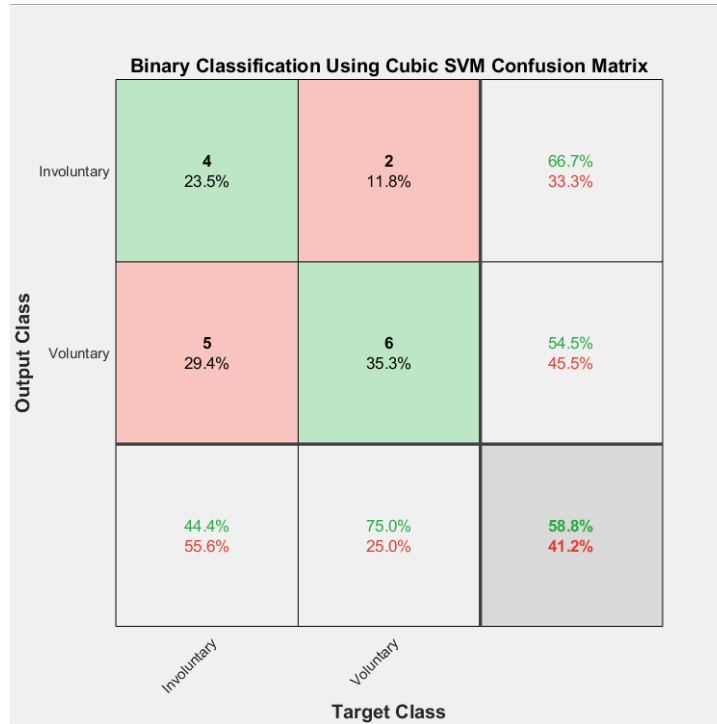


Figure 7.15: Confusion Matrix for Cubic SVM Model (old plug-in).

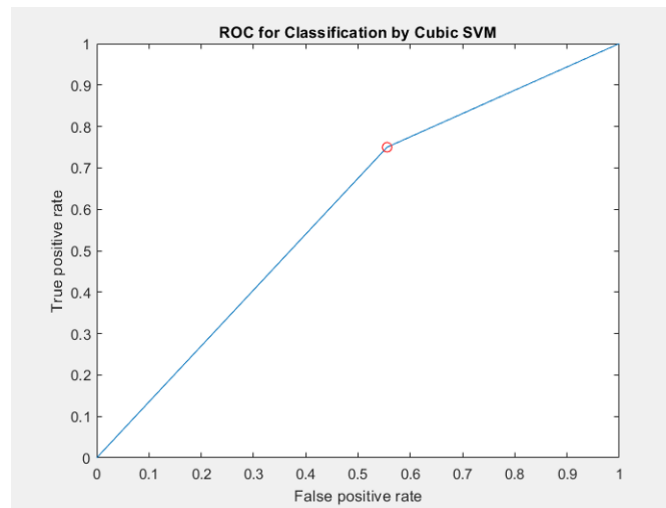


Figure 7.16: ROC curve of Cubic SVM Model (old plug-in).

k-NN

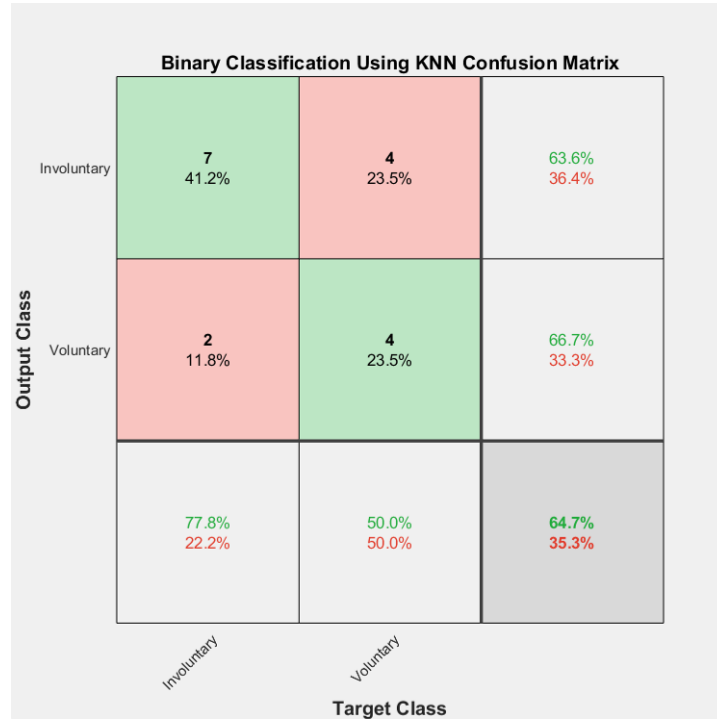


Figure 7.17: Confusion Matrix for k-NN Model (old plug-in).

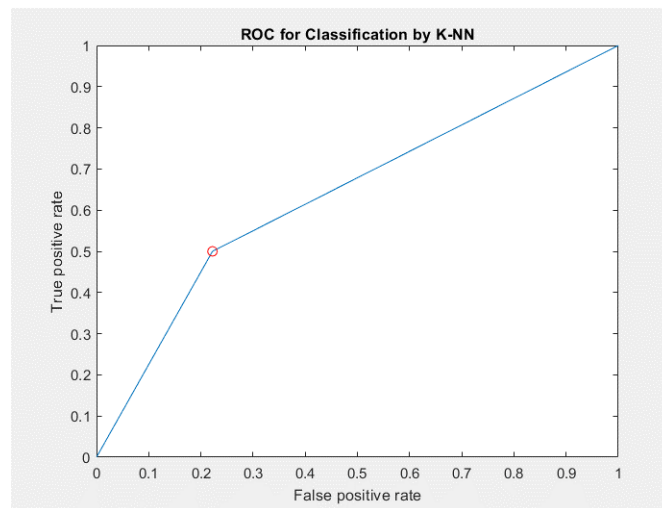


Figure 7.18: ROC curve of k-NN Model (old plug-in).

Decision Tree

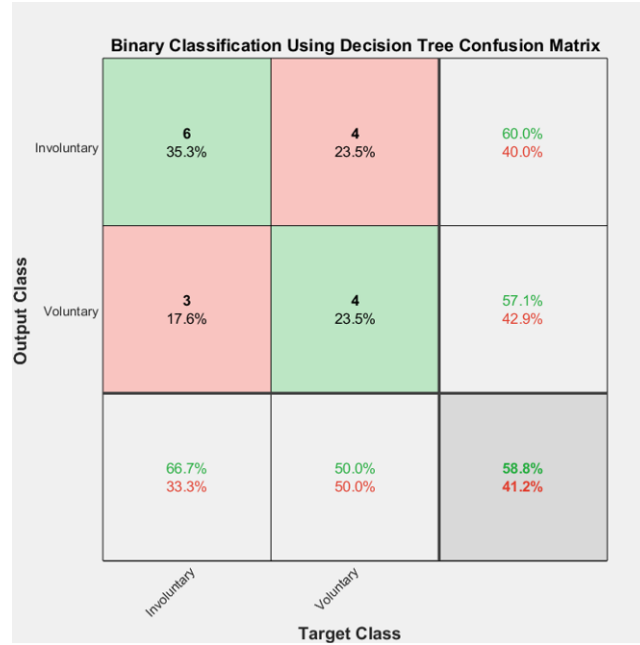


Figure 7.19: Confusion Matrix for Decision Tree Model (old plug-in).

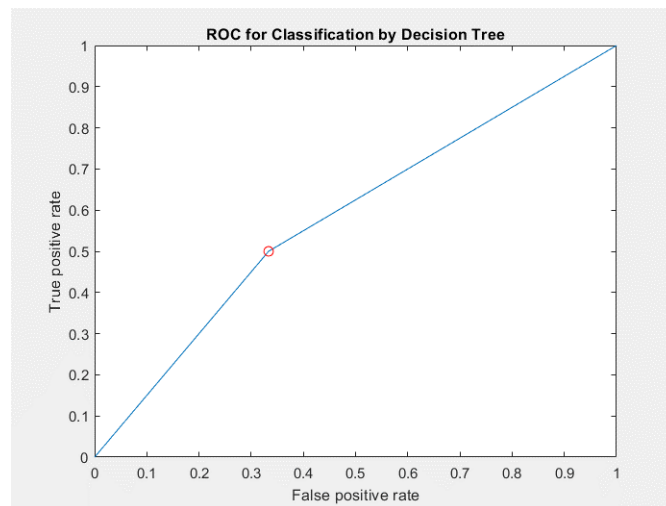


Figure 7.20: ROC curve of Decision Tree Model (old plug-in).

Performance Tables (with Feature Selection)

	Linear SVM	Cubic SVM	k-NN	Decision Tree
AIC	26.53	18.71	16.75	18.71
K Statistics	5.56%	19.44%	27.78%	16.67%
Specificity	50%	54.55%	66.67%	57.14%
Sensitivity	55.56%	66.67%	63.64%	60%
Accuracy	52.9%	58.8%	64.7%	58.8%

Table 7.4: Table of classification performances of the *old* plug-in with the algorithm for feature selection (*4 features*).

The k-NN classifier shows the highest overall classification performance, with the lowest AIC value and the highest K Statistics, Specificity, Sensitivity, and Accuracy. The Cubic SVM and Decision Tree classifiers exhibit moderate performance, while the Linear SVM performs less favorably with the highest AIC and lower classification metrics.

Performance Tables (without Feature Selection)

	Linear SVM	Cubic SVM	k-NN	Decision Tree
AIC	0.44	0.52	0.50	0.66
K Statistics	40.97%	50%	45.83%	64.58%
Specificity	-18.06%	0%	-8.33%	29.17%
Sensitivity	37.5%	NaN%	40%	62.50%
Accuracy	41.2%	52.9%	47.1%	64.7%

Table 7.5: Table of classification performances of the *old* plug-in without the algorithm for feature selection (*17 features*).

It can be observed that the results obtained are slightly worse compared to the previous table. Specifically, all classifiers have higher AIC values, indicating lower model goodness. The metrics of K Statistics, Specificity, Sensitivity, and Accuracy also show lower or negative values in some cases.

7.3 Comparison between the New and Old EEGLAB Plugins

In this section, the RP graphs and their corresponding SNR (C line and Fc line) are presented for each subject to visually demonstrate the differences in the outputs of the two different plugins.

7.3.1 RP and SNR of voluntary subjects

AL858070 - voluntary subject

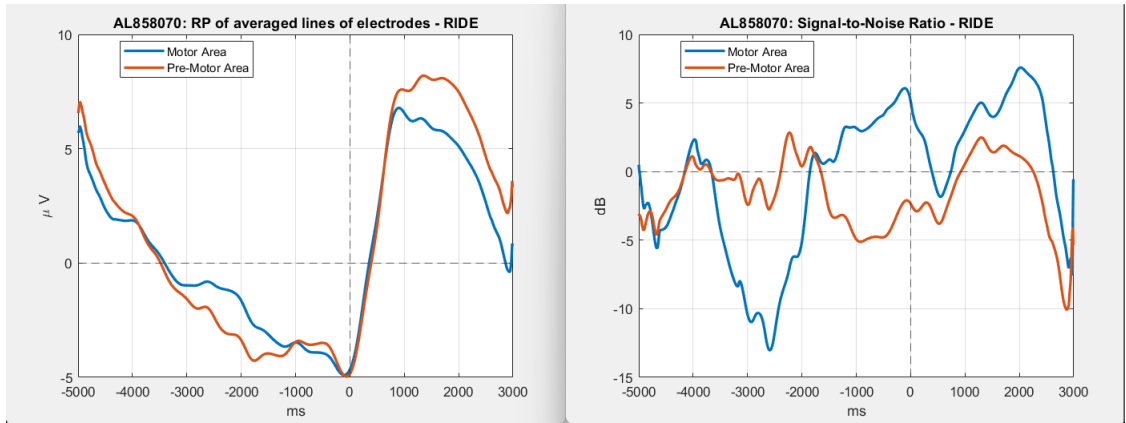


Figure 7.21: Subject graph AL858070 (old plugin). Left: RP; Right: SNR.

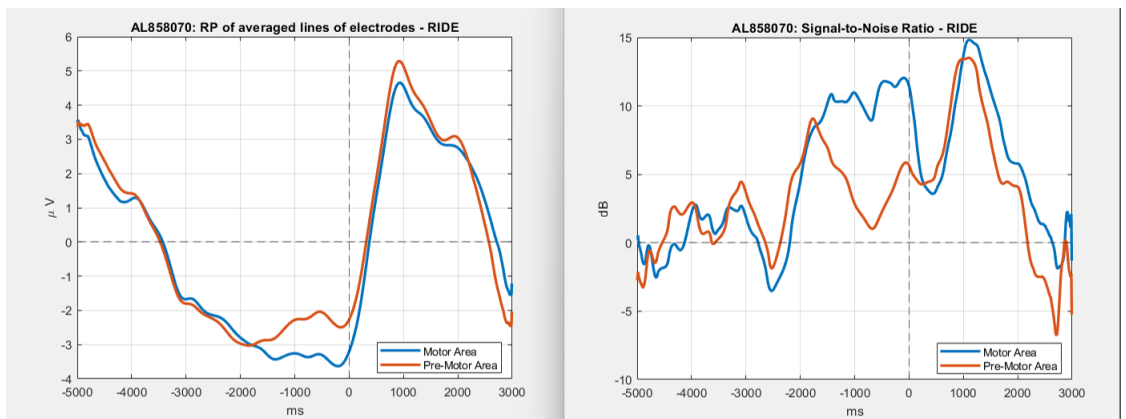


Figure 7.22: Subject graph AL858070 (new plugin). Left: RP; Right: SNR.

AP996111 - voluntary subject

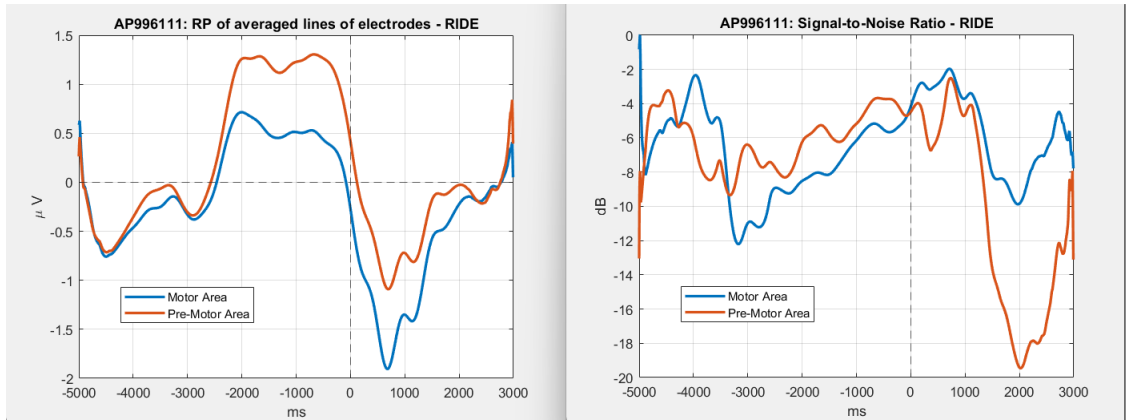


Figure 7.23: Subject graph AP996111 (old plugin). Left: RP; Right: SNR.

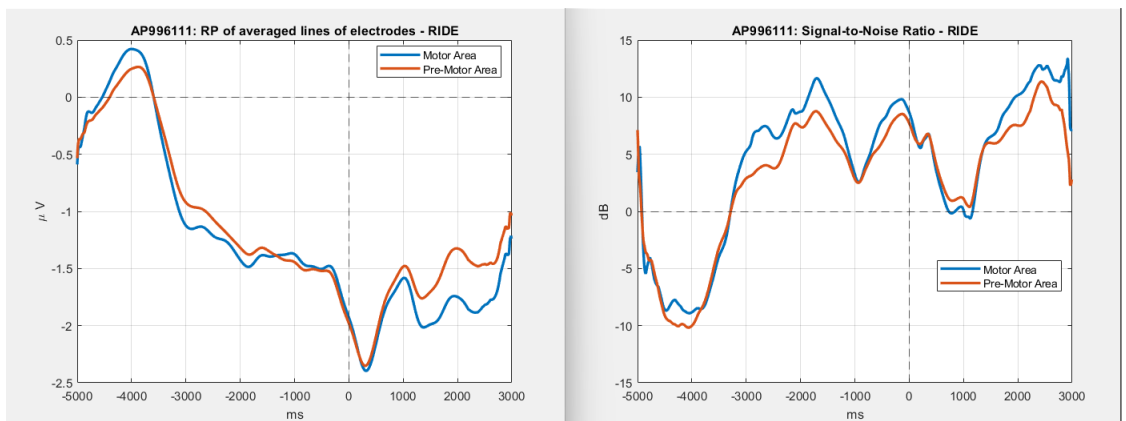


Figure 7.24: Subject graph AP996111 (new plugin). Left: RP; Right: SNR.

SD874070 - voluntary subject

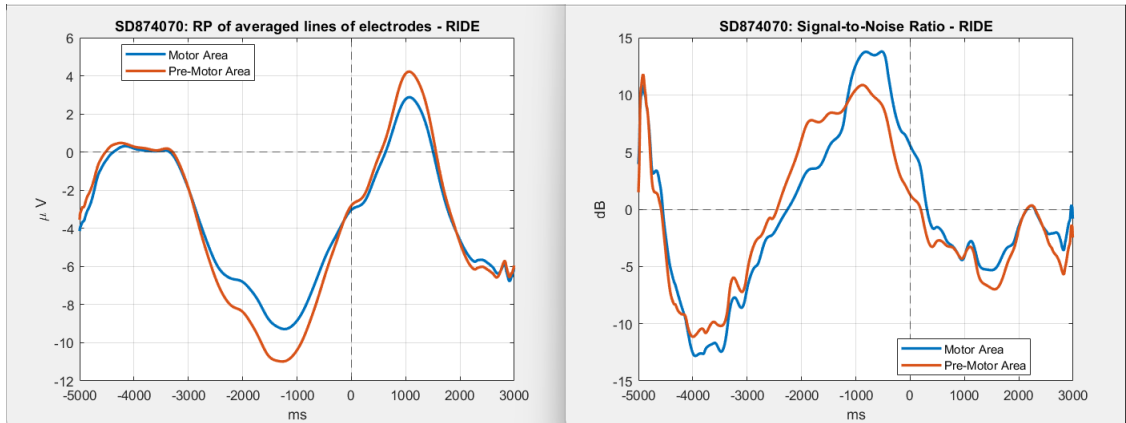


Figure 7.25: Subject graph SD874070 (old plugin). Left: RP; Right: SNR.

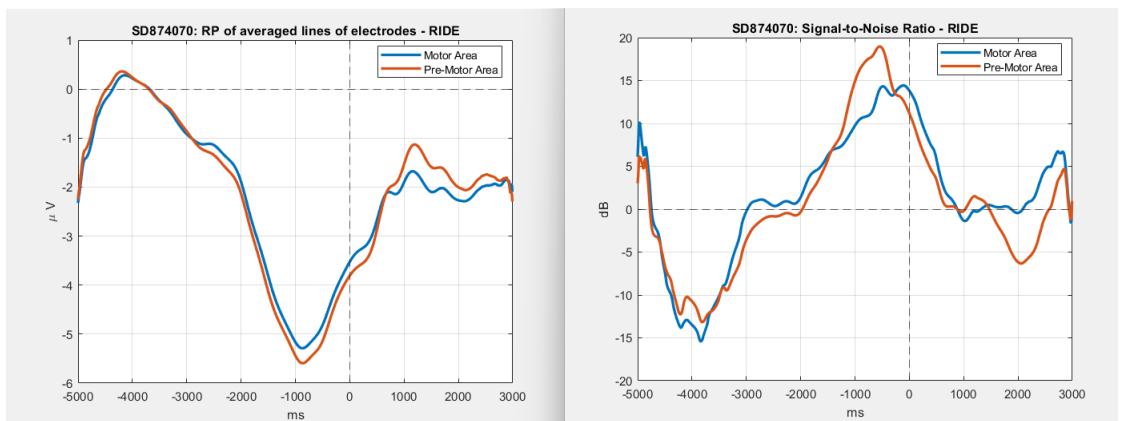


Figure 7.26: Subject graph SD874070 (new plugin). Left: RP; Right: SNR.

MI993011 - voluntary subject

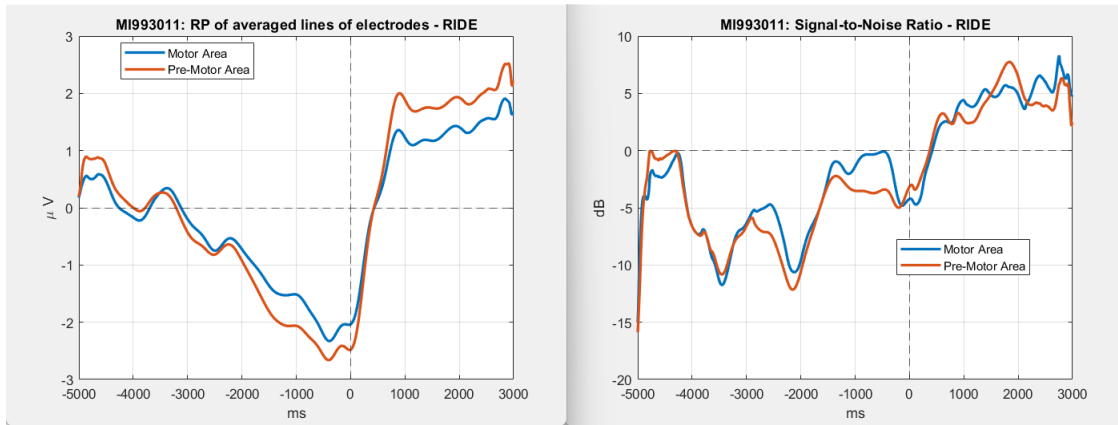


Figure 7.27: Subject graph MI993011 (old plugin). Left: RP; Right: SNR.

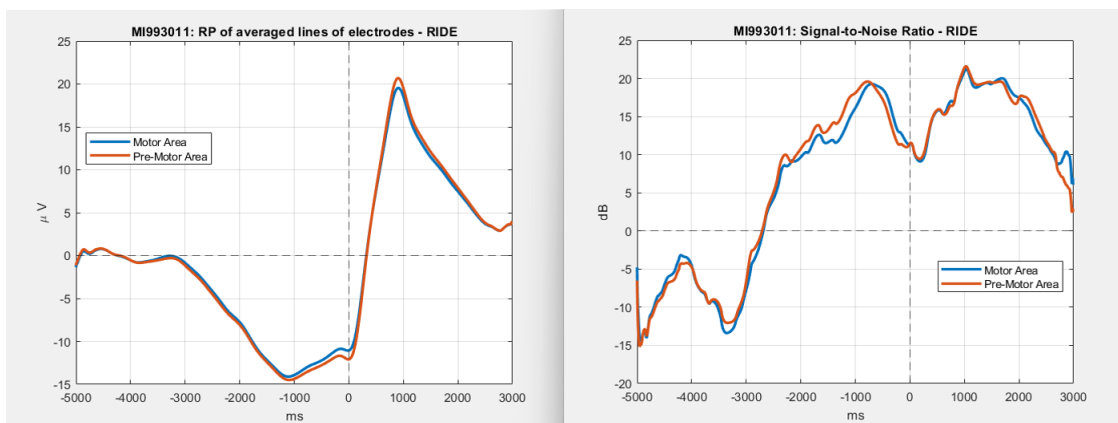


Figure 7.28: Subject graph MI993011 (new plugin). Left: RP; Right: SNR.

RB890071 - voluntary subject

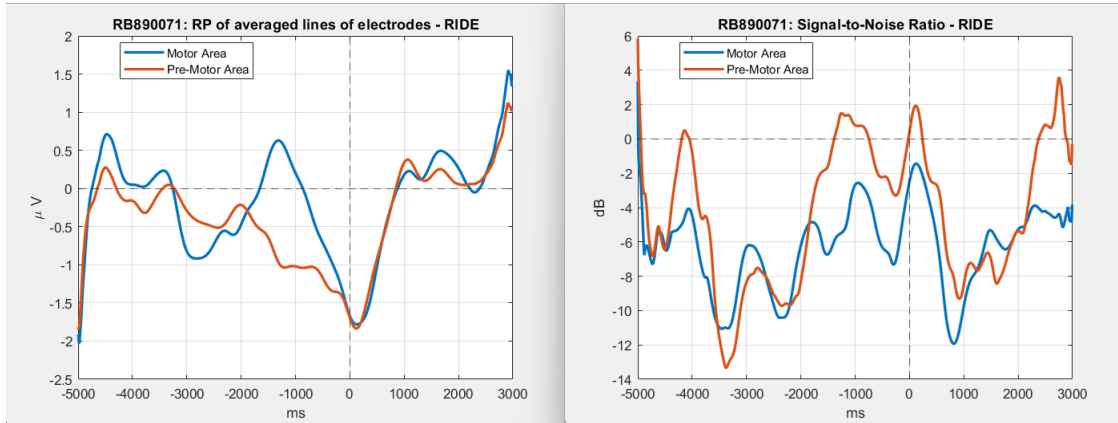


Figure 7.29: Subject graph RB890071 (old plugin). Left: RP; Right: SNR.

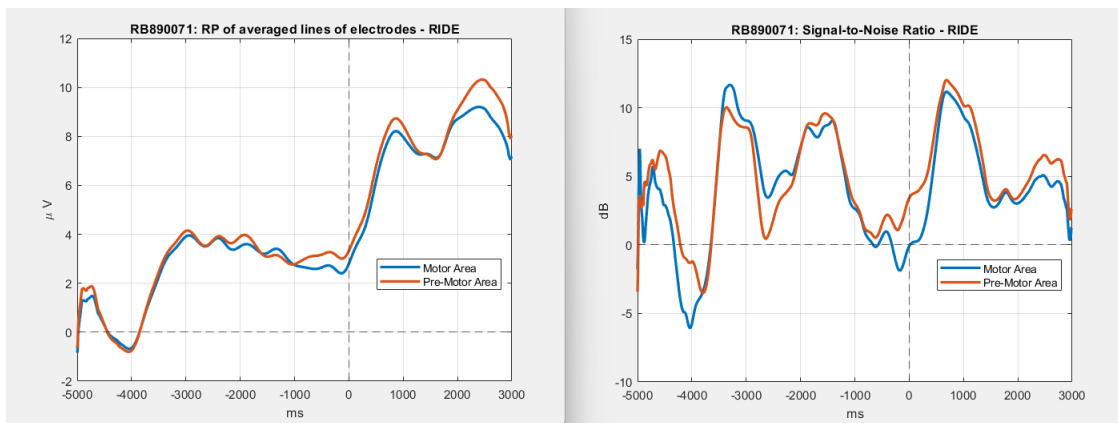


Figure 7.30: Subject graph RB890071 (new plugin). Left: RP; Right: SNR.

MS861070 - voluntary subject

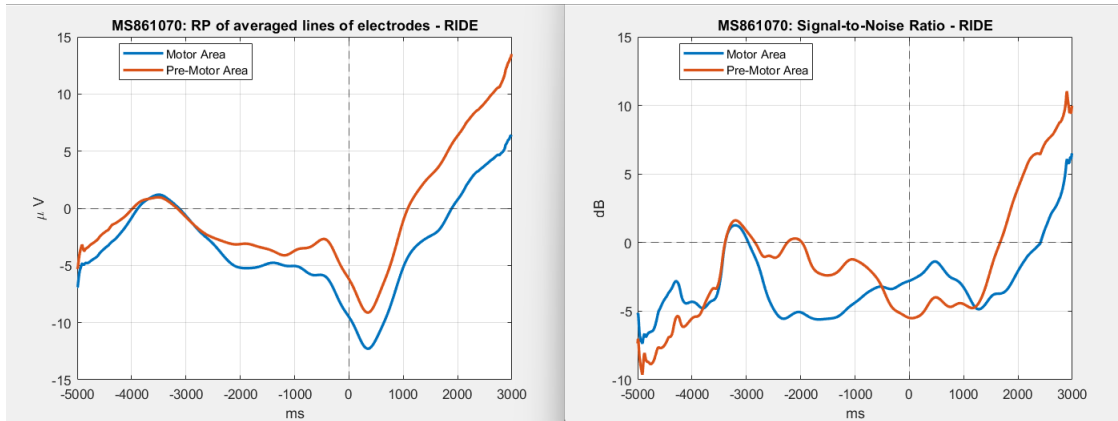


Figure 7.31: Subject graph MS861070 (old plugin). Left: RP; Right: SNR.

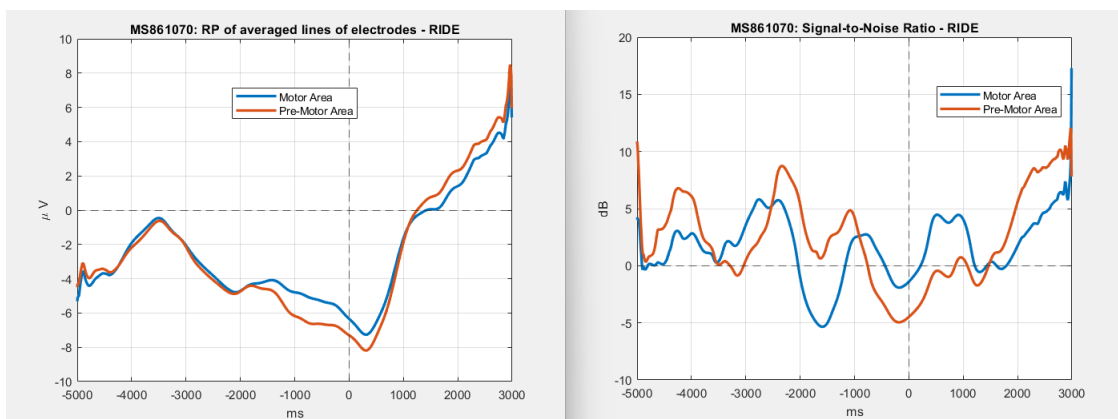


Figure 7.32: Subject graph MS861070 (new plugin). Left: RP; Right: SNR.

GF892070 - voluntary subject

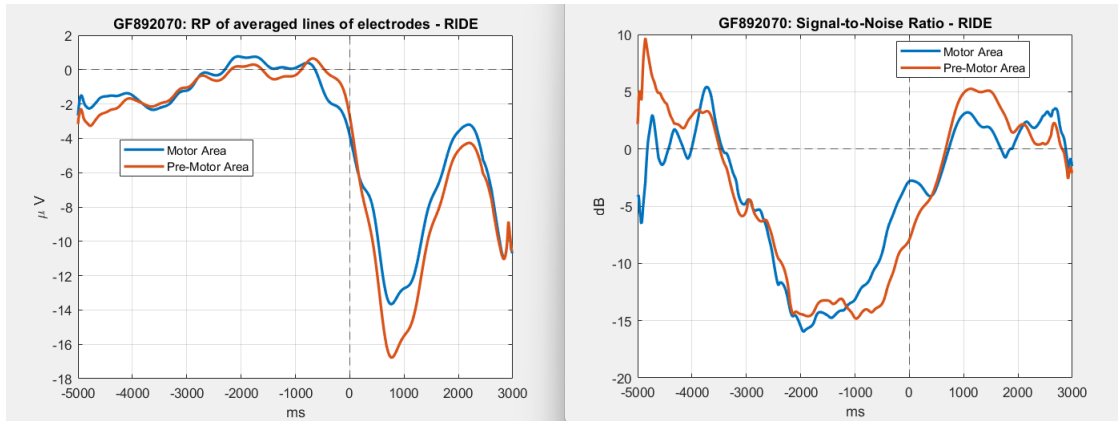


Figure 7.33: Subject graph GF892070 (old plugin). Left: RP; Right: SNR.

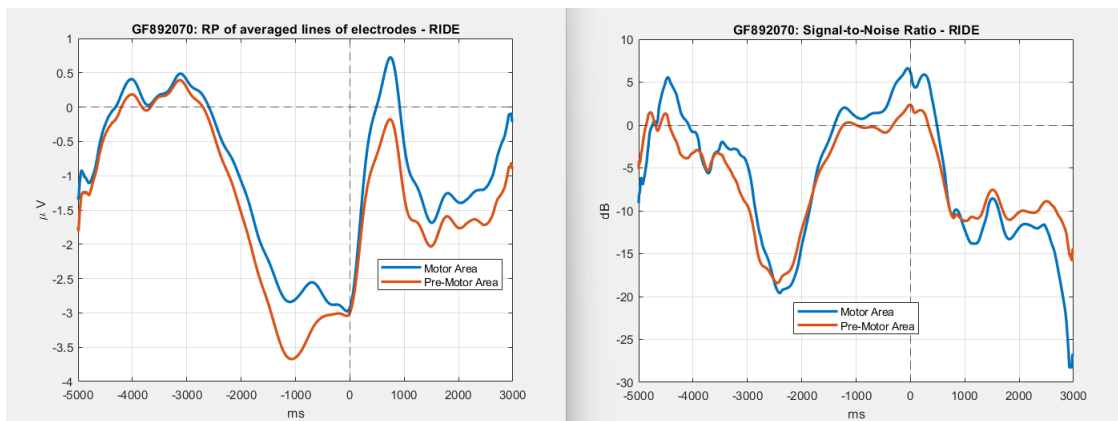


Figure 7.34: Subject graph GF892070 (new plugin). Left: RP; Right: SNR.

TC995011 - voluntary subject

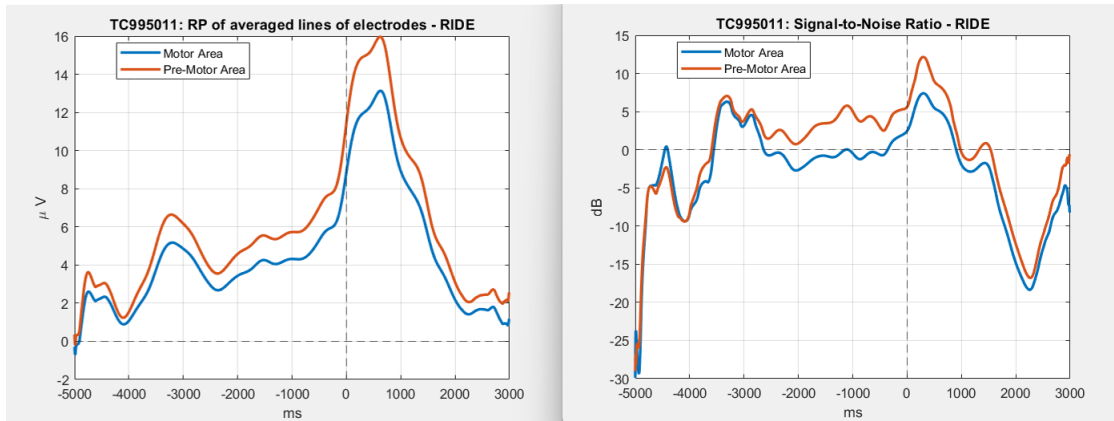


Figure 7.35: Subject graph TC995011 (old plugin). Left: RP; Right: SNR.

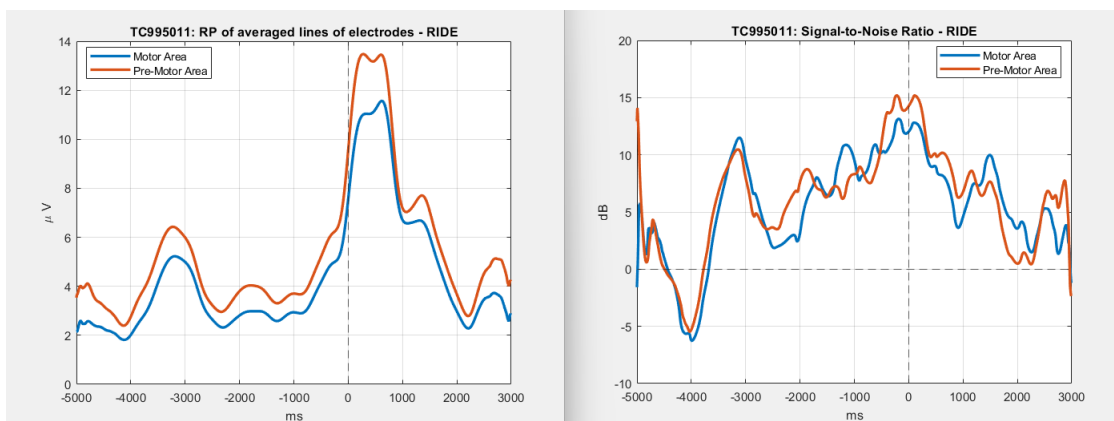


Figure 7.36: Subject graph TC995011 (new plugin). Left: RP; Right: SNR.

7.3.2 RP and SNR of involuntary subjects

AP996111 - involuntary subject

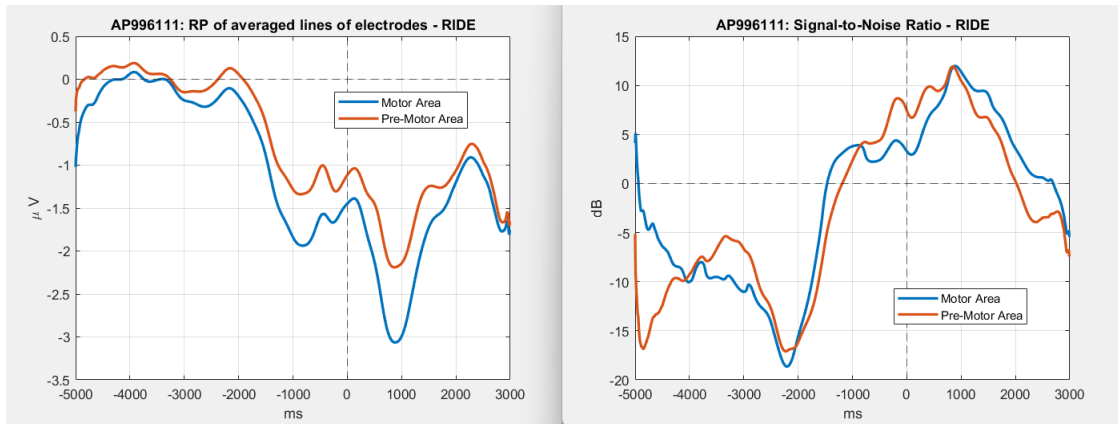


Figure 7.37: Subject graph AP996111 (old plugin). Left: RP; Right: SNR.

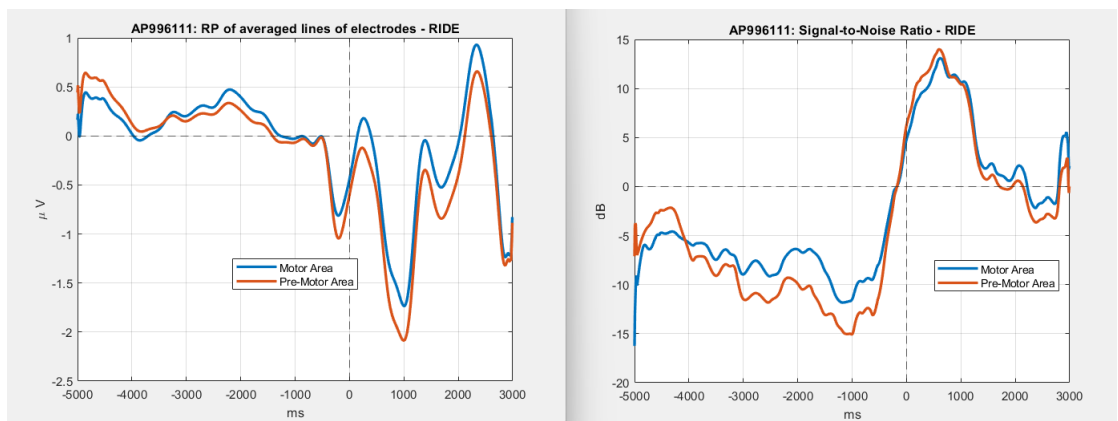


Figure 7.38: Subject graph AP996111 (new plugin). Left: RP; Right: SNR.

LL993111 - involuntary subject

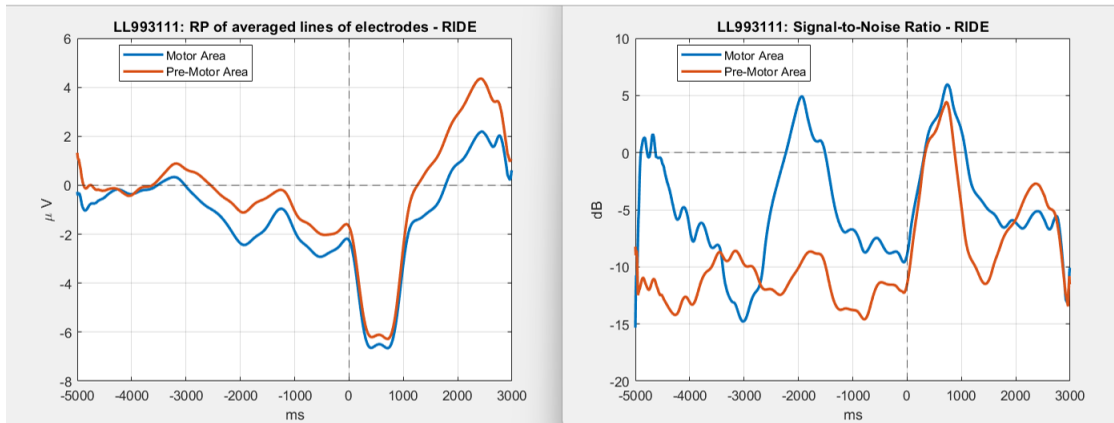


Figure 7.39: Subject graph LL993111 (old plugin). Left: RP; Right: SNR.

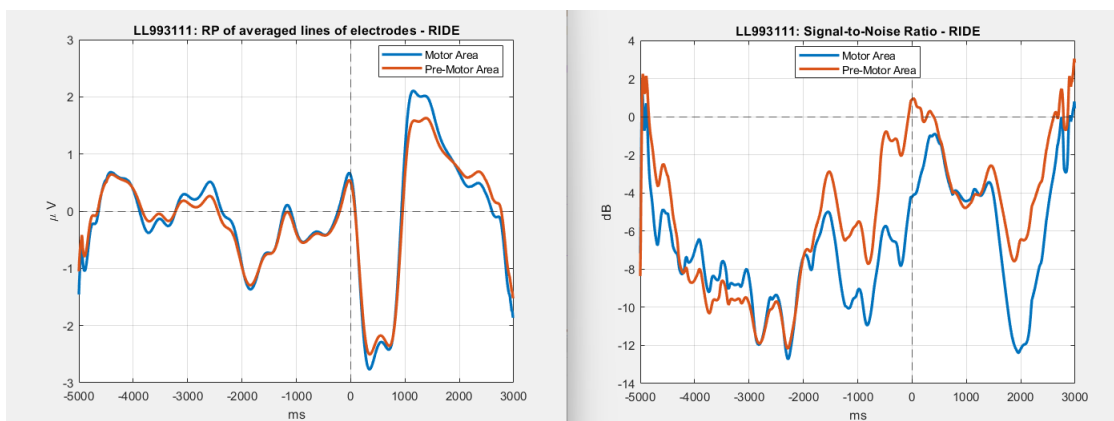


Figure 7.40: Subject graph LL993111 (new plugin). Left: RP; Right: SNR.

RG865070 - involuntary subject

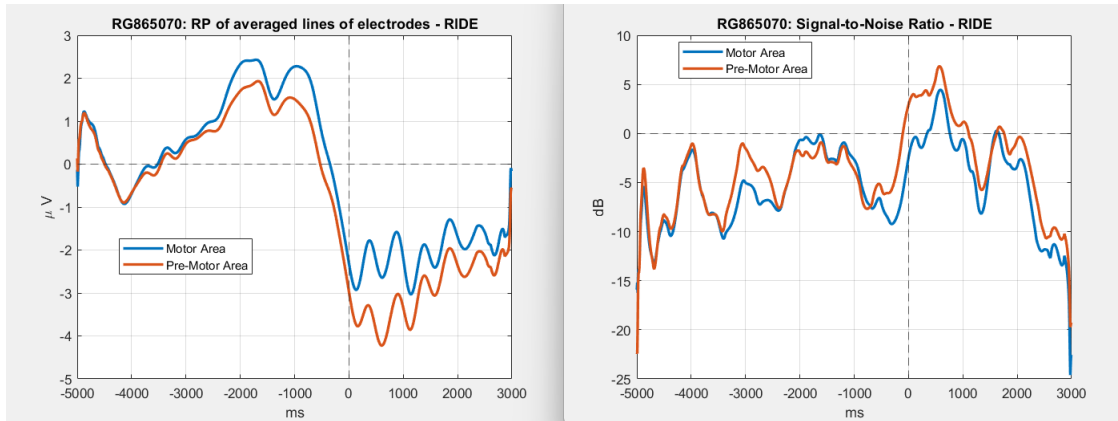


Figure 7.41: Subject graph RG865070 (old plugin). Left: RP; Right: SNR.

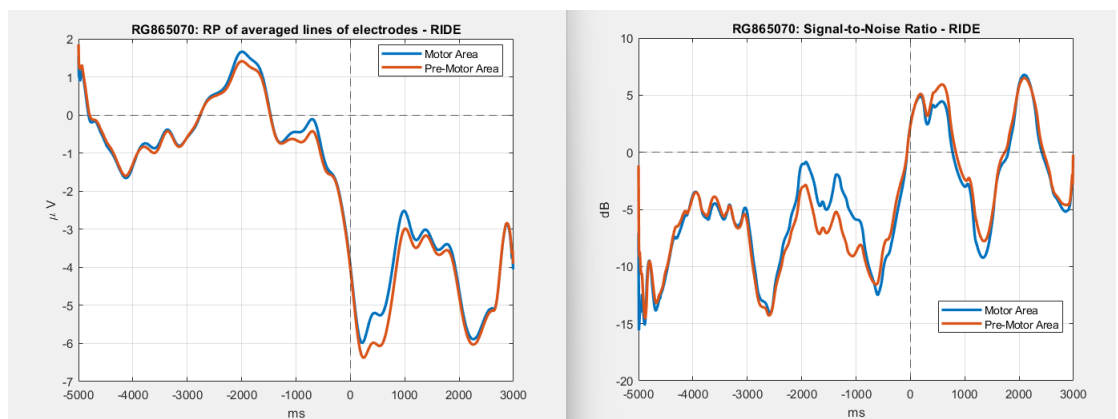


Figure 7.42: Subject graph RG865070 (new plugin). Left: RP; Right: SNR.

LF864071 - involuntary subject

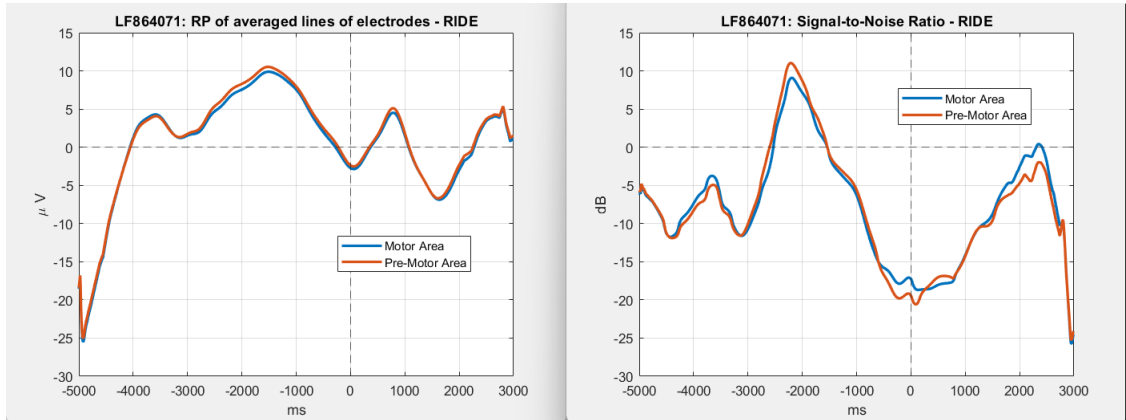


Figure 7.43: Subject graph LF864071 (old plugin). Left: RP; Right: SNR.

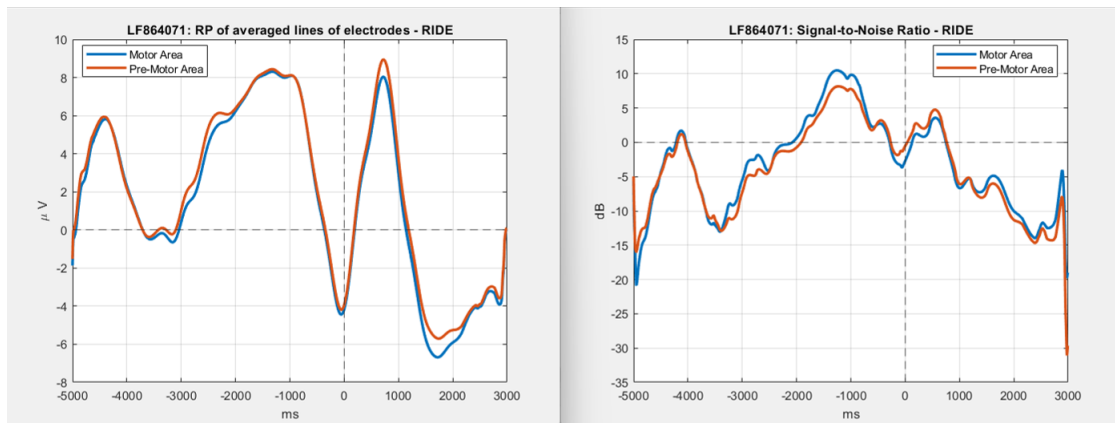


Figure 7.44: Subject graph LF864071 (new plugin). Left: RP; Right: SNR.

AP996120 - involuntary subject

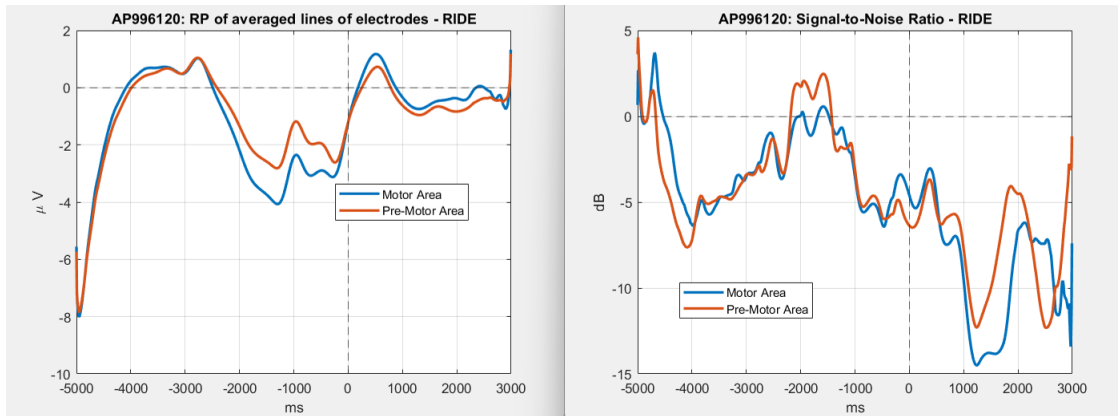


Figure 7.45: Subject graph AP996120 (old plugin). Left: RP; Right: SNR.

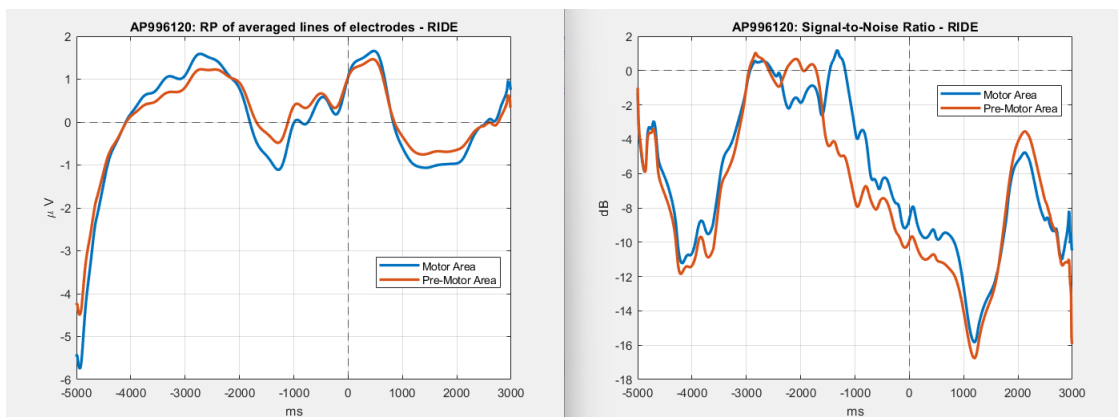


Figure 7.46: Subject graph AP996120 (new plugin). Left: RP; Right: SNR.

GO862071 - involuntary subject

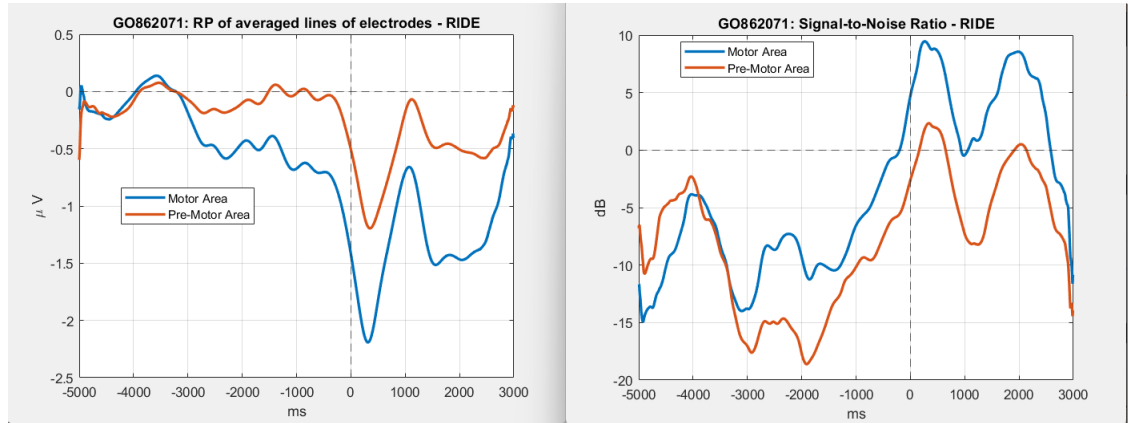


Figure 7.47: Subject graph GO862071 (old plugin). Left: RP; Right: SNR.

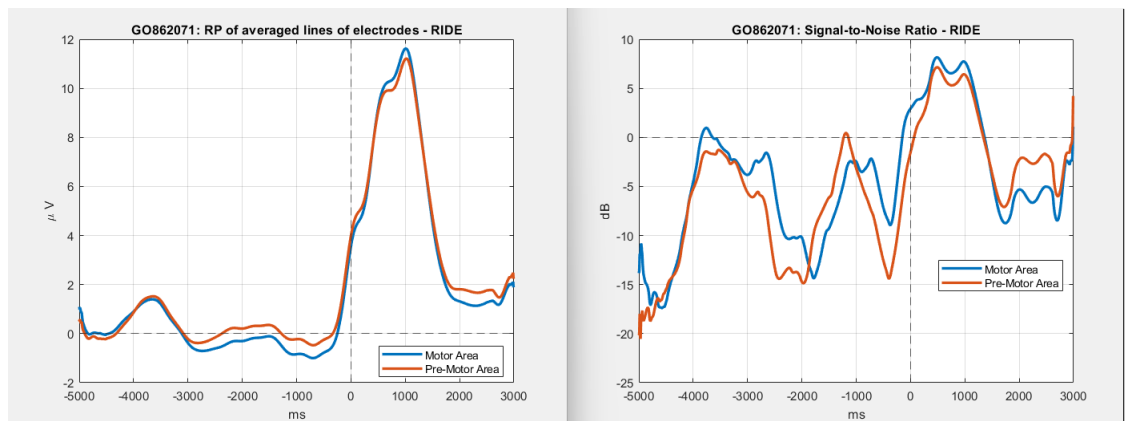


Figure 7.48: Subject graph GO862071 (new plugin). Left: RP; Right: SNR.

FM893061 - involuntary subject

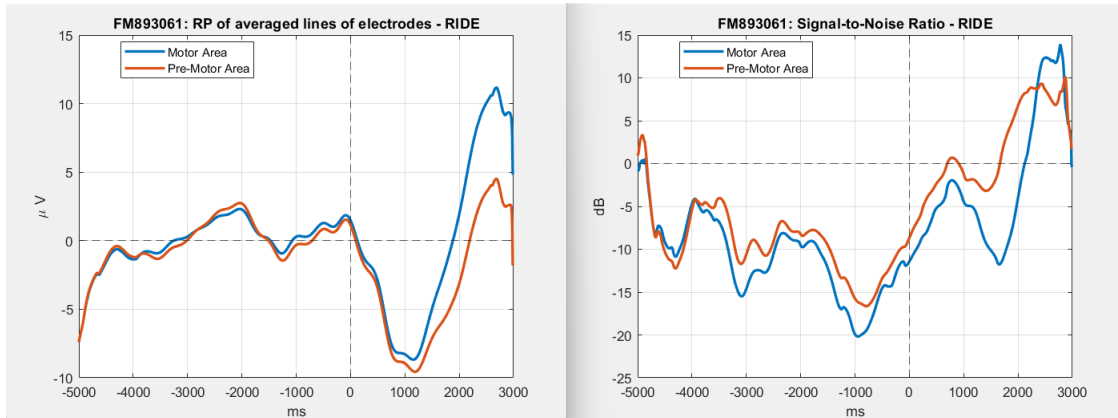


Figure 7.49: Subject graph FM893061 (old plugin). Left: RP; Right: SNR.

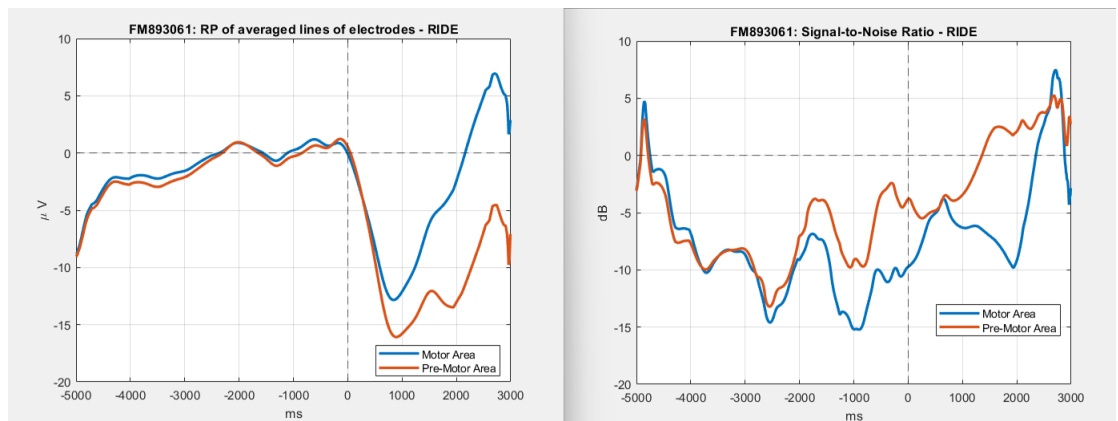


Figure 7.50: Subject graph FM893061 (new plugin). Left: RP; Right: SNR.

SP880071 - involuntary subject

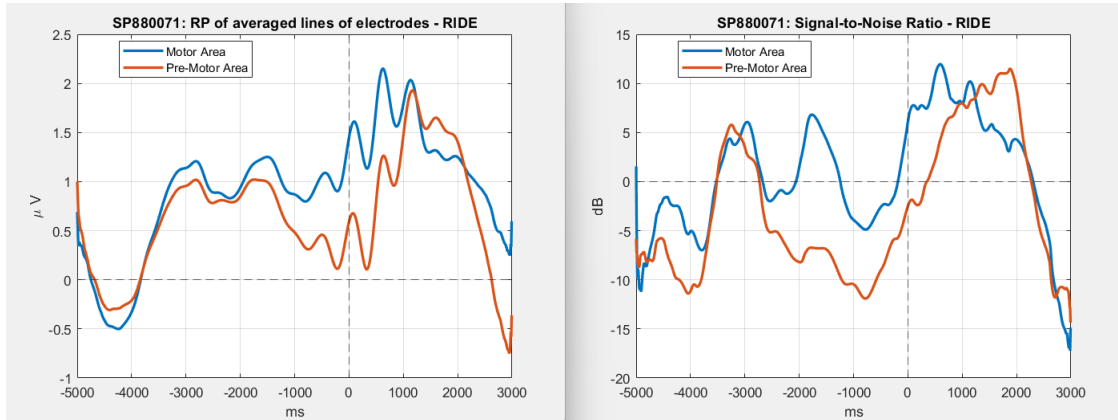


Figure 7.51: Subject graph SP880071 (old plugin). Left: RP; Right: SNR.

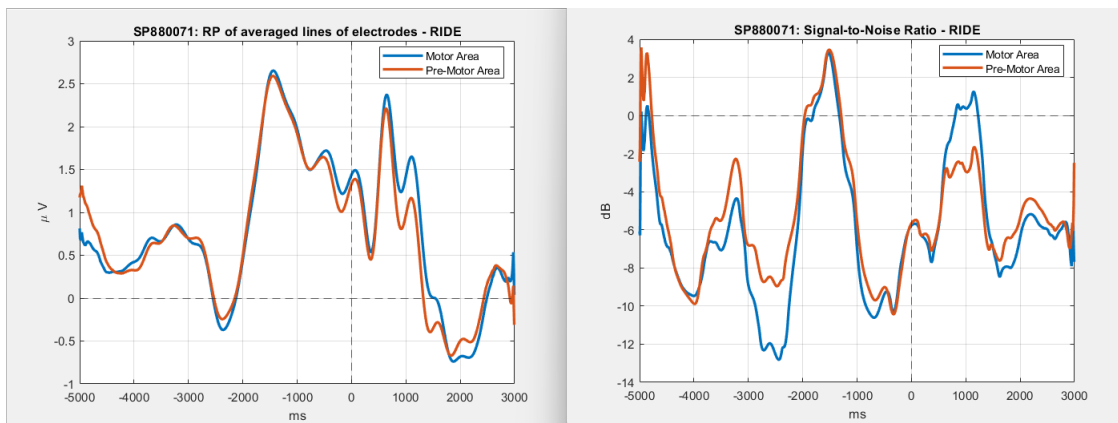


Figure 7.52: Subject graph SP880071 (new plugin). Left: RP; Right: SNR.

AL858070 - involuntary subject

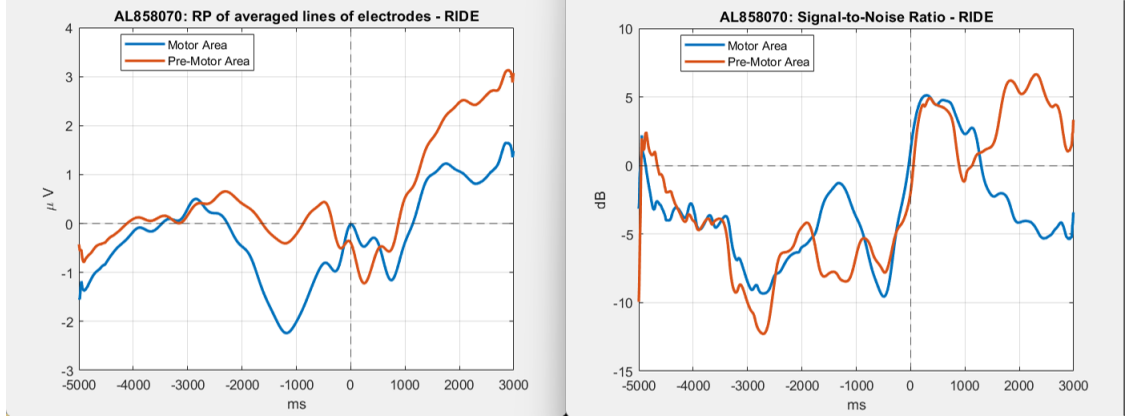


Figure 7.53: Subject graph AL858070 (old plugin). Left: RP; Right: SNR.

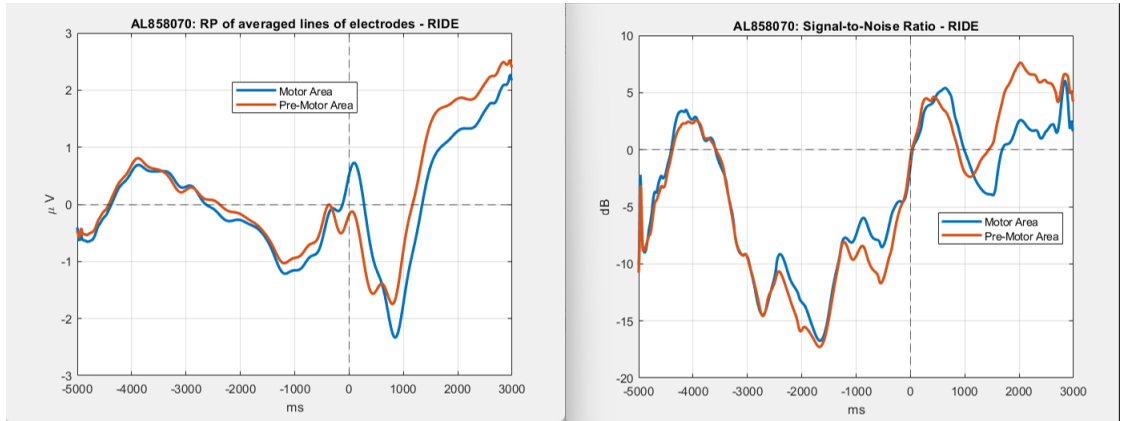


Figure 7.54: Subject graph AL858070 (new plugin). Left: RP; Right: SNR.

It can definitely be said from these graphs that the SNR improves and some artifacts are compensated in the case of the new plugin. These visually noticeable improvements in the new and improved preprocessing are attributed to two specific enhancements, as said before: improved *artifact correction* and *spatial filtering* (small laplacian low-pass spatial filter). The spatial filtering was not present in the previous version of the plugin, while the artifact correction has been improved.

Artifact Correction

Before explaining why the shapes of the RP (Readiness Potential) signals and their corresponding SNR (Signal-to-Noise Ratio) improve, here's a brief explanation

of **ICA** (Independent Component Analysis) for better understanding. ICA is a computational statistical technique for signal processing and machine learning that helps to filter signals, because it separates mixed signals into their independent components, in order to isolate the neural activity related to the motor task from the unwanted artifacts. By applying ICA, the algorithm can extract and remove the components related to artifacts, resulting in an improved representation of the RP signals and higher SNR. This enhancement helps in identifying the brain's intentions and responses more clearly, making the classification of the signals more accurate and reliable. For example, during a motor task, various brain activities, ocular artifacts, and muscular artifacts might be mixed together in the EEG signal.

The automated algorithm utilized in MRCPLAB employs Independent Component Analysis (ICA) and conducts a comprehensive analysis of components, subsequently applying necessary corrections. The algorithm in the recent MRCPLAB was improved by *Cristina Del Prete* ([34]) by incorporating the EOG signal in the analysis prior to evaluating the independent components (ICs). This allows for the calculation of Pearson's coefficient between the ICs and EOG, facilitating the identification of components that are strongly correlated with EOG activity. After correcting these components, additional features were examined and compared against specific thresholds to detect other types of artifacts. These identified artifacts are then removed, resulting in corrected EEG signals [34].

The types of artifacts that were corrected include:

- Ocular artifacts, which exhibit a high correlation with EOG signals [34].
- Muscular artifacts, characterized by a low fit-error and prominent peaks in the 25 Hz-40 Hz frequency band [34].
- Artifacts related to eye blinking, cardiac activity, and intense muscle activity, indicated by high skewness and kurtosis values [34].
- Noisy channels, identified by the presence of high focal components [34].
- Other unpredictable and unexpected artifacts, determined based on high entropy values [34].

Spatial Filtering

The low-pass Laplacian spatial filtering, in the context of EEG signals, is a processing technique aimed at improving signal quality by reducing high-frequency interference and noise (which may be caused by muscle movements, electrical activity, or other external sources), in order to attenuate these components while preserving the more relevant low-frequency information.

In the spatial domain, the Laplacian filter calculates the second derivative of the signal, which corresponds to the variation in the potential distribution along different directions in the brain's electric field. This operation helps identify regions in the brain where significant changes in the EEG signal occur.

The algorithm in the recent MRCPLAB was created by Andrea Bonomi ([45]). The low pass versions provided improvements of the RPs waveforms and enhancement of their signal-to-noise ratio.

Chapter 8

Conclusions

There are significant differences in terms of performance between the two classifications. For the Linear SVM classifier, the first classification (new plugin) achieved perfect scores in all metrics; the second classification (old plugin) with the same classifier showed decreased performance across all metrics. These results suggest that the second classification may have encountered challenges in accurately separating the two classes. Similarly, for the Cubic SVM classifier, the first classification had higher performance in terms of AIC, K Statistics, Specificity, Sensitivity, and Accuracy compared to the second classification. In the case of the k-NN classifier, the first classification had higher scores but the second classification showed improvement compared to the first in terms of K Statistics and Specificity, but still had lower values compared to the first classification. Finally, the Decision Tree classifier showed a decline in performance in the second classification compared to the first.

Overall, the differences between the two classifications suggest that the first set of results achieved better classification performance across all classifiers. The better results obtained in the first case are due to the improvements made in the data preprocessing. Using a plugin with the recent *artifact correction* can help reduce the influence of unwanted or noisy signals in EEG recordings, thereby improving the quality of the signals. Additionally, the *spatial filtering* can help mitigate interference from external sources. Everything leads to the better distinction between features of voluntary and involuntary signals, because these improvements have specifically targeted the reduction of ocular and muscular artifacts, which are common sources of interference in EEG recordings that distort the underlying brain activity of interest.

Specifically, the *artifact correction* techniques employed have allowed for the identification and removal of unwanted components, resulting in cleaner and more reliable EEG signals and the integration of *low-pass Laplacian spatial filtering* has

proven beneficial in reducing high-frequency interference and noise while preserving essential low-frequency information.

The application of these improved techniques in the context of EEG can result in higher-quality signals, reducing unwanted interferences and enhancing the detection and analysis of relevant brain events. This can contribute to a better understanding of brain activities and their implications in the field of Brain-Computer Interfaces (BCIs).

Regarding the selected features, that are the SNR of the motor line and premotor line, the area of the motor line in the intention interval and the PCA of the PSD, turned out to be meaningful for distinguishing between volunteers and non-volunteers for several reasons.

Firstly, the **Signal-to-Noise Ratio** (SNR) is an indicator of signal quality and represents the ratio between the power of the signal and the power of the background noise. A higher SNR indicates that the signal is more dominant compared to the noise, making the differences between the groups more evident. Remembering that the signals were chosen according to the quality of their extraction in the phase of EEG signal recording from subjects, if the higher SNR is present in voluntary subjects, the following conclusions can be drawn: a) action-specific related neuronal activation could be more focused and intense than involuntary activation. This could generate a signal that is stronger and more distinctive than the background noise. In cases of involuntary signals, neuronal activation could be less focused or weaker, making the signal less relevant and more susceptible to noise; b) neural signals generated during a voluntary action could be more synchronized and correlated with each other, making them more distinguishable than noise. In contrast, in cases of involuntary activities, temporal coherence might be reduced, making the signal weaker and less distinguishable than in noise; c) during a voluntary action, involved areas may generate stronger and more distinctive signals than other brain regions not involved in the action. In cases of involuntary activity, there might be a lack of involvement of such specific areas, leading to weaker and less distinctive signals.

The **area** of the motor line in the intention interval is an indication of the spatial distribution of neural activity during the intention to perform a movement. This measure can reveal significant differences between the groups as voluntary and non-voluntary subjects. In the context of a voluntary Readiness Potential (RP), a larger area is expected, since a voluntary RP indicates intention or preparation to perform a volitional movement (so the motor line occupies a longer period of time). On the other hand, in the case of an involuntary RP, a more restricted area of the motor line might be present, as the activity might be less controlled or less directly related to a voluntary movement.

Lastly, **PCA** on the **Power Spectral Density** (PSD) is a dimensionality

reduction technique that allows identifying the main patterns of variability within the signal. The PSD reflects the spectral distribution of brain activity and can reveal relevant differences between the groups in terms of specific frequency activity.

In conclusion, it is demonstrated that these features hold great potential for the development of Brain-Computer Interfaces (BCIs). The improved performance achieved through an accurate and targeted preprocessing aimed at *cleaning* the signal and the utilization of the SNR of the motor and premotor lines, area of the motor line during the intention interval, and PCA of the PSD, indicates their suitability for robust and accurate classification of EEG signals. This finding can be useful for the application of these features in real-world scenarios, where the reliable detection and classification of voluntary and involuntary signals are crucial for the development of BCIs.

8.0.1 Special Case

A subject from involuntary patients was included in the involuntary dataset, but he produced a RP similar to the volunteers (Figure 8.1): LF864071.

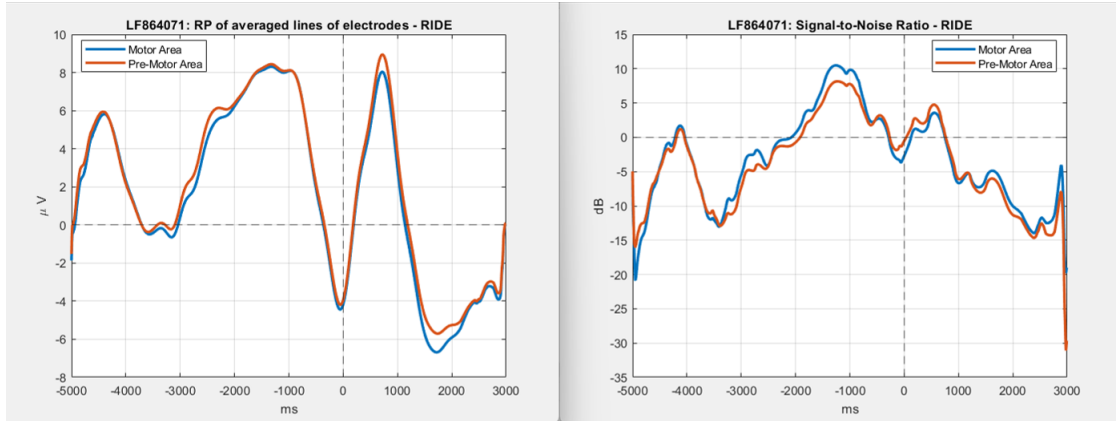


Figure 8.1: Subject graph LF864071 (**new** plugin). Left: RP; Right: SNR.

Understanding the RP (Readiness Potential) and SNR (Signal-to-Noise Ratio) of someone who performed the involuntary task but moved voluntarily can be useful. In this case, it is exhibited an RP peak and a high SNR similar to a voluntary subject. In the case of someone who performed the involuntary task this may appear contradictory. The RP is typically associated with the peak of intention, indicating a voluntary movement initiation. Similarly, a high SNR is often indicative of a clear and strong signal, typically observed in voluntary movements, as explained before. Further investigation would be necessary to understand the underlying factors contributing to this observation. It could involve exploring potential confounding

variables, such as subconscious intentions or unintended muscle activation, that may have influenced the RP and SNR in this particular scenario. In fact, this signal is correctly recognized as involuntary only by the Linear SVM; all the others misclassify it.

8.0.2 Issues and limitations

While this thesis has provided valuable insights into the classification of EEG signals for distinguishing voluntary and involuntary actions, it is important to acknowledge the issues and limitations of the described approach. One of the main challenges faced during the project was the quality of the available datasets, particularly in relation to the Protocol 2018, in which some measurements were affected by poor signal quality. This leads to a poor dataset: few subjects were selected. Studying the effects of both plugins on the signal and noise was necessary in order to understand their impact on the classification performance.

Another limitation lies in the classification aspect, which is closely tied to the quality of the EEG recordings. In the preliminary study, only binary classification was feasible due to the poor signal quality of the semi-voluntary tasks. Expanding the classification capabilities to include non-binary classifications, such as distinguishing different types of movements or intentions, would require datasets of higher quality and a more comprehensive analysis approach.

Furthermore, an inherent limitation of this approach is the possibility of undetectable involuntary reflexes in patients. While the presence of the patient's will to move serves as an indication of consciousness, the absence of this will cannot be definitively interpreted as a sign of unconsciousness.

8.0.3 Ideas for the future

There are several areas for potential improvement:

1. Increase dataset size: collect more high-quality measurements to improve the accuracy and reliability of the classification algorithms and enhance the generalizability of the findings.
2. Explore ensemble models: combine the outputs of different models, such as K-NN and Decision Tree, to create a more powerful and robust classification system.
3. Introduce additional classes: include different types of movements or analyze lateralized readiness potential (LRP) to capture specific brain activations and improve the differentiation of actions.

Bibliography

- [1] Adrian M Owen. «Improving diagnosis and prognosis in disorders of consciousness». In: *Brain* 143.4 (Apr. 2020), pp. 1050–1053 (cit. on p. i).
- [2] Eoin Travers, Nima Khalighinejad, Aaron Schurger, and Patrick Haggard. «Do readiness potentials happen all the time?» In: *NeuroImage* 206 (2020), p. 116286. ISSN: 1053-8119. DOI: <https://doi.org/10.1016/j.neuroimage.2019.116286>. URL: <https://www.sciencedirect.com/science/article/pii/S1053811919308778> (cit. on p. i).
- [3] Tonya Hines. «Anatomy of the Brain». In: (2018) (cit. on pp. 1–3, 5–8).
- [4] Jan Helm. «Brain and consciousness». In: (May 2021) (cit. on pp. 1, 14).
- [5] *Brain MRI Scan: Everything You Need to Know*. URL: <https://www.echelon.health/ar/brain-mri-scan-everything-you-need-to-know/> (cit. on p. 2).
- [6] *Your Brain: An Introduction to Its Anatomy*. URL: <https://mapp.mgh.harvard.edu/your-brain-an-introduction-to-its-anatomy/> (cit. on pp. 2–5).
- [7] URL: <https://www.simplypsychology.org/left-brain-vs-right-brain.html> (cit. on p. 3).
- [8] URL: https://it.freepik.com/vettori-premium/diagramma-di-infographics-di-anatomia-del-cervello-umano-con-sezioni-e-descrizione-del-testo-piatta_13740869.htm (cit. on p. 4).
- [9] URL: <https://quizlet.com/247788722/chapter-12-reading-flash-cards/> (cit. on p. 5).
- [10] *The Meninges*. URL: <https://teachmeanatomy.info/neuroanatomy/structures/meninges/> (cit. on p. 7).
- [11] URL: <https://www.google.com/url?sa=i&url=https> (cit. on p. 7).
- [12] Hiroshi Shibasaki. «Clinical Neurophysiology». In: (2012), pp. 229–243 (cit. on p. 9).

- [13] Department of Neurobiology and McGovern Medical School Anatomy at The University of Texas Health Science Center at Houston. *Motor Cortex*. 2000. URL: <https://nba.uth.tmc.edu/neuroscience/s3/chapter03.html> (cit. on p. 10).
- [14] Bhidayasiri R. Virameteekul S. «We Move or Are We Moved? Unpicking the Origins of Voluntary Movements to Better Understand Semivoluntary Movements». In: (2022) (cit. on p. 11).
- [15] Mark Hallet. «Volitional control of movement: the physiology of free will». In: (2007), pp. 1179–1192 (cit. on p. 11).
- [16] Alessandra Zanetta. «Machine Learning algorithms to classify voluntary and involuntary movements from EEG in a BCI for post-coma non-responsive patients». MA thesis. Politecnico di Torino, 2022 (cit. on pp. 11, 42).
- [17] Shibasaki H. «Cortical activities associated with voluntary movements and involuntary movements.» In: (2012) (cit. on p. 11).
- [18] URL: <https://iep.utm.edu/hard-problem-of-consciousness/> (cit. on p. 12).
- [19] URL: <https://en.wikipedia.org/wiki/Consciousness> (cit. on pp. 12, 13, 62).
- [20] Steven Rose. «Il cervello e la coscienza». In: (Nov. 1977), pp. 569–571 (cit. on p. 13).
- [21] James Kingsland. «How does the human brain create consciousness, and why?» In: (Jan. 2023). URL: <https://www.medicalnewstoday.com/articles/how-does-the-human-brain-create-consciousness-and-why> (cit. on p. 14).
- [22] Tindall SC. *Level of Consciousness*. Vol. 3. Chapter 57. 1990 (cit. on p. 15).
- [23] NHS. «Disorders of consciousness». In: (2022). URL: <https://www.nhs.uk/conditions/disorders-of-consciousness> (cit. on pp. 15, 16).
- [24] Aaron Schurger, Pengbo 'Ben' Hu, Joanna Pak, and Adina L. Roskies. «What Is the Readiness Potential?» In: *Trends in Cognitive Sciences* 25.7 (2021), pp. 558–570. ISSN: 1364-6613. DOI: <https://doi.org/10.1016/j.tics.2021.04.001>. URL: <https://www.sciencedirect.com/science/article/pii/S1364661321000930> (cit. on pp. 19–21, 48).
- [25] URL: <https://sabrinasingh.medium.com/the-power-of-brain-computer-interfaces-in-neurorehabilitation-db3511234892> (cit. on p. 19).
- [26] «International 10-20 System». In: (2022). URL: <https://www.evokedpotential.com/international-10-20-system.html> (cit. on pp. 19, 20).
- [27] H. Shibasaki and M. Hallett. «What is the Bereitschaftspotential?» In: (Apr. 2006), pp. 26–28 (cit. on pp. 22, 23).

- [28] Luca Mesin Alessio Mascolini Imran Khan Niazi. «Non-linear optimized spatial filter for single-trial identification of movement related cortical potential». In: (Mar. 2022) (cit. on pp. 23, 24).
- [29] Ji-Hoon Jeong, No-Sang Kwak, Min-Ho Lee, and Seong-Whan Lee. «Decoding of walking Intention under Lower limb exoskeleton Environment using MRCP Feature». In: *Graz Brain-Computer Interface Conference*. 2017 (cit. on pp. 23, 24).
- [30] Peter G.H. Clarke. «The Libet Experiment and its Implications for Conscious Will». In: (May 2023). URL: <https://www.bethinking.org/human-life/the-libet-experiment-and-its-implications-for-conscious-will> (cit. on pp. 23–25).
- [31] Chiara Botrugno. «Enhancement of Readiness Potentials’ Pre-Processing Chain in an Brain Computer Interface for nonresponsive patients». MA thesis. Politecnico di Torino, 2022 (cit. on pp. 24, 26–31, 33, 42, 46).
- [32] Alessandra Zanetta. «Machine Learning algorithms to classify voluntary and involuntary movements from EEG in a BCI for post-coma non-responsive patients». MA thesis. Politecnico di Torino, 2022 (cit. on pp. 24, 34).
- [33] Federica Sgrò. «Disorders of Consciousness: using the Perturbational Complexity Index to distinguish between voluntary and involuntary movements». MA thesis. Politecnico di Torino, 2019 (cit. on p. 24).
- [34] Cristina Del Prete. «Enhancements of EEG Artifact Automatic Correction Algorithm and Processing of Hemiplegic Patients’ EEG». MA thesis. Politecnico di Torino, 2023 (cit. on pp. 26–31, 33, 42, 85).
- [35] URL: <https://mitsloan.mit.edu/ideas-made-to-matter/machine-learning-explained> (cit. on p. 35).
- [36] IBM. *Machine Learning*. 2022. URL: <https://www.ibm.com/topics/machine-learning> (cit. on p. 35).
- [37] Shiv Kumar Mudgal, Suresh K Sharma, Jitender Chaturvedi, and Anil Sharma. «Brain computer interface advancement in neurosciences: Applications and issues». In: *Interdisciplinary Neurosurgery* 20 (2020), p. 100694. DOI: <https://doi.org/10.1016/j.inat.2020.100694>. URL: <https://www.sciencedirect.com/science/article/pii/S2214751920300098> (cit. on p. 35).
- [38] Zhihan Lv, Liang Qiao, Qingjun Wang, and Francesco Piccialli. «Advanced Machine-Learning Methods for Brain-Computer Interfacing». In: *IEEE/ACM Transactions on Computational Biology and Bioinformatics* 18.5 (2021), pp. 1688–1698. DOI: 10.1109/TCBB.2020.3010014 (cit. on p. 36).

- [39] Rohith Gandhi. *Support Vector Machine — Introduction to Machine Learning Algorithms*. 2018. URL: <https://towardsdatascience.com/support-vector-machine-introduction-to-machine-learning-algorithms-934a444fca47> (cit. on p. 37).
- [40] Javatpoint. *Support Vector Machine (SVM) Algorithm*. 2022. URL: <https://www.javatpoint.com/machine-learning-support-vector-machine-algorithm> (cit. on p. 37).
- [41] *Support Vector Machines(SVM) - A Complete Guide for Beginners*. 2021. URL: <https://www.analyticsvidhya.com/blog/2021/10/support-vector-machinessvm-a-complete-guide-for-beginners/> (cit. on p. 38).
- [42] Wikipedia. *Polynomial kernel — Wikipedia, The Free Encyclopedia*. 2023. URL: https://en.wikipedia.org/wiki/Polynomial_kernel (cit. on p. 38).
- [43] *K-Nearest Neighbor(KNN) Algorithm for Machine Learning*. 2022. URL: <https://www.javatpoint.com/k-nearest-neighbor-algorithm-for-machine-learning> (cit. on pp. 38, 39).
- [44] *Machine Learning Decision Tree Classification Algorithm*. 2021. URL: <https://www.javatpoint.com/machine-learning-decision-tree-classification-algorithm> (cit. on pp. 39, 40).
- [45] Andrea BONOMI. «Role of spatial filtering in the pre-processing chain of a BCI for non-responsive patients». MA thesis. Politecnico di Torino, 2022 (cit. on pp. 43, 86).
- [46] Guang Ouyang, Werner Sommer, and Changsong Zhou. «A toolbox for residue iteration decomposition (RIDE)—A method for the decomposition, reconstruction, and single trial analysis of event related potentials». In: *Journal of Neuroscience Methods* 250 (2015), pp. 7–21. DOI: <https://doi.org/10.1016/j.jneumeth.2014.10.009>. URL: <https://www.sciencedirect.com/science/article/pii/S0165027014003690> (cit. on pp. 43, 44).
- [47] Guang Ouyang, Werner Sommer, and Changsong Zhou. «Reconstructing ERP amplitude effects after compensating for trial-to-trial latency jitter: A solution based on a novel application of residue iteration decomposition». In: *International Journal of Psychophysiology* 109 (2016), pp. 9–20. ISSN: 0167-8760. DOI: <https://doi.org/10.1016/j.ijpsycho.2016.09.015>. URL: <https://www.sciencedirect.com/science/article/pii/S0167876016307103> (cit. on pp. 43–47).
- [48] Enes Zvornicanin. *What Is Feature Importance in Machine Learning?* URL: baeldung.com/cs/ml-feature-importance (cit. on pp. 47, 50).
- [49] *Principal Component Analysis*. URL: <https://www.javatpoint.com/principal-component-analysis> (cit. on p. 50).

- [50] Kai Zhao. *Feature Extraction using Principal Component Analysis — A Simplified Visual Demo*. URL: <https://towardsdatascience.com/feature-extraction-using-principal-component-analysis-a-simplified-visual-demo-e5592ced100a> (cit. on p. 50).
- [51] Ryan J. Urbanowicz, Melissa Meeker, William La Cava, Randal S. Olson, and Jason H. Moore. «Relief-based feature selection: Introduction and review». In: *Journal of Biomedical Informatics* 85 (2018), pp. 189–203. ISSN: 1532-0464. DOI: <https://doi.org/10.1016/j.jbi.2018.07.014>. URL: <https://www.sciencedirect.com/science/article/pii/S1532046418301400> (cit. on p. 50).
- [52] Musa Peker, Serkan Ballı, and Ensar Sağbaş. «Predicting Human Actions using a Hybrid of ReliefF Feature Selection and Kernel-Based Extreme Learning Machine». In: Dec. 2018, pp. 379–397. ISBN: 9781522547662. DOI: 10.4018/978-1-5225-4766-2.ch017 (cit. on p. 51).
- [53] Igor Kononenko, Marko Robnik-Sikonja, and Uros Pompe. *ReliefF for estimation and discretization of attributes in classification, regression, and ILP problems*. URL: <http://lkm.fri.uni-lj.si/rmarko/papers/kononenko96-aims.pdf> (cit. on p. 51).
- [54] *LOOCV (Leave One Out Cross-Validation) in R Programming*. URL: <https://www.geeksforgeeks.org/loocvleave-one-out-cross-validation-in-r-programming> (cit. on p. 52).
- [55] The R4DS Online Learning Community. *Advantages of LOOCV over Validation Set Approach*. 2023. URL: <https://r4ds.github.io/bookclub-islr/advantages-of-loocv-over-validation-set-approach.html> (cit. on p. 52).

Acknowledgements

I write these words with tears in my eyes and a heart filled with joy. I want to express my heartfelt thanks to Professoressa Olmo for giving me the opportunity to be part of this project and to experience one of the most important journeys of my life. I am deeply grateful to Professor De Feo for his constant availability, understanding, and guidance throughout this project, and for making me feel part of an amazing group of students.

Thank you, Cristina, Micaela, and Andrea, for your help and support. Especially to the girls (sorry, Andre), I want to say thank you for enduring me, standing by my side, laughing with me, and becoming not only friends but also confidants. I will never forget you.

I can't help but thank my family: mom, dad. Thank you because it's because of you that I'm here and that I've become who I am. Thank you for teaching me that you have to build yourself up in life but also for being my safe haven.

Thank you, Dani. I couldn't have asked for a better sister. You are the greatest gift life has given me.

Grandma, thank you. You are my number one fan. You see me as the smartest and most talented person in the world, and you have a belief in me that I don't think I will ever fully possess. I carry you with me always, even when you're not physically here, and I know that when I return, your lasagna will be waiting for me.

To my friends in Turin and to those who have always been there for me, thank you. I love you all.

